8èmes Journées Nationales sur la Récupération et le Stockage d'Energie

8th National Days on Energy Harvesting and Storage

May 14-15, 2018, Besançon, France

https://jnrse-2018.sciencesconf.org/

Table of Contents

Posters

8èmes Journées Nationales sur la Récupération et le Stockage d'Energie
8th National Days on Energy Harvesting and Storage

Organizing Committee

Program Committee

- Adrien BADEL, SYMME, Annecy
- Philippe BASSET, ESIEE, Paris
- Skandar BASROUR, TIMA, Grenoble
- Noureddine BOUHADDI, FEMTO-ST, Besançon
- Hélène DEBEDA, IMS, Bordeaux
- Jean-Marie DILHAC, LAAS, Toulouse
- Mickaël LALLART, LGEF, INSA-Lyon
- Elie LEFEUVRE, IEF, Paris

Local Committee

- Ausryne BARTASYTE, FEMTO-ST, co-chair
- Magali BARTHES, FEMTO-ST, co-chair
- Noureddine BOUHADDI, FEMTO-ST, chair
- Sandrine CHATRENET, FEMTO-ST, co-chair
- Christine FROIDEVAUX, FEMTO-ST, co-chair
- Najib KACEM, FEMTO-ST, co-chair
- François LANZETTA, FEMTO-ST, co-chair
- Claudia LAOU-HUEN, FEMTO-ST, co-chair
- Francis MILLER, FEMTO-ST, co-chair
- Sandrine QUARROZ, FEMTO-ST, co-chair
- Micky RAKOTONDRABE, FEMTO-ST, co-chair
- Delphine TRAVAGLINI, co-chair

Preface

The « Journées Nationales sur la Récupération et le Stockage d'Energie » (JNRSE – literally "National Days on Energy Harvesting and Storage") aims at gathering the French and international community from the felds of energy conversion, harvesting and storage, especially at small scale, as well as the design of complete "selfpowered" devices that are energetically autonomous.

The context, motivations and challenges behind this conference series lie in the increasing demands in terms of energetically autonomous devices, both at public and industrial scales, covering domains like domotics or widespread sensors and sensor networks for control and security. Scientifc and industrial progresses in terms of autonomous, wireless devices begin however still limited by out-of-board energy demands which currently cannot be fully addressed by primary batteries, it becomes mandatory to fnd and use other energy sources. Hence, using the energy that is directly available from the surrounding environment of the device (in the form of heat, vibrations, electromagnetic wave and so on), leading to the concept of energy harvesting, is an attractive alternative.

Nevertheless, capabilities in terms of energy conversion, extraction and storage must sustain the energy demand of the targeted system. Similarly, the optimal design of a complete self-powered device, ranging from the material to the electrical aspects, through the mechanical, thermal or radiofrequency domains, require considering the global energy transfer chain.

After the previous editions in various places in France, the JNRSE of 2018 is organized by the FEMTO-ST research institute in Besançon, France, and will take place at the ENSMM engineering school, 26 rue de l'Epitaphe on the 14th and the 15th of May, 2018.

We deeply thank you for your valuable participation to the JNRSE 2018 and wish you a pleasant and fruitful stay in Besançon.

JNRSE 2018 Organizing Committee

Program

Besançon, May 14-15, 2018

femto-st SCIENCES & TECHNOLOGIES — UBFC UNIVERSITÉ BOURGOGNE FRANCHE-COMTE — cnrs — UFC UNIVERSITÉ DE FRANCHE-COMTÉ — ensmm École Nationale Supérieure de Mécanique et des Microtechniques — Labex Action Integrated smart systems

Conference Program

	Day 1
08h30	Registration
09h15	Welcome speech (M. SCHAUSS, Vice President, Enseignement Supérieur et Recherche, Grand Besançon)
09h30	Conference opening (chair and co-chairs)
	Session 1 (chairs: N. BOUHADDI / M. RAKOTONDRABE)
09h45	Invited 1: **An NGUYEN-DINH**, VERMON & CAIRDAC Powering autonomous sensors and therapeutic medical implants with miniaturized piezoelectric energy harvesting devices
10h25	Invited 2: **Antoine FERREIRA**, PRISME Laboratory, INSA Centre Val de Loire Energy harvesting for locomotion of micro and nano robotics in medical applications
11h05	Coffe Break
	Session 2 (chairs: N. KACEM / M. BARTHES)
11h30	Talk 1: **Luis Fonseca**, Inci Donmez, Marc Dolcet, Andrej Stranz, Marc Salleras, Gerard Gadea, Mercè Pacios, Alex Morata, Albert Tarancón Research on thermoelectric microgenerators based on Si and SiGe nanowires as thermoelectric material
11h50	Talk 2: **Thomas Huguet**, Adrien Badel, Olivier Druet, Mickaël Lallart Significant enhancement of bistable energy harvesters bandwidth: subharmonic orbits and their stability robustness
12h10	Talk 3: **Adrien Morel**, Adrien Badel, pierre gasnier, David Gibus, Gaël Pillonnet Short Circuit Synchronized Electric Charge Extraction (SC-SECE): a tunable interface for wideband vibration energy harvesting
12h30	Lunch
	Session 3 (chairs: F. LANZETTA / A. BARTASYTE)
14h00	Invited 3: **Fabien FORMOSA**, SYMME Laboratory, Université Savoie Mont-Blanc A story about micro-Stirling design and fabrication
14h40	Invited 4: **Luis ORTIZ**, CEDRAT TECHNOLGIES From Amplified Piezoelectric Actuators to high performance & resistant piezo harvester
15h20	
15h40	Talk 4: **Julien Le Scornec**, Benoit GUIFFARD, Raynald SEVENO, Vincent Le Cam Flexible piezoelectric micro-generator with interdigitated electrodes for energy harvesting
16h00	Coffe break
	Session 4 (chairs: N. BOUHADDI / N. KACEM)
16h25	Talk 5: **Rubaiyet Haque**, Olivier CHANDRAN, Sébastien LANI, Danick Briand Use of 3D printing to build self-powered triboelectric sensors
16h45	Talk 6: David Gibus, pierre gasnier, Adrien Morel, Sébastien Boisseau, Adrien Badel Modeling and design of highly-coupled piezoelectric energy harvesters for broadband applications
17h05	
17h25	Coffe break/Poster session/JNRSE Live
19h00	End of day

Day 2	
	Session 5 (chairs: N. KACEM / M. BARTHES)
09h00	Invited 5: **Marian WIERCIGROCH,** Centre for Applied Dynamics Research, University of Aberdeen Vibrational energy harvesting from complex dynamics of pendula
09h40	Invited 6: **Sebastian BADER**, Department of Electronics Design, Mid Sweden University Energy harvesting for self-powered sensors in hydraulic motors
10h20	Coffe break
	Session 6 (chairs: N. BOUHADDI / M. RAKOTONDRABE)
10h50	Talk 7: **Zakaria Zergoune**, Najib Kacem, Jean-Louis Raynaud, Noureddine Bouhaddi Design of broadband nonlinear vibration energy harvester with magnetic coupling
11h10	Talk 8: **Saïma Siouane**, Slavisa Jovanovic, Etienne Tisserand, Philippe Poure Towards fault tolerant two-stage DC-DC converters under open-circuit switch fault: an original circuit design approach
11h30	Talk 9: **Bogdan Vysotskyi**, Denis Aubry, Philippe Gaucher, Xavier Le Roux, Fabien Parrain, Elie Lefeuvre Heartbeat Electrostatic Energy harvesting using Multimodal-shaped springs MEMS and Fractioning Interface Circuit
11h50	Talk 10: **Giacomo Clementi**, Ausrine BARTASYTE, Bernard DULMET, Samuel MARGUERON Energy Harvesting with lead free LiNbO3
12h10	
12h30	Lunch
	Session 7 (chairs: F. LANZETTA / A. BARTASYTE)
14h00	Invited 7: **Paul MURALT**, EPFL Piezoelectric energy harvesting with ferroelectric thin films coupled to interdigitated electrodes
14h40	Invited 8: **Paul MITCHESON**, Imperial College London Wireless power transfer: an alternative to harvesting
15h20	Talk 11: **Alpha Dassimou Diallo**, Ravinder Chutani, Magali Barthès, Sylvie BEGOT, Sylwester Bargiel, Michel De Labachelerie, François Lanzetta Design and microfabrication of a Microscale-Stirling Engine (M-SE) for low temperature heat recovery
15h40	Talk 12: **Dimitri Tainoff**, Anais Proudhom, Sébastien Dufresnes, Sylvain Dumont, Daniel Bourgault, Olivier Bourgeois Thermoelectric nanogenerator networks: a viable source of power for autonomous wireless sensors
16h00	Best presentation and best poster awards
16h20	Conference closing (chair and co-chairs)
16h30	End of conference

Posters

Poster ID

199946	Clémence ROGIER, Grégory POGNON, Paolo BONDAVALLI, Gaëtan BRACCIALE, Christophe GALINDO, Tran Minh Giao NGUYEN, Frédéric Vidal and Pierre-Henri AUBERT *Development of nanostructured carbon/MnO2 hybrid electrodes for energy storage applications*
202652	Abbas HOMAYOUNI-AMLASHI, Abdenbi MOHAND-OUSAID and Micky RAKOTONDRABE *Optimization Of A Bimorph Piezoelectric Energy Harvester Using Neural Network-Based Genetic Algorithm*
202925	Giulia LOMBARDI and Mickaël LALLART *Hybrid synchronized switch harvesting using piezoelectric and electromagnetic conversion*
203450	Anjneya VERMA *Growth of KNN Nanostructure and thin-films for vibrational energy harvesters*
203568	Robin DARLEUX, Boris LOSSOUARN and Jean-François DEÜ *Plate electrical analogue for multimodal energy transfer*
204715	Kaouthar AOUALI *Enhancement of the performances of a quasi-periodic electromagnetic vibration energy harvester by energy localization*
204907	Quentin MICARD, Anna L. PELLEGRINO, Gugliemo G. CONDORELLI and Graziella MALANDRINO *Dy-doped BiFeO3 films grown by MOCVD on single crystal substrate*
206320	Adrian RENDON-HERNANDEZ, Skandar BASROUR *A PSpice model of a thermo-magnetically triggered piezoelectric generator*
207244	Mihaela IVAN, Ioan IVAN, Joel AGNUS, Thomas BARON and Philippe LUTZ *MEMS Harvester based on PMN-PT/SOI bimorph beam*
207276	Gabriel BARRIENTOS *Autonomous Wireless Network Sensor (WSN) general approach for Energy Harvesting (EH) power supply solutions*
207545	Bastien POLITI, Alain FOUCARAN, Marie PIQUEMIL and Nicolas CAMARA *Harvesting indoor light to supply power to nomad embedded systems*
208122	Matthias PEREZ, Simon CHESNE, Claire JEAN-MISTRAL, Sandrine BOUVET and Christian CLERC *An electromagnetic vibration energy harvester using a two degree of freedom oscillator for railway applications*

Invited Talks

Powering autonomous wireless sensors and therapeutic medical implants with miniaturized piezoelectric energy harvesting devices

An NGUYEN-DINH, Dr / CEO

VERMON & CAIRDAC, Tours France

an.nguyendinh@vermon.com

Abstract

Harvesting energy from ambient sources such as motions, temperature changes or light can be very efficient and replace many conventional power supply systems such as batteries, fuel cells or wiring. There are 3 main methods for mechanical energy harvesting: Electrostatic, Electromagnetic and Piezoelectric.
This paper will cover piezoelectric energy harvesting and its related products in medical and industry. Piezoelectric is so far one of the very common technique for harvesting mechanical energy (movements, pressure, etc.) Number of designs and concepts have been disclosed for years and some are already commercialised. The principle of piezoelectricity is herein exploited using material's intrinsic properties such as elastic compliance (s), strain (d31) and stress (g31) constants or relative dielectric constant (epsilon). Two use-cases of piezoelectric energy harvesters will be disclosed and discussed. The first use-case regards a cardiac leadless stimulation implant wherein a miniaturized low frequency PEH system is incorporated to powering the device's electronics for telemetry, pacing and communication functions, while the second use-case is dedicated to industrial monitoring through for autonomous wireless sensing network applications wherein autonomous single nodes are concerned.
This work has been performed by both VERMON and CAIRDAC companies who are respectively specialised in piezoelectric technologies for ultrasonic transducers and autonomous leadless pacing systems for CRM (Cardiac Rhythm Management).

MSc in µ-Mechanics, Electronics & µ-Systems, An NGUYEN-DINH joined the new start-up company VERMON SA in 1987 as Ultrasound transducer Engineer. From this date, he held several managing positions: R&D Manager in 1989, Director of technology in 1997 and Vice President in charge of Innovation since 2014.
In 2016, An NGUYEN-DINH co-founds CAIRDAC SAS company with the objective to develop innovative Autonomous Leadless Pacing System (ALPS) using piezoelectric energy harvesters as power supply.

His domain of interest covers ultrasound technologies & systems, cMUT (capacitive micro-machined ultrasonic transducer), advanced piezoelectric materials, energy harvesting devices, wireless sensor network & implants, leadless cardiac pacing system.

An NGUYEN-DINH is author or co-author of several international patents (>20) and scientific publications in the field of ultrasound, transducers, imaging, diagnostic, energy harvesting and wireless sensing systems.

Energy harvesting for locomotion of micro and nano robotics in medical applications

Antoine FERREIRA, Professor

PRISME Laboratory, INSA Centre Val de Loire

antoine.ferreira@insa-cvl.fr

Abstract

Untethered robots miniaturized to the length scale of millimeter and below attract growing attention for the prospect of transforming many aspects of health care and bioengineering. As the robot size goes down to the order of a single cell, previously inaccessible body sites would become available for high-resolution in situ and in vivo manipulations. At such small scales, on-board energy is challenging. At micro-scale, storing, harvesting, and transmitting power is not feasible in the conventional sense we are used to in our macroscopic world. Therefore, a significant effort has been concentrated on various power sources. For micro-robot actuation, wireless power transmission techniques such as inductive powering and radio frequency, microwave radiation, and piezoelectric ultrasound. For nano-robot actuation systems, self-powering techniques including biological bacteria, self-electrophoresis, self-diffusiophoresis, and self-thermophoresis are actually preferred. This talk will provide a state-of-the-art in the energy harvesting to achieve remote or autonomous microrobot actuation for long durations in a wide range of mobility and inside deep regions of the human body.

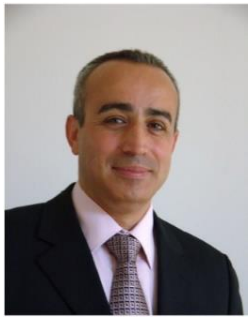

Antoine FERREIRA received his MS and PhD degrees in electrical and mechanical engineering from University of Franche-Comté, Besançon, France, in 1993 and 1996, respectively.
In 1997, he was a Visiting Researcher at the ElectroTechnical Laboratory, Tsukuba, Japan. He is currently a Professor of robotics engineering with Laboratoire PRISME, Institut National des Sciences Appliquées Centre Val de Loire, campus Bourges, France.

His main research interests are focused on the design, modeling and control of micro and nanorobotic systems using active materials, micro-nanomanipulation systems, biological nanosystems, bio-nanorobotics. He has authored three books on micro- and nanorobotics and more than 250 journal and conference papers, as well as book contributions.

A story about micro Stirling design and microfabrication

Fabien FORMOSA, Associate Professor

SYMME Laboratory, Université Savoie Mont-Blanc

fabien.formosa@univ-smb.fr

Abstract

Power MEMS engines are miniaturized thermodynamics machines. Making use of the scale effects and novel fabrication strategies, these complex systems are high potential research subject. However, to date few proofs of concept are available from which some of the main technical constraints are underlined: lack of assembly technologies, lack of technological standard components, non-conventional planar architecture…
Engines, even more micro-engines design call for multi-physics modeling.

In such an uncertain background, how can we achieve conception and sizing taking into account dynamics, fluids, thermodynamics and electromechanical transduction together?

Some answers will be given using the microStirling case study. We will retrace the steps of multiple design from the performance potential, the promising applications and preliminary architecture selections to the modeling strategies attempts.

Fabien Formosa holds a PhD in Mechanical engineering from the "Laboratoire de Mécanique et de Technologie" of the Ecole Normale Supérieure de Cachan (2002). Associate Prof. since 2003, he has been working in the field of power MEMS for 10 years.

His research interest includes vibration energy harvesting, phase change and Stirling micro-engines.

From Amplified Piezoelectric Actuators to high performance and resistant piezo harvester

Luis ORTIZ

CEDRAT TECHNOLGIES

luis.ortiz@cedrat-tec.com

Abstract

APA® Amplified Piezoelectric Actuators from CEDRAT TECHNOLOGIES have been designed to offer a high electro mechanical efficiency and a high resistance to shock and vibration in a compact size. In addition their metallic shell allows for building monolithic structures integrating several functions. All these advantages have been used for delivering operational mechanisms for air, space, optronic and machine-tool fields. They have also been used for making various robust shock or vibration energy harvesters in either proof-mass configurations or bistable buckling structures: This last design invented by SYMME is especially interesting because able to generate more than 2mW with 0.6g at 70Hz.

This presentation will review APA design and limits as well as some applications from mechanisms to harvesters.

Luis Arturo Ortiz Brunicardi is a PhD candidate for the ENHANCED project, awarded Marie Skłodowska-Curie fellowship, Early State Researcher 13, position between CEDRAT TECHNOLOGIES in Grenoble and INSA Lyon, both in located France. His previous experience as an Assistant Professor and Researcher in rational mechanics, linear and nonlinear vibrations, and rotodynamics -Simon Bolivar University, Venezuela- has led him to extend his career towards ways for obtaining energy through the studies of mechanical vibrations.

He did his Bachelor in Mechanical Engineering at the Simon Bolivar University of Venezuela, and extended his studies by obtaining a Master's Degree in Engineering Acoustics and Vibrations, at Valladolid University and Leon University, both of them from Spain.

Vibrational energy harvesting from complex dynamics of pendula

Marian WIERCIGROCH, Professor

Centre for Applied Dynamics Research, University of Aberdeen

m.wiercigroch@abdn.ac.uk

Abstract

Complex dynamics of pendula systems is being analysed with a view of vibrational energy harvesting and vibration isolation. The main focus of the paper is a new concept of energy conversion, where a predominantly vertical oscillatory motion is being converted into rotations by means of a pendulum or pendulums system. The simplest physical configuration of this idea is a parametric pendulum operating in the fully rotational motion. Practically this can be envisaged as a floating structure excited to which pendulums are mounted at their pivots. These vertical oscillations of the structure will generate the pendulums rotational motion. Numerical, analytical and experimental studies have been undertaken on a parametric pendulum, a pendulum excited by a planar motion and a set of four pendula. They suggest the rotational motion is persisting and occurs for a large range of frequencies and excitation amplitudes, which are the main control parameters. These investigations reinforce the viability of this new concept of the energy conversion. In the lecture, I outline this new concept and review the current theoretical and experimental developments. Specifically, I will present the physical and mathematical modelling of a single pendulum, a system comprised of two pendulums and a system of four double pendulums. Details of the experimental rigs and a correlation between the theory and experiments will be given. Detailed numerical and analytical results showing complex dynamical behaviour will be discussed. I will conclude with a brief study on nonlinear control to maintain rotational motion.

Professor Marian Wiercigroch educated in Poland, UK and US holds a prestigious Sixth Century Chair at the University of Aberdeen. He is a founding director of the internationally renowned Centre for Applied Dynamics Research and a Director of Internationalisation for the College of Physical Sciences at the University of Aberdeen.

His area of research is theoretical and experimental nonlinear dynamics, which he applies to various engineering problems such as oil & gas drilling, rotor systems, underwater acoustics, fatigue and vibration isolation and renewable energy harvesting. Professor Wiercigroch has published extensively (over 350 journal and conference papers) and sits on some eight editorial boards of peer review journals. He is an editor of Acta Mechanica Sinica and an Editor-In-Chief of International Journal of Mechanical Sciences. He is a frequent keynote and plenary speaker at major international conferences.

He has received many awards and distinctions including a Senior Fulbright Scholarship in 1994. In 2009 for his contribution to engineering and mathematics he was elected a Fellow of the Royal Society of Edinburgh, the Scotland national academy and in 2013 he was awarded an honorary doctorate, DSc honoris causa, by the Lodz University of Technology, the best Polish University for mechanical engineering.

Energy harvesting for self-powered sensors in hydraulic motors

Sebastian BADER, Assistant Professor

Department of Electronics Design, Mid Sweden University

sebastian.bader@miun.se

Abstract

Similar to many other industrial systems, hydraulic motors are envisioned to undergo a development towards being smart components. Such components should be able to monitor key system parameters in order to detect abnormal conditions, as well as to communicate such findings to other components, systems or the operator. As it can be inconvenient or costly to power the required equipment from the mains or batteries, self-powered sensor systems based on energy harvesting are a desirable alternative. This talk will discuss two approaches of energy harvesting in hydraulic motors: energy harvesting from slow motor rotations based on the variable reluctance principle; and energy harvesting from hydraulic pressure fluctuations based on the piezoelectric effect. For both cases, principles, challenges and solutions will be discussed.

Sebastian Bader is currently an assistant professor at the Department of Electronics Design at the Mid Sweden University, Sundsvall, Sweden. He holds a PhD-degree in electronics and his research and teaching interests lie in the areas of low-energy embedded systems and self-powered sensor systems.

Dr Bader has worked in the area of energy harvesting and self-powered sensor systems for about ten years and published a number of articles in this field in academic journals and international conference proceedings. He has experience in transducer design, modeling and optimization, as well as on energy harvesting system integration. He has, amongst others, worked with energy harvesting from solar irradiation, ambient light, pressure fluctuations, vibrations and low-speed rotations. Besides his interest in transducer optimization, he has a research interest in output power estimations and design methodologies for energy harvesting systems.

Dr Bader is an active reviewer for journals, such as the IEEE Transactions on Industrial Electronics and the IEEE Sensors Journal, and has on several occasions been a TPC member and organizer of conferences, workshops and sessions in the field of energy harvesting.

Piezoelectric energy harvesting with ferroelectric thin films coupled to interdigitated electrodes

Paul MURALT, Professor / Dr. Sc. Nat.

Ecole Polytechnique Fédérale de Lausanne (EPFL)

paul.muralt@epfl.ch

Abstract

Interdigitated electrode (IDE) transducers with ferroelectric thin films offer some different options than the usual parallel plate geometry, and are also different to standard transducers for the excitation and detection of surface acoustic waves, because the local polarization can be aligned to the sense of the electric field. In the direct mode, a homogeneous strain applied to the IDE transducer will lead a constructive accumulation of charges at all electrode pairs. This property is useful for energy harvesting and sensors, particularly also because the capacitance is lower for the same film thickness as compared to the parallel plate case. The talk will describe the present understanding of how such IDE's work, based on analytical and finite element modeling. The application in energy harvesting is discussed in terms of figures of merit, and some device examples are presented

Paul Muralt received a diploma in experimental physics in 1978 at the Swiss Federal Institute of Technology ETH in Zurich. He accomplished his Ph.D. thesis in the field of commensurate-incommensurate phase transitions at the Solid State Laboratory of ETH. In the years 1984 and 1985 he held a post-doctoral position at the IBM Research Laboratory in Zurich where he pioneered the application of scanning tunneling microscopy to surface potential imaging.

In 1987 he joined the Balzers group in Liechtenstein. He specialized in sputter deposition techniques, and managed since 1991 a department for development and applications of Physical Vapor Deposition and PECVD processes. In 1993, he joined the Ceramics Laboratory of EPFL in Lausanne. As group leader for thin films and MEMS devices, he specialized in piezoelectric and pyroelectric MEMS with mostly Pb(Zr,Ti)O3 and AlN thin film. His research interests are in thin film growth in general, and more specifically in property assessment of small ferroelectric structures, in integration issues of ferroelectric and other polar materials, property-microstructure relationships, and applications of polar materials in semiconductor and micro-electro-mechanical devices.

More recently he extended his interests to oxide thin films of ionic conductors. The focus in piezoelectric thin films was directed towards AlN-ScN alloys. He gives lectures in thin film processing, micro fabrication, and surface analysis. He authored or co-authored more than 230 scientific articles. He became Fellow of IEEE in 2013. In 2005, he received an outstanding achievement award at the International Symposium on Integrated Ferroelectrics (ISIF), and in 2016 the B.C. Sawyer Memorial award.

Wireless power transfer: an alternative to harvesting

Paul MITCHESON, Professor

Imperial College London

paul.mitcheson@imperial.ac.uk

Abstract

Energy harvesting has been used in wireless sensor network deployments and has seen enabled several new products. However, the power levels that are possible are low, partly because of technology limitations but also due to fundamental physical limits. An alternative solution in some cases is to use wireless power delivery. In this talk, I will discuss recent work on inductive power delivery, covering magnetic links, transmit and receive-side electronics and control of throughput power. I will conclude with some applications of the technology and show its use in sensor networks via two prototypes.

Paul Mitcheson received the MEng degree in Electrical and Electronic Engineering in 2001 and the PhD degree in 2005 both from Imperial College London.

He is currently Professor of Electrical Energy Conversion in the Control and Power Research Group in the Electrical Engineering Department at Imperial and has research interests in energy harvesting systems, wireless power transfer and power electronics. He is a fellow of the higher education academy and senior member of the IEEE. He was general co-chair of PowerMEMS 2013, held in the Royal Society, London and sits on the Executive Committee of the UK Power Electronics Centre.

Oral Presentations

Research on thermoelectric microgenerators based on Si and SiGe nanowires as thermoelectric material

Inci DONMEZ[1], Marc DOLCET[1], Andrej STRANZ[1], Marc SALLERAS[1], Luis FONSECA[1]*, Gerard GADEA[2], Mercè PACIOS[2], Alex MORATA[2], Albert TARANCON[2]

[1] *IMB-CNM (CSIC,) C/Til·lers s/n Campus UAB, Bellaterra 08193, Spain*

[2] *IREC, Jardins de les Dones de Negre 1, Sant Adrià de Besòs 08930, Barcelona, Spain*

*luis.fonseca@csic.es

***Abstract*—The work of our two groups on all-silicon thermoelectric microgeneration will be reviewed. Our devices use low-dimension silicon as thermoelectric material including SiGe nanowires for the first time. A new redesign leading to a significant reduction in device thermal conductance and electrical resistance has been tested and a route for the integration of a heat exchanger onto it has been attempted. Power densities of a few tens of μW/cm^2 have been achieved.**

I. INTRODUCTION

Thermoelectricity offers a way of converting waste heat into electricity. Since it does not feature moving parts, it is a technology-friendly approach. It can help in waste heat recovery scenarios for improving the energy efficiency of industrial processes or engines, and it can also play a role in energy harvesting, powering sensor nodes where hot surfaces are available in IoT scenarios. For the latter, small size may be a request and microgenerators would be advised. However, standard thermoelectric technology is not prone to automation and miniaturization. In this context, our two groups have collaborated in an approach for devising all-silicon thermoelectric microgenerators [1]. Silicon technology is the archetypical miniaturization technology and it enables device large scale production with economy of scale. Silicon itself is not a good thermoelectric material because of its large thermal conductivity but low-dimension silicon may offer a way of circumventing this handicap [2]

II. SILICON MICROGENERATORS

A. *MEMS suspended platform*

The core of the microgenerator (μTEG) is a planar micromachined device featuring a 1 mm^2 suspended micro-platform, defined by MEMS processes, surrounded by a bulk Si rim as shown in FIGURE 1. The device is built on 500 μm SOI wafers with a 15 μm (110) Si device layer. The platform vertical walls are aligned to (111) planes. Three of the sides contain 1 to 4 trenches that will be filled up with nanowires, and the fourth contains the mechanical supports attaching the platform to the rim and also holding the electrical connections to the platform.

B. *Silicon based Nanowires*

Nanowires (NWs) are grown on the device as a post-process in a CVD reactor following a Vapor-Liquid-Solid mechanism after first have seeded the vertical trenches with gold nanoparticles [3]. NWs grow laterally from (111) surfaces and bridge the gap between the platform and the Si rim along three of the sides. The attachment of the NWs to the Si of the vertical walls is quasi-epitaxial, leading to optimally low electric and thermal contact resistances. Dense arrays of Si and SiGe NWs have been grown following this procedure. When placing the device on a hot surface, a temperature difference will develop between the bulk rim and the platform and will be transduced into a Seebeck voltage by the silicon nanowire arrays.

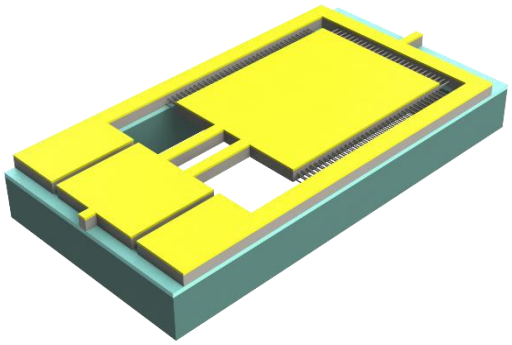

FIGURE 1. SKECTCH OF THE UNIT CELL OF THE THERMOELECTRIC MICROGENERATOR

C. *Thermal and electrical optimization*

The thermal performance of the μTEG, which is linked to the attainable ΔT, has been enhanced by revising its architecture reducing the parasitic thermal losses between the hot and cold ends of the μTEG. This is achieved by replacing the original bulk Si connecting bridges in the fourth side with a thin dielectric membrane. The thermal conductance of the platform has been decreased by 34% with this new arrangement. The electrical performance of the μTEG has been also enhanced by decreasing the device internal resistance. The resistances of the metal collectors have been lowered by redesign, and additional processing steps have been employed to minimize the metal/Si contact resistance. As a result, the device internal resistance has decreased 7 to 20 times compared to the preceding μTEG.

Optimized μTEGs with different number of trenches (T1 to T4) filled with NWs have been characterized to investigate the effect of NW length on the Seebeck voltage and power output.

Even though the highest Seebeck voltage has been obtained for the µTEG with the highest number of trenches (T4), the same trend is not observed for the power output since the electrical resistance of NWs also increases with their effective length (i.e. number of trenches). Maximum power densities of 0.34 and 7.3 µW/cm^2 have been obtained for Si and SiGe NW based µTEGs, respectively, when they are placed under natural convection conditions on a waste heat source of 200 ◦C. SiGe NWs were much more electrically resistive than Si NWs, so the above result is a clear consequence of the much lower thermal conductance of the former.

D. Heat exchanger

One important limitation of µTEGs is the quite moderate temperature difference that develop across the thermoelectric material when placed on a waste heat source due to the small size of the device. The thermal resistance to the ambient of a bare small surface is so high that under natural convection the device is only capturing a minimum fraction of the total temperature difference existing between the heat source and the ambient. Therefore, routes for the integration of a heat exchanger on the proposed planar µTEGs have been designed, simulated and characterized. A simulation result is shown in FIGURE 2.

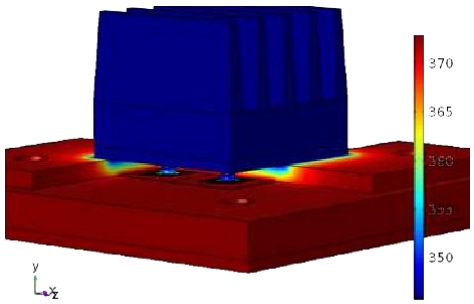

FIGURE 2. SIMULATED TEMPERATURE DISTRIBUTION AFTER MINI HEAT EXCHANGER INTEGRATION

With the integration of the heat exchanger a significant amount of improvement has been observed for all tested µTEGs. Heat exchanger integrated µTEGs were able to harvest 41.2 (Si NWs) and 45.2 (SiGe NWs) when they were placed on a waste heat source of 100 ◦C. This is 100 times more that for similar devices without heat exchanger at the same hot plate temperature. Clearly, the presence of the heat exchanger changes the device internal balance of thermal resistances in a way that makes the thermal conductivity of the thermoelectric material less relevant, while making electrical parameters (Seebeck coefficient and electric resistance) to gain importance.

III. CONCLUSION

The study presented deals with the optimization of a planar thermoelectric microgenerator (µTEG) based on the use of Si and SiGe nanowire arrays as thermoelectric material. Dense arrays of such nanowires (NWs) have been monolithically integrated by means of VLS-CVD into a silicon micromachined device composed of a suspended microplatform and a surrounding bulk Si rim. A previous design has been optimized leading to a significant reduction in device thermal conductance and electrical resistance and, consequently, higher power output. Power output boosted after the integration of a mini heat exchanger on top of the device, featuring values that could help powering IoT nodes.

ACKNOWLEDGMENT

This work has been partially supported by the Spanish project TEC2016-7828-4-C3-1/2-R (AEI/FEDER, UE).

REFERENCES

[1] D. Dávila, A. Tarancón, C. Calaza, M. Salleras, M. Fernández-Regúlez, A. San Paulo, and L. Fonseca, "Monolithically integrated thermoelectric energy harvester based on silicon nanowire arrays for powering micro/nanodevices" *Nanoenergy* 1(6), 812-819, 2012.

[2] A. I. Boukai, Y. Bunimovich, J. Tahir-Kheli, J-K Yu, W. A. Goddard III & J. R. Heath, "Silicon nanowires as efficient thermoelectric materials" *Nature* 451,168–171, 2008.

[3] G. Gadea, A. Morata, J.D. Santos, D. Dávila, C. Calaza, M. Salleras, L. Fonseca, A. Tarancón, "Towards a full integration of vertically aligned silicon nanowires in MEMS using silane as a precursor" *Nanotechnology* 26, 195302 (13pp), 2015

Significant enhancement of bistable energy harvesters bandwidth: subharmonic orbits and their stability robustness

Thomas HUGUET[1,2], Adrien BADEL[2,*], Olivier DRUET[3] and Mickaël LALLART[1,□]

[1]*Laboratoire LGEF, INSA-Lyon, Université de Lyon, Villeurbanne, France*
[2]*Laboratoire SYMME, Université Savoie Mont-Blanc, Annecy, France*
[3]*Institut Camille Jordan, Université Lyon 1, Villeurbanne, France*

* adrien.badel@univ-smb.fr □ mickael.lallart@insa-lyon.fr

***Abstract*— This paper focuses on vibration energy harvesting in order to propose an alternative to batteries for stand-alone, left-behind wireless devices. More particularly, it aims at giving new insights on bistable harvesters already known for their wide bandwidth. Indeed, this study highlights new exploitable steady-state behaviors for bistable generators, namely subharmonic behaviors for which the mass oscillates at a frequency lower than the excitation frequency. Analytical study and associated experimental validation conducted here with a buckled beam show that the use of subharmonic 3 behavior, in addition to the well-known harmonic 1 behavior, leads to a tripling of the useful frequency band compared to the sole exploitation of the harmonic 1 motion. The second part of this study starts from the experimental observations showing that the behaviors are not equally sensitive to disturbances. Some of them are easier to reach and maintain over time thanks to their low sensibility to disturbances. Hence a new analytical criterion is introduced, defined as the stability robustness, giving the sensitivity of the behaviors to external disturbances. For low stability robustness, the behavior will be considered as non-suitable for energy harvesting (as it cannot be secured in steady state) leading to a new description of bistable generators frequency bandwidth. Analytical results following this method show very good agreement with experimental results, hence validating the relevance of the stability robustness criterion.**

I. Introduction

Considering the multiplication of stand-alone, left behind wireless devices, ambient vibration energy harvesting is of significant interest to ensure their energy supply, hence acting as an interesting alternative to batteries. In this goal, linear oscillators have been studied to harvest energy when the ambient vibration spectrum matches with their resonance frequency [1]. However, for more complex or inconstant excitations, their efficiency fast collapse. One of the solutions first studied by Erturk et al. [2] to face this challenge is to introduce nonlinearities in the oscillators. This is the case of bistable generators for instance [3] which present a wider operating frequency bandwidth compared to linear generators and a similar maximal harvested power. Moreover, these generators admit several different coexisting behaviors on certain frequency ranges. Some of them, *i.e.*, subharmonic behaviors, are reached when the mass oscillates at a frequency lower than the excitation frequency (n times lower for subharmonic n behavior). It can be noted that these particular behaviors are not visible with conventional methods used to characterize bistable harvesters (frequency-sweep characterization) which can explain the little attention they received. A few paper mentioned their existence [4-7] but have only been considered as curiosities, and mainly in the pure mechanical domain. Arietta et al. [8] and Syta et al. [9] however reported the energy harvested on some subharmonic orbits but did not investigate their total frequency ranges.

This research proposes to analytically and experimentally investigate such subharmonic behaviors and their help to enhance the global bandwidth of the bistable generator. A new criterion is introduced, namely the stability robustness, to take into account the sensitivity of all the behaviors to external disturbances. A behavior will be defined as robust if its sensitivity to external disturbances is low. This behavior will be considered as suitable for energy harvesting because it is easier to reach and secure over time. Some numerical considerations about robustness have also been reported by Harne et al. [10] with a different approach consisting of adding a white noise to the sinusoidal excitation on the harmonic behavior. The analytical approach proposed here introduces a pulse disturbances and calculate the minimum disturbance leading to instability. This new analytical criterion show very good agreement with experiments, confirming its relevance for realistic bistable harvesters.

II. Subharmonic orbits and their stability robustness

The bistable oscillator considered here is obtained with a buckled beam and a mass at its center as shown in Figure 1. The frame is subjected to the excitation. The transducer linked to this oscillator for energy conversion purposes is composed of a magnet fixed on the mass and a coil fixed on the frame.

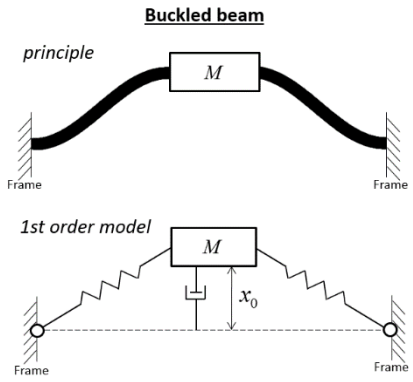

Figure 1: 1 degree of freedom nonlinear model of a common bistable oscillator.

Resolving the governing equation of this energy harvester for a polychromatic response leads to find different steady-state

behaviors: the harmonic 1 orbit and the subharmonic orbits. A stability analysis with small disturbances is conducted on those responses to find all the stable behaviors. Then the new criterion of stability robustness is applied on those stable orbits. The idea is to add a bigger perturbation (*i.e.*, which cannot be linearized anymore) to the stable orbits and to calculate the minimum disturbance needed to destabilize the stable orbits. The stability robustness is then defined by the energy of this minimal disturbance leading to instability normalized by the energy brought by the ambient vibration per period of vibration. A high stability robustness therefore means that the minimum energy needed to destabilize the orbit is high so the orbit has a low sensitivity to external disturbances. Figure 2 shows the analytical results with the new criterion of stability robustness and the comparison with experimental results conducted in this study.

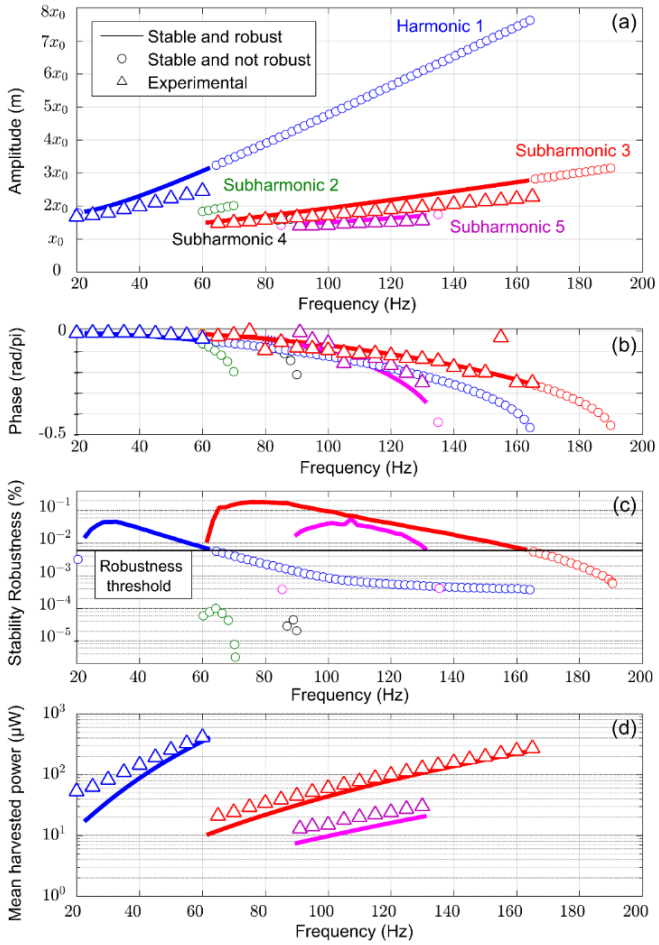

Figure 2: Bistable harvester experimental and analytical spectra showing stable orbits for an excitation amplitude of 5 m/s² including the new criterion of stability robustness indicating their sensitivity to disturbances: (a) amplitude, (b) phase of the excitation displacement when the position of the mass reaches a maximum, (c) stability robustness and (d) average harvested power.

A threshold is experimentally defined for the stability robustness under which the orbits will be considered as not robust enough for energy harvesting because too difficult to maintain over time. The definition of this threshold, unique for all the behaviors, leads to a better match between theory and experiment for both harmonic 1 and all the subharmonic behaviors.

III. Discussion and Conclusion

The analytical results shows good agreement with the experimental results and confirms 2 major new features for bistable energy harvesters introduced in this study: (i) the subharmonics behaviors and more particularly subharmonic 3 behavior leads, in addition to the well-known harmonic 1 behavior, to an increase by 180 % of the frequency range on which the generator harvest more than 100 µW compared to the sole exploitation of the harmonic 1 motion; (ii) the different behaviors have different sensibilities to external disturbances (*i.e.*, different stability robustness) as suggested by the experimental observations. The stability robustness criterion appears to be relevant to characterize bistable generators as the experimental and analytical results agreed only when it is added.

Acknowledgment

The authors acknowledge the support of Région Auvergne-Rhône-Alpes through the ARC 4 Energies program.

References

[1] Williams CB, Yates RB, "Analysis Of A Micro-electric Generator For Microsystems", Sensors and Actuators A: Physical, 52, 8–11 (1996).

[2] Erturk A, Hoffmann J, Inman DJ, "A piezomagnetoelastic structure for broadband vibration energy harvesting", Applied Physics Letters, 94(25), 128-130 (2009).

[3] Harne R.L, Wang KW, "A review of the recent research on vibration energy harvesting via bistable systems", Smart Materials and Structures, 22, 23001 (2013).

[4] Moon FC, Shaw SW, "Chaotic vibrations of a beam with non-linear boundary conditions", Non-Linear Mechanics, 18(6), 465-477 (1983).

[5] Emam SA, Nayfeh AH, "Nonlinear Responses of Buckled Beams to Subharmonic-Resonance Excitations", Nonlinear Dynamics, 35, 105-122 (2004).

[6] Arrieta AF, Neild SA, Wagg DJ, "Nonlinear dynamic response and modeling of a bi-stable composite plate for applications to adaptive structures", Nonlinear Dynamics, 58(1-2), 259-272 (2009).

[7] Mahmoodi SN, Jalili N, Ahmadian M, "Subharmonics analysis of nonlinear flexural vibrations of piezoelectrically actuated microcantilevers", Nonlinear Dynamics, 59(3), 397-409 (2010).

[8] Arrieta AF, Hagedorn P, Erturk A, Inman DJ, "A piezoelectric bistable plate for nonlinear broadband energy harvesting", Applied Physics Letters, 97(10), 104102 (2010).

[9] Syta A, Litak G, Friswell MI, Adhikari S, "Multiple solutions and corresponding power output of nonlinear piezoelectric energy harvester", The European Physical Journal B, 89-99 (2016).

[10] Harne RL, Dai Q, "Characterizing the robustness and susceptibility of steady-state dynamics in post-buckled structures to stochastic perturbations", Journal of Sound and Vibration, (2017).

Short Circuit Synchronized Electric Charge Extraction (SC-SECE): a tunable interface for wideband vibration energy harvesting

Adrien MOREL[1,2*], Adrien BADEL[2], Pierre GASNIER[1], David GIBUS[1,2], Gaël PILLONNET[1]
[1] Univ. Grenoble Alpes, CEA, LETI, MINATEC, F-38000 Grenoble, France
[2] Univ. Savoie Mont Blanc, SYMME, F-74000 Annecy, France
*adrien.morel@cea.fr

***Abstract*— In this paper, we present a new harvesting interface, called Short Circuit Synchronous Electric Charge Extraction (SC-SECE). The SC-SECE strategy includes a tunable short-circuit time thanks to two tuning parameters, ϕ_S and $\Delta\phi$. ϕ_S stands for the phase between the mechanical displacement extrema and the energy harvesting event. $\Delta\phi$, stands for the angular time spent in the short-circuit phase. The theoretical analysis and modelling of this short-circuit influences are derived in this paper. When associated with highly coupled harvesters, it is shown that both the harvested power and bandwidth are greatly improved. These results have been numerically validated and they demonstrate the potential of this strategy for extending the bandwidth of piezoelectric vibration energy harvesters.**

I. INTRODUCTION

In order to make small systems and sensors autonomous scavenging ambient energy has been widely investigated in the last two decades as an alternative to batteries. Piezoelectric energy harvesters (PEH) are of particular interest in closed confined environments, where there are few solar radiations and thermal gradients.

In order to maximize the energy harvested from piezoelectric harvesters, the electrical interface is a key point to consider. Several non-linear synchronous strategies, such as Synchronous Electric Charge Extraction (SECE) and Synchronized Switch Harvesting on Inductance (SSHI) have been introduced [1], and have been implemented using discrete components [2,3] or dedicated ASIC [4,5]. Those strategies exhibit high performance for lowly coupled and/or highly damped piezoelectric harvesters. However, for highly coupled and/or lowly damped piezoelectric harvesters, these strategies may overdamp the mechanical resonator, leading to low performances. To face this challenge, researchers started to propose new tunable strategies inducing lower damping [6], and even tuning the PEH resonant frequency thanks to the important influences of the electrical interface on the mechanical resonator [7].

In this paper, we introduce a strategy based on the SECE interface, which introduces a tunable short-circuit phase. As detailed extensively in this paper, this short-circuit allows to reduce the damping induced by the electrical interface. Furthermore, for high coupling harvesters, it allows to tune the PEH resonant frequency, leading to an enhanced harvesting bandwidth.

II. THEORETICAL MODELLING

A. Linear PEH modelling

A linear PEH under a periodic excitation can usually be modelled by a system of linear differential equations, given by (1).

$$\begin{cases} M\ddot{x} + D\dot{x} + K_{sc}x + \alpha v_p = -\mathrm{F} = -M\ddot{y} \\ i = \alpha\dot{x} - C_p\dot{v_p} \\ x(t) = X_m\cos(\theta) = X_m\cos(\omega t) \end{cases} \quad (1)$$

where y, F and x stand for the ambient displacement, the force applied on the PEH, and the tip mass displacement, respectively. M, K_{sc}, D, C_p and α stand for the equivalent mass of the PEH, its short-circuited stiffness, its mechanical damping, the capacitance of the piezoelectric material, and the piezoelectric force coefficient, respectively. Fig.1 shows the electrical circuit modelling these equations.

B. Expression of the piezoelectric voltage

In order to find the harvested power expression, we have to solve (1) and find the mechanical displacement magnitude X_m. As $\mathrm{v_p}$ is a variable in (1), finding a linear expression of v_p would greatly simplify the calculations. The piezoelectric harvester is either working in open or short-circuit, as illustrated in Fig.2. Thus, the piezoelectric voltage during a semi-period of vibration is given by (2).

$$\mathrm{v_p}(\theta) = \begin{cases} \dfrac{\alpha}{C_p}\displaystyle\int_{\phi_s+\Delta\phi-\pi}^{\theta} \dot{x}(\theta)\mathrm{d}\theta\,, \forall\theta \in]\phi_s + \Delta\phi - \pi, \phi_s] \\ 0, \forall\theta \in]\phi_s, \phi_s + \Delta\phi] \end{cases} \quad (2)$$

$\phi_s \in [0, \pi]$ corresponds to the angular phase between the harvesting process and the precedent displacement extremum. $\Delta\phi \in [0, \pi]$ stands for the angular time spent in the short-circuit phase. A system implementing this extraction strategy is depicted in Fig.1, and an example of the voltage waveform is shown in Fig.2. As expressed by (2), $\mathrm{v_p}$ is not sinusoidal. Only the first harmonic of $\mathrm{v_p}$ is considered in order to analytically solve (1) while simplifying the calculations.

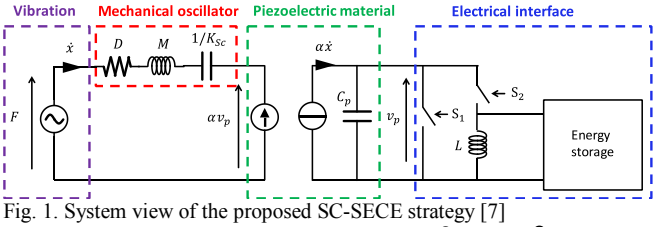

Fig. 1. System view of the proposed SC-SECE strategy [7]

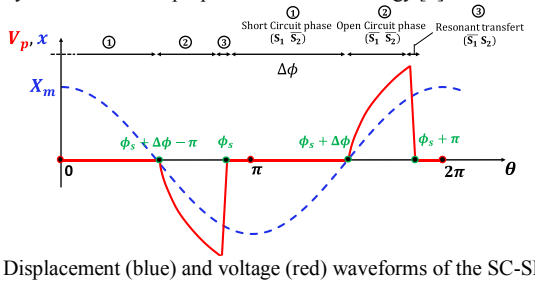

Fig. 2. Displacement (blue) and voltage (red) waveforms of the SC-SECE

From (2), we eventually find the expression of the Fourier series coefficients a_1 and b_1 associated with v_p:

$$\begin{cases} a_1 = \dfrac{\alpha X_m}{\pi C_p}\left[\pi - \Delta\phi + \dfrac{\sin(2\phi_s + 2\Delta\phi)}{2} + \dfrac{\sin(2\phi_s)}{2} \right. \\ \qquad \left. +2\cos(\phi_s + \Delta\phi)\sin(\phi_s)\right] \\ b_1 = -\dfrac{\alpha X_m}{\pi C_p}[\cos\phi_S + \cos(\phi_S + \Delta\phi)]^2 \end{cases} \quad (3)$$

Hence, the first harmonic of v_p, $\underline{v_{p_1}}$, is expressed by (4).

$$\underline{v_{p_1}} = \underline{x}\left(\frac{a_1}{X_m} - j\frac{b_1}{X_m}\right) = \underline{x}(a_1^* - jb_1^*) \quad (4)$$

where $\underline{x}$ is the mechanical displacement in the Fourier domain. a_1^* and b_1^* are the first Fourier coefficients a_1 and b_1 divided by the displacement amplitude, X_m.

C. Expression of the harvested power

Due to the filtering effect of the resonator, we consider that the first voltage harmonic may impact the PEH dynamics. We can hence substitute the voltage expression (4) in (1) to find the displacement amplitude. Solving (1) in the Fourier domain, the mechanical displacement amplitude can be expressed by (5).

$$X_m = \frac{|M\ddot{y}|}{\sqrt{(K_{sc} - M\omega^2 + \alpha a_1^*)^2 + (\omega D + \alpha b_1^*)^2}} \quad (5)$$

For each vibration's semi-period, the harvested energy is the one stored in C_p when $\theta = \phi_s$. Thus, from (1), we can derive the harvested power expression:

$$P_{harv} = \frac{\omega\alpha^2}{2\pi C_p} X_m^2[\cos(\phi_s + \Delta\phi) + \cos(\phi_s)]^2 \quad (6)$$

This power P_{harv}, divided by the maximum harvestable power $P_{max} = D^{-1}|M\ddot{y}|^2/8$ [6] has been computed in Figure 3 with optimized parameters $(\phi_S, \Delta\phi)$ as a function of the normalized vibration frequency $\Omega_m = \omega/\omega_0$ with three normalized squared coupling coefficients k_m^2 and a mechanical quality factor of Q_m=25. These normalized parameters have been extensively described in [6,7]. We can observe that the bandwidth gain becomes more important as k_m^2 is increased.

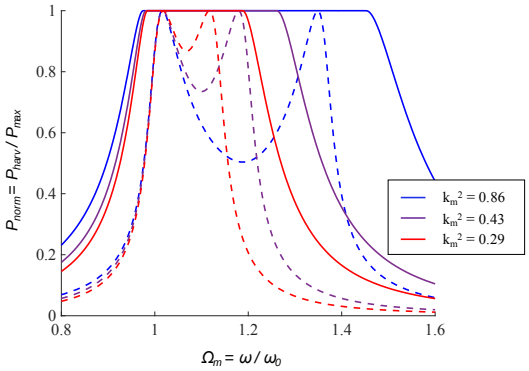

Fig. 3. Frequency responses of highly coupled PEH with optimized resistive loads (dashed lines) and the proposed SC-SECE interface (straight lines)

III. Conclusion

In this paper, we present a theoretical analysis of the SC-SECE strategy. Numerical results show that this strategy could both enhance the harvested power and the harvesting bandwidth of highly coupled PEH. Experiments confirming these theoretical predictions will be presented during the conference.

References

[1] E. Lefeuvre *et al.*, "A comparison between several vibration-powered piezoelectric generators for standalone systems", Sensors and Actuators A: Physical, vol. 126, no. 2, pp. 405–416, Feb. 2006.

[2] G. Shi *et al.*, "An efficient self powered synchronous electric charge extraction interface circuit for piezoelectric energy harvesting systems" Journal of Intelligent Material Systems and Structures, vol. 27, no. 16, pp. 2160–2178, Sep. 2016.

[3] Y. Wu *et al.*, "Piezoelectric vibration energy harvesting by optimized synchronous electric charge extraction" Journal of Intelligent Material Systems and Structures 24(12): 1445–1458, 2012.

[4] A. Quelen *et al.*, "A 30nA Quiescent 80nW to 14mW Power Range Shock-Optimized SECE-based Piezoelectric Harvesting Interface with 420% Harvested Energy Improvement", IEEE International Solid State Circuit Conference, 2018.

[5] T. Hehn *et al.*, "A Fully Autonomous Integrated Interface Circuit for Piezoelectric Harvesters", IEEE Journal of Solid-State Circuits, vol. 47, no. 9, pp. 2185–2198, Sep. 2012.

[6] A. Morel *et al.*, "Regenerative synchronous electrical charge extraction for highly coupled piezoelectric generators", *IEEE Midwest symposium of circuits and systems (MWSCAS) 2017*, 2017.

[7] A. Morel *et al.*, "Short Circuit Synchronous Electric Charge Extraction(SC-SECE) Strategy for Wideband Vibration Energy Harvesting", *IEEE International Symposium of Circuits And Systems (ISCAS) 2018*, 2018.

Flexible piezoelectric micro-generator with interdigitated electrodes for energy harvesting

J. Le Scornec[1,*] B. Guiffard[1], R. Seveno[1], and V. Le Cam[2]

[1] *IETR UMR CNRS 6164, UBL University, University of Nantes, 2 rue de la Houssinière, 44322 Nantes Cedex 3, France*

[2] *IFSTTAR, COSYS, SII, Route de Bouaye, 44344 Bouguenais, France*

*corresponding author: julien.le-scornec@etu.univ-nantes.fr

***Abstract*—This research work deals with the development of high performance flexible piezoelectric microgenerators, able to harvest low frequency (<10 Hz) mechanical energy from wind flows, for instance. Such hybrid microsystems are made of lead zirconate titanate (PZT) films easily transferred onto an insulating polymeric substrate. In order to optimize the output voltage and harvested power, an interdigitated electrode structure is adopted. By manually subjecting the micro device to a pseudo-sinusoidal excitation of about 2 Hz, an output voltage of 7.7 V and a power of 220 nW are obtained, using a resistive load of 100 MΩ. Owing to the IDE design, the optimum load resistance is found to be about 71 GΩ, yielding calculated huge maximum voltage values (6.2 kV) and power (137 µW). These results make the studied micro-generators promising candidates to electrically power miniature, autonomous wireless electronic micro devices, such as distributed sensor networks**

I. INTRODUCTION

Nowadays, the energy harvesting from ambient and renewable sources is a major objective to make autonomous wireless self-powered microsystems, such as sensor networks. In this sense, the objective is to replace or at least reload batteries necessary for the power supply of these sensors which are sometimes spread by hundreds on great distances, confronted with a severe environment or simply difficult to access. Piezoelectric energy harvesting devices called microgenerators have been proposed and developed by many researchers, in order to harvest electrical energy from ambient mechanical energies created by natural sources or from human movements.

Recently, researchers have focused on the development of a low-cost manufacturing process by producing piezoelectric structures on flexible substrates, which preserves the lightness of the micro-generator and thus makes it sensitive to air flow. For instance, thin films of lead zirconate titanate (PZT) have been prepared using a chemical deposition process on a flexible metal substrate: a commercial aluminum foil (Al) with a thickness less than 30 µm have been used [1].

To obtain a high electrical energy density, the interdigital electrodes (IDE structure (FIGURE 1-B) is more efficient than the metal-insulator-metal (MIM) design (FIGURE 1-A) because it reduces the linear capacitance of the generator. Besides, it has the advantage of working in the 33 (longitudinal) piezoelectric mode with piezoelectric coefficients ~3 times greater than in 31 (transverse) mode. To realize this structure, PZT films must be separated from the aluminium ground plane before the realization of IDE. The solution proposed by Dufay and al [2] is to use polymer materials as PZT substrates which present a flexibility and a natural insulation. However, the major drawback with these soft polymers is their low resistance against thermal treatment which does not allow the direct drop-off of PZT. Park and al. [3] successfully transferred a PZT thin film onto a polymer substrate by using the laser lift-off (LLO) process. However, this method is expensive and could be difficult to transfer to the industry.

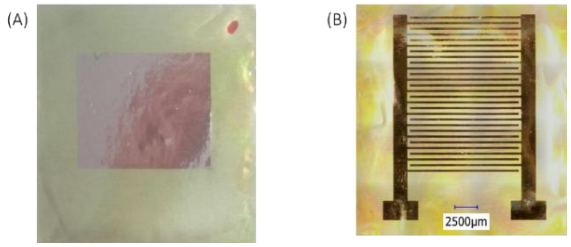

FIGURE 1. PHOTO OF THE (A) MIM AND (B) IDE STRUCTURE

In this paper, we present the fabrication and the mechanical energy harvesting performances of PZT thin film/polymer bilayers with an interdigital electrode structure. This latter design has been realized using photolithography techniques followed by lift-off process.

II. EXPERIMENTAL PROCEDURE

PZT thin films were prepared by a sol-gel process. Lead acetate trihydrate $[Pb(CH_3CO_2)_2,3H_2O]$ with 30% molar excess is dissolved in acetic acid. An excess of lead is used in order to compensate the PbO loss during the annealing treatment due to the formation of volatile PbO. Zirconium $[Zr(O(CH_2)_2CH_3)_4]$ and titanate $[Ti((CH_3)_2CHO)_4]$ n-propoxides are then added to the solution in order to obtain the $Pb(Zr_{0.57}\ Ti_{0.43})O_3$ composition. In addition, Ethylene glycol $[HO\text{-}CH_2\text{-}CH_2OH]$ is used to reduce the appearance of cracks during the crystallization of the films.

The precursor solution was deposited onto the commercial aluminium foil at 6000 rpm during 20 s by a multi-step spin coating process and each layer was annealed during 2 min in a preheated open air furnace at 650°C. The deposition and annealing steps are repeated 10 times in order to get an overall thickness of the PZT film of 3 µm.

FIGURE 2 illustrates the transfer of PZT to a flexible polymer substrate -125 µm thick polyethylene terephthalate (PET)-and the realization of the interdigitated electrodes. The interdigitated electrodes (IDE, 170 nm-thick Al) with a finger length of 1.5 cm, an electrode width of 200 µm, an inter-electrode gap of 400 µm, and 14 finger pairs were deposited onto PZT thin films using photolithography and lift-off

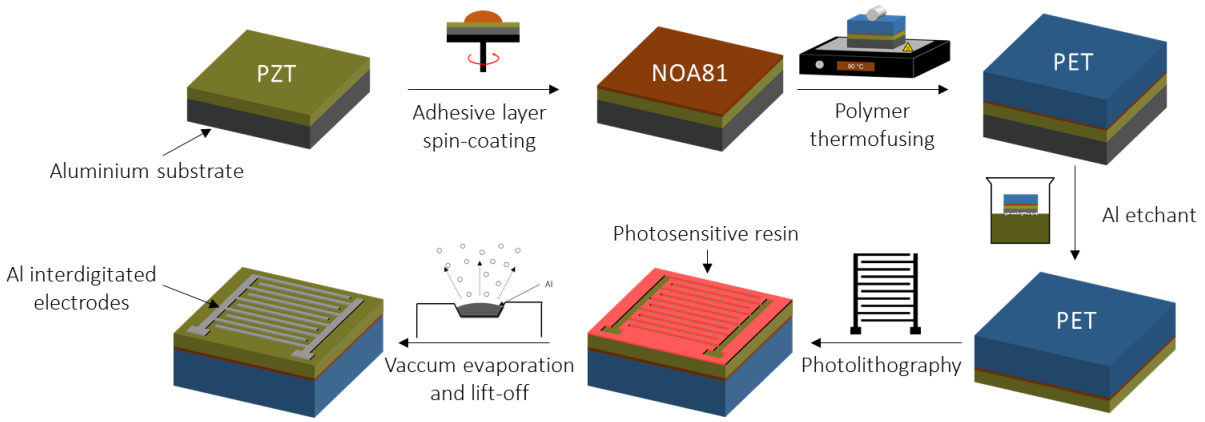

FIGURE 2. SCHEMATIC ILLUSTRATION OF THE PROCESS OF PZT TRANSFER AND LIFT-OFF

procedures. Finally, thin Cu wires were fixed onto metal terminals by conductive paste and a poling process was performed at 100 °C onto a hot-plate by under an applied DC electric field of 50 kV/cm for approximately 2 hours.

III. RESULTS AND DISCUSSION

The voltage across a load resistance in parallel with the micro-generator for a pseudo-sinusoidal mechanical excitation of approximately 2 Hz applied manually, is recorded using an oscilloscope (see FIGURE 3). The sample has a very low capacitance around 1.3 pF (static capacitance) and the optimal load resistance is close to 71 GΩ.

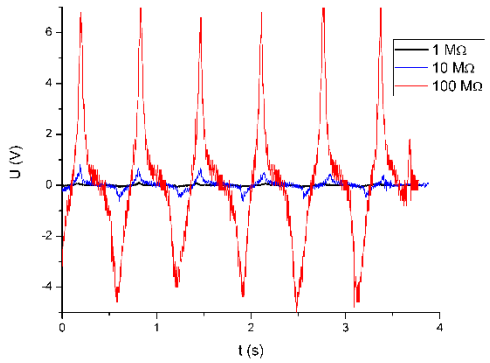

FIGURE 3. TIME DEPENDENCE OF THE MEASURED OUTPUT VOLTAGE FOR LOAD RESISTANCES OF 1 MΩ, 10 MΩ AND 100 MΩ.

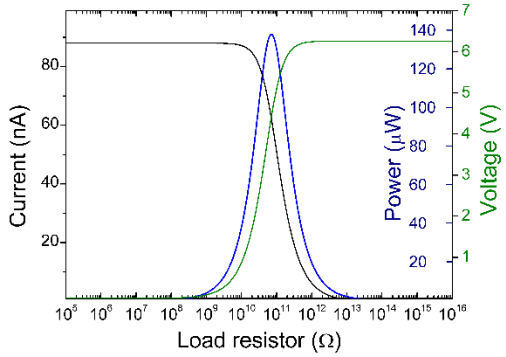

FIGURE 4. THEORETICAL VOLTAGE, CURRENT AND POWER DELIVERED BY MICRO-GENERATOR WITH AN MECHANICAL EXCITATION AT ~2 HZ

FIGURE 4 shows the calculated voltage, the current and the power as a function of the load resistance. In theory, at the optimum load resistance the open circuit voltage may reach up to 6.2 kV and the maximum power of 137 µW.

As expected, it is found a large dependence of the maximum output voltage upon the load resistance value (R). For R= 100 MΩ, an output voltage of 7.7 V is obtained, yielding an harvested power of 220 nW.

IV. CONCLUSION

In this work, the interdigitated electrodes structure was successfully realized on a PZT thin film/polymer film bilayer using lift-off process. The micro-generator may work at very low frequencies (less than 2 Hz) and theoretically provide an output voltage (in open-circuit condition) of about 6.2 kV. Moreover, the use of the IDE structure instead of the MIM structure would lead to the maximum power of 137 µW against 18 nW [4] for the MIM structure. Besides, this electrode configuration makes the piezoelectric generator operate in more efficient longitudinal mode, instead of transverse mode (d_{33}>d_{31}). Ongoing investigations concern output current and voltage measurements using higher resistive loads to confirm the expected theoretical large values. Besides, in order to increase the output current, future work will also be devoted to the improvement of the piezoelectric properties of the PZT with IDE by optimizing the poling procedure.

REFERENCES

[1] R. Seveno et D. Averty, « Ultra light tunable capacitor based on PZT thin film deposited onto aluminium foil », *J. Sol-Gel Sci. Technol.*, vol. 68, n° 2, p. 175‑179, nov. 2013.

[2] T. Dufay, R. Seveno, B. Guiffard, et J. C. Thomas, « New process for transferring PZT thin film onto polymer substrate », in *2016 Joint IEEE International Symposium on the Applications of Ferroelectrics, European Conference on Application of Polar Dielectrics, and Piezoelectric Force Microscopy Workshop (ISAF/ECAPD/PFM)*, 2016, p. 1‑4.

[3] K.-I. Park *et al.*, « Highly-Efficient, Flexible Piezoelectric PZT Thin Film Nanogenerator on Plastic Substrates », *Adv. Mater.*, vol. 26, n° 16, p. 2514‑2520, avr. 2014.

[4] R. Seveno, J. Carbajo, T. Dufay, B. Guiffard, et J. C. Thomas, « Flexible PET/Al/PZT/Al/PET multi-layered composite for low frequency energy harvesting », *J. Phys. Appl. Phys.*, vol. 50, n° 16, p. 165502, 2017.

Use of 3D printing to build self-powered triboelectric sensors

Rubiayet HAQUE[1,*], Olivier CHANDRAN[2], Sébastien LANI[2] and Danick BRIAND[1]

[1] *École Polytechnique Fédérale de Lausanne, Soft Transducers Laboratory, Rue de la Maladière, 2002 Neuchâtel, Switzerland*

[2] *CSEM, Rue Jaquet-Droz 1, 2002 Neuchâtel, Switzerland*

*rubaiyet.haquel@epfl.ch

***Abstract*— Triboelectric sensing and energy harvesting module using 3D printed materials have been developed. The functional triboelectric layers and spring are prepared using 3D printing method. The device shows potential of determining mechanical deformation and generates electrical signal in response, and exhibits sensitivity towards changing operational frequencies and forces. Under hand tapping condition at 1.0±0.1 Hz, the device provides optimum average power of 28.7 μW for the load resistance (R_L) of 273.7 MΩ, which corresponds to the average power density of 4.6 μW/cm². Ultimately, 3D printing will enable the complete digital manufacturing of triboelectric cells embedded in objects.**

I. Introduction

In recent time, harvesting mechanical energy has emerged as a promising alternative to non-renewable energy sources. Several triboelectric generators have been reported for mechanical energy harvesting and sensing applications [1]–[4]. Different materials and fabrication methods were utilized to develop these devices. Most of these devices involve multiple fabrication steps and require assembling. With the ultimate goal of eliminating assembly steps, digital printing technique was introduced in this work that is capable of 3D manufacturing of different functional materials [5], [6].

Herein, we present investigations on different 3D printed materials as functional triboelectric layer, and the development of triboelectric device, having simple vertical-contact separation design, made of all 3D printed active layers and spring structure. Responses of the devices were studied under different mechanical stimuli.

II. Experiments

A. Process flow

At first, 3D printing of acrylonitrile butadiene styrene (ABS-M30), polyamide (PA 2200), polydimethylsiloxane (PDMS-KER-4690, from Shin-Etsu) and TangoBlack (TB) was performed using STRATASYS Fortus 400mc, EOSINT P 395, Aether 1 and OBJET Connex 500 3D printing systems. The spring structure for the vertical mode device is also 3D printed using PA materials as it gave structural strength and flexibility. Table 1 listed the physical parameters of the 3D printed parts. Composites made of dispersing Ketjenblack EC-600JD conductive carbon black pellets from Akzo-Nobel into PDMS and polyurethane (PU) elastomers were film casted as electrode layers. Triboelectric properties of the 3D printed layers were examined and the best materials combination having opposite charge affinity was identified. Finally, the triboelectric device was fabricated by assembling best pair of triboelectric layers facing each other, having active area of 6.5 cm², separated by the 3D printed spring using PDMS based adhesive and then wiring was then performed (Figure 1).

TABLE 1. Physical parameter of 3D printed materials and spring

Physical parameters	
Sprint height [mm]	5
Thickness of ABS layer [μm]	250
Thickness of PA layer [μm]	500
Thickness of PDMS layer [μm]	160
Thickness of Tango black layer [μm]	250

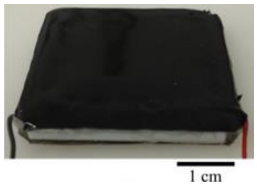

FIGURE 1. Photographs of the 3D printed materials based (a) spring structure and (b) triboelectric tactile device.

B. Characterizations

The triboelectric characterizations were performed by custom made linear motor based mechanical vibrator, which allows to control the gaps, applied force and operational frequencies. The responses were recorded over wide range of load resistances (R_L) using the oscilloscope. While characterizing 3D printed layers, 3×3 cm² layers were mounted on the holder as presented in Figure 2(a). For triboelectric device characterization, 2×2 cm² piston was used (Figure 2(b)).

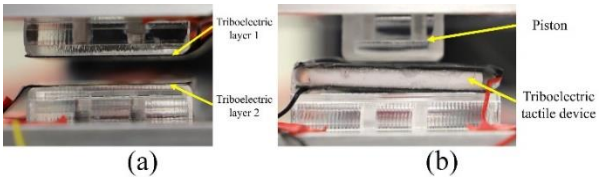

FIGURE 2. Photographs of the 3D printed materials based (a) spring structure and (b) triboelectric tactile device.

III. Results and Discussions

A. Evaluation of 3D printed materials

Figure 3 presents the average power outputs of different pair of 3D printed layers with respect to the load resistances (R_L).

Results showed that amongst the tested 3D printed materials, the pair of TB and PDMS demonstrated the best triboelectric responses. For the optimum R_L of 76.0 MΩ, the TB and PDMS pair generated the optimum average power response of 33.5 µW (optimum average power density of 3.7 µW/cm^2). Therefore, for the device fabrication 3D printed TB and PDMS layers were used as functional layers.

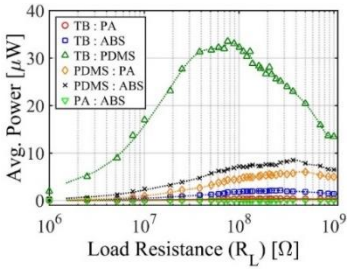

FIGURE 3. AVERAGE POWER OUTPUTS WITH RESPECT TO R_L FOR THE APPLIED FORCE OF 20 N AND SPACING OF 5 MM AT OPERATION FREQUENCY OF 2 HZ.

B. Performances of triboelectric sensor

Once the best material pairs were detected, the triboelectric device, having simple vertical-contact separation mode design (Figure 4), were developed. The experiment showed that the device was enabled to detect the variation of operational frequencies and applied forces (Figure 5).

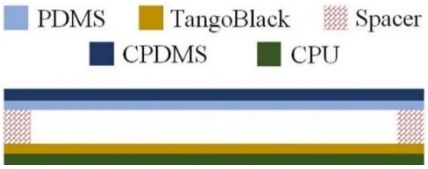

FIGURE 4. SCHEMATIC DIAGRAM OF THE DESIGN OF 3D PRINTED MATERIALS BASED TRIBOELECTRIC DEVICE.

The device exhibited enhanced output responses with the increasing operational frequency. Under constant applied force of 20 N, the device generated optimum average power outputs of 6.3 µW (for optimum R_L of 273.7 MΩ), 29.2 µW (for optimum R_L of 273.7 MΩ) and 62.5 µW (for optimum R_L of101.0 MΩ) for the operational frequencies of 1 Hz, 2 Hz and 5 Hz, respectively, as presented in **Figure 5**. In addition, for the fixed operational frequency of 2 Hz, the voltage (rms value) of 264.4 V was obtained and the optimum average power of 29.2 µW was observed for the optimum R_L of 273.7 MΩ, and the optimum average power of 48.9 µW was generated for the optimum R_L of 101.0 MΩ for the applied force of 40 N.

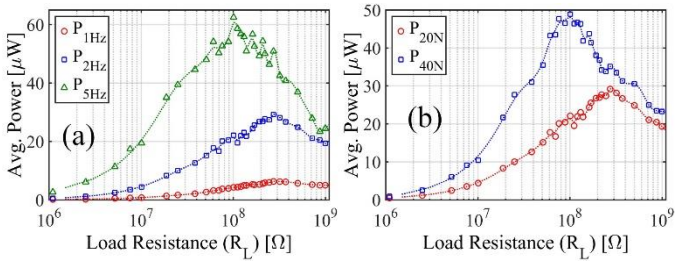

FIGURE 5. AVERAGE POWER OUTPUTS OF THE TRIBOELECTRIC DEVICE WITH RESPECT TO R_L FOR THE ACTIVE SURFACE AREA OF 4 CM^2, (A) DIFFERENT OPERATIONAL FREQUENCIES AND (B) APPLIED FORCE.

Eventually, the device was tested under hand tapping condition for tapping frequency of 1.0±0.1 Hz and 2.0±0.1 Hz for the R_L of 273.7 MΩ. For the tapping frequency of 1±0.05 Hz, peak-to-peak voltage (V_{pp}) of 771.3 V (rms value of 88.7 V) was generated, which corresponded to the peak power (P_P) of 0.6 mW (average power of 28.7 µW) and peak power density of 97.6 µW/cm^2 (average power density of 4.6 µW/cm^2). While tapping at 2±0.05 Hz, the V_{pp} of 1020.5 V over the R_L of 273.7 MΩ and the P_P of 1.2 mW (average power of 98.5 µW) was obtained. Figure 6 illustrates the average power outputs of the device for the hand tapping over the R_L of 273.7 MΩ.

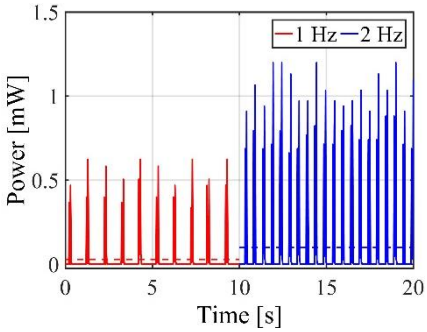

FIGURE 6. OUTPUT POWER SENSING RESPONSES OF TRIBOELECTRIC DEVICE UNDER HAND TAPPING FOR R_L OF 273.7 MΩ (AREA OF 6.5 CM^2).

IV. CONCLUSION

We have presented a triboelectric device that consists of 3D printed TangoBlack and PDMS materials functional triboelectric layers and polyamide spring structure. The devices operated in a simple vertical-contact separation mode and acted as self-powered sensor. We are now working on the complete printing of the triboelectric cells. Such devices can also be employed as energy harvesting device where charge can be stored in capacitor to power energy efficient electronics.

ACKNOWLEDGMENT

The authors would like to acknowledge Swiss National Science Foundation (SNSF) and NanoTera.ch for the funding and support of this work within the framework of BodyPowerSenSE project. CSEM is grateful to Aether© for the donation of the Aether 1 printing system.

REFERENCES

[1] R. I. Haque, P.-A. Farine, and D. Briand, "Soft triboelectric generators by use of cost-effective elastomers and simple casting process," *Sensors and Actuators A: Physical*, vol. 271, pp. 88–95, Mar. 2018.

[2] Feng-Ru Fan, Zhong-Qun Tian, and Zhong Lin Wang, "Flexible Triboelectric Generator," *Nano Energy*, vol. 1, no. 2, pp. 328–334, Mar. 2012.

[3] H. Liu *et al.*, "Large-Scale and Flexible Self-Powered Triboelectric Tactile Sensing Array for Sensitive Robot Skin," *Polymers*, vol. 9, no. 11, p. 586, Nov. 2017.

[4] Ya Yang *et al.*, "Human Skin Based Triboelectric Nanogenerators for Harvesting Biomechanical Energy and as Self-Powered Active Tactile Sensor System," *ACS Nano*, vol. 7, no. 10, pp. 9213–9222, Oct. 2013.

[5] R. Bogue, "3D printing: an emerging technology for sensor fabrication," *Sensor Review*, vol. 36, no. 4, pp. 333–338, Sep. 2016.

[6] Y. Ni, R. Ji, K. Long, T. Bu, K. Chen, and S. Zhuang, "A review of 3D-printed sensors," *Applied Spectroscopy Reviews*, vol. 52, no. 7, pp. 623–652, Aug. 2017.

Modeling and design of highly-coupled piezoelectric energy harvesters for broadband applications

David GIBUS[1,*], Pierre GASNIER[1], Adrien MOREL[12], Sebastien BOISSEAU[1] and Adrien BADEL[2]

[1] *Univ. Grenoble Alpes, CEA, LETI, MINATEC, F-38000 Grenoble, France*

[2] *Univ. Savoie Mont Blanc, SYMME, 74000 Annecy, France*

* david.gibus@cea.fr

***Abstract*— This paper reports on a method to model and design highly-coupled piezoelectric energy harvesters. Such devices are necessary to improve the frequency bandwidth when specific non-linear electrical techniques are used. A 2-degree of freedom (2-DOF) analytical model for cantilever with long tip mass is proposed and is in close agreement with finite element analyzes for the first resonance mode. This model is used to maximize the global electromechanical coupling for a given PMN-PT patch. The proposed structure demonstrates a strong coupling coefficient (k^2=39.7% for the 1st mode) which allows to considerably increase the frequency bandwidth.**

I. INTRODUCTION

During the last decade, there has been a certain enthusiasm for finding ways to replace or complement batteries in order to power wireless sensor nodes. Energy scavenging is a promising alternative to batteries as it allows to use the ambient available energy to make sensors autonomous and self-powered. Vibrations energy harvesting is of particular interest in places with few solar radiations or low thermal gradients.

In order to harvest vibrations, researchers developed electromechanical systems based on mechanical resonators. The energy transferred in such oscillators is relatively important as long as the input vibration frequency remains close to the natural frequency of the resonator. However, one of the main challenge is to harvest enough energy when the vibration frequency gets farther from the resonant frequency.

Recently, new methods have been proposed to enlarge the harvesting bandwidth, and are based on the influence of the electrical interface on the mechanical resonator dynamics. In order to maximize these influences, it has been shown that it is necessary to use highly-coupled piezoelectric generators [1-3]. One of these generators, which has been introduced by [1], is a cantilever-based piezoelectric harvester with a long tip mass and has a coupling coefficient k^2 equal to 53%. Nevertheless, this work did not propose any mechanical modeling or design method. Furthermore, 1-degree of freedom models based on static assumptions used in literature for piezoelectric energy harvesters do not give accurate results when such a mass is used [4]. Other models using continuous beam analysis do not give analytical expressions of the resonant frequencies [5].

In this paper, a 2-degree of freedom (2-DOF) analytical model is presented and used to design highly coupled piezoelectric energy harvesters. In section II, the principle of this proposed model, which is an evolution of the one presented by [4], is detailed. In section III, the optimal dimensions that maximize the electromechanical coupling of the first mode are introduced. Finally, we discuss about the validation of the model as well as the benefits of the proposed geometry.

II. PROPOSED APPROACH

The studied system is the commonly used bimorph cantilever with a tip proof mass as shown in FIGURE 1(a). Electrodes cover piezoelectric patches at the bottom and the top surfaces and are connected in parallel. The piezoelectric patches are clamped, as well as the substrate, at one end of the beam. To study this device, a 2-degree of freedom (2-DOF) model based on the Euler-Bernoulli assumptions and neglecting the beam mass is proposed. In addition to the analysis of the deflection *u* and the force *F* (done in the 1-degree of freedom model), the effect of the rotation θ of the tip mass and the resultant couple *C* are analyzed (FIGURE 1(b)). This can be done by taking into account both rotary inertia I_t of the tip mass and the distance between its center of gravity and the end of the beam [4].

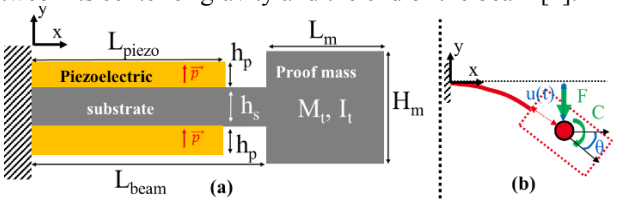

FIGURE 1: (a) BIMORPH CANTILEVER (b) DURING BENDING

The following constitutive equations of piezoelectric [6] and substrate material (1) are used to calculate the internal bending moment of the beam [7].

$$\begin{cases} T_1^p = c_{11}^{eff} S_1^p - e_{31}^{eff} E_3 \\ D_3 = e_{31}^{eff} S_1^p + \epsilon_{33}^{eff} E_3 \end{cases} \qquad T_1^S = Y_s S_1^S \qquad (1)$$

where $c_{11}^{eff} = 1/s_{11}^E$, $\epsilon_{33}^{eff} = \epsilon_{33}^T - d_{31}^2/s_{11}^E$ and $e_{31}^{eff} = d_{31}/s_{11}^E$ are the effective piezoelectric coefficients obtained with plane-stress consideration [7] and Y_s is the Young modulus of the substrate.

The bending moment allows to determine the stiffness matrix of the beam and then the following system of equations (2) is derived thanks to the force equilibrium analysis:

$$\begin{bmatrix} M_t & 0 \\ 0 & I_t \end{bmatrix} \begin{pmatrix} \ddot{u} \\ \ddot{\theta} \end{pmatrix} + \begin{bmatrix} K_1 & K_2 \\ K_3 & K_4 \end{bmatrix} \begin{pmatrix} u \\ \theta \end{pmatrix} + \begin{bmatrix} \alpha_1 \\ \alpha_2 \end{bmatrix} V = \begin{bmatrix} M_t \gamma \\ 0 \end{bmatrix}$$
$$\alpha \dot{\theta} + C_p \dot{V} = I \qquad (2)$$

where γ is the excitation acceleration of the clamped end, V and I are the voltage across and the current through the electrodes respectively. C_p, α, α_1, α_2 and the coefficients of the stiffness matrix [K] depend on the geometry and the material

coefficients. M_t and I_t are the mass and rotary inertia of the tip mass respectively.

The first and the second resonant frequencies as well as the displacement and strain distributions can be determined for open and short-circuit conditions from (2). The global coupling coefficient can be expressed as of function of the resonant frequencies for both modes [6]:

$$k_i^2 = \frac{f_{i_{oc}}^2 - f_{i_{sc}}^2}{f_{i_{oc}}^2} \quad (3)$$

where $f_{i_{oc}}$ and $f_{i_{sc}}$ are respectively the open-circuit and short-circuit resonant frequencies for the i^{th} mode.

III. Modeling and Simulation Results

A 45x10x0.5mm PMN-PT plate is used and the geometrical parameters (h_s, L_{beam}, H_m and L_m in FIGURE 1) have been optimized to maximize the global coupling coefficient of the first mode. The second mode electromechanical coupling does not show any interest as the second resonant frequency is far from the first one. The material parameters are given in TABLE 1, where ϵ_0 is the permittivity of free space and $k_{31}^2 = d_{31}^2/s_{11}^E\epsilon_{33}^T$ [6] is the material coupling coefficient. The tip mass is made of the substrate material and has the same width as the beam. The first resonant frequency is sought around 50Hz and the total length (L_m+L_{beam}) has to be less than 90mm.

TABLE 1: Material Parameters

Coefficient	d_{31} ($pm.V^{-1}$)	s_{11} ($x10^{-12}Pa^{-1}$)	ϵ_{33}^T ($F.m^{-1}$)	k_{31}^2	ρ_{piezo} ($kg.m^{-3}$)	$\rho_{substrate}$ ($kg.m^{-3}$)	Y_s (GPa)
Value	488	14.16	3880 ϵ_0	48.98%	8000	7930	200

We performed a parametric study to find the best configuration. A value of k_1^2=39.7% is obtained for the following optimal parameters (TABLE 2):

TABLE 2: Parameters for Optimal Configuration

L_p	L_m	H_m	h_s
45mm	45mm	5mm	0.42mm

We use Finite Element method (COMSOL) on the optimal configuration to verify our model. The first and the second resonant frequencies as well as the corresponding coupling coefficients are computed and compared with the proposed model (TABLE 3). The normalized displacement and strain mode shapes are also given in FIGURE 2.

TABLE 3: Obtained Frequencies and Coupling

	First mode			Second mode		
	$f_{1_{sc}}$	$f_{1_{oc}}$	k_1^2	$f_{2_{oc}}$	$f_{2_{oc}}$	k_2^2
Analytical	50,56 Hz	65,3 Hz	40,06%	700,5 Hz	717,97 Hz	4,81%
Numerical	50,1 5Hz	64,6 Hz	39,74%	544,6 Hz	557,55 Hz	4,78%
Error	0,82%	1,09%	0,80%	28,75%	28,77%	0,56%

IV. Discussion

Our model gives a good approximation of the resonant frequency and mode shapes for the first mode (TABLE 3 and FIGURE 2). As the tip mass is long, the device can be modeled as a 2-DOF system. The second mode coupling coefficient well predicted even if there is 29% error on the resonant frequencies. This comes from the fact that the beam is too heavy in comparison with the tip mass.

The design optimization gives a considerable first mode coupling coefficient (39.74% in TABLE 3), i.e. 81% of the piezoelectric coupling coefficient k_{31}^2. As a comparison, the mentioned ratio (k^2/k_{31}^2) is equal to 63% for the device presented in [1]. These interesting results are obtained thanks to the large value of the L_m/L_p ratio. Indeed, increasing the distance between the center of gravity of the proof mass and the end of the beam homogenizes the strain distribution along the piezoelectric patches, which improves the coupling coefficient. Moreover, this homogenization allows to have a more robust structure by smoothening the stress distribution.

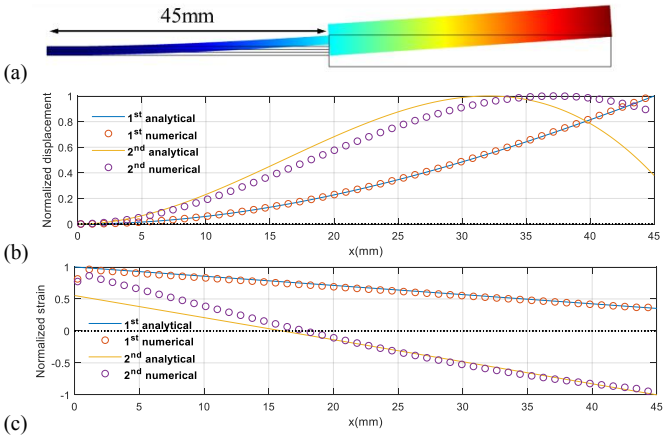

FIGURE 2: (a) COMSOL FIRST MODE DISPLACEMENT SHAPE, (b) NORMALIZED DISPLACEMENT AND (c) STRAIN SHAPES OF PIEZOELECTRIC PATCH

Conclusion

A 2 degree of freedom model was improved to find a piezoelectric cantilever configuration that considerably maximizes the global coupling coefficient (k^2=39.7%). Future work will focus on fabricating the optimized prototype to validate the analytical and simulation results. Furthermore, non-linear techniques for piezoelectric energy harvesting will be experimented. As an example, a harvesting bandwidth of approximately 60% of the mechanical resonant frequency can be expected by using the SC-SECE technique presented in [3]. Thanks to the 2-DOF, we will also be able to analyze the switches impact on the second resonance mode.

References

[1] A. Badel and E. Lefeuvre, 'Wideband Piezoelectric Energy Harvester Tuned Through its Electronic Interface Circuit', *J. Phys. Conf. Ser.*, vol. 557, p. 012115, Nov. 2014.

[2] B. Ahmed-Seddik, G. Despesse, S. Boisseau, and E. Defay, 'Self-powered resonant frequency tuning for Piezoelectric Vibration Energy Harvesters', *J. Phys. Conf. Ser.*, vol. 476, p. 012069, Dec. 2013.

[3] A. Morel, P. Gasnier, Y. Wanderoild, G. Pillonnet, and A. Badel, 'Short Circuit Synchronous Electric Charge Extraction (SC-SECE) Strategy for Wideband Vibration Energy Harvesting', *IEEE International Symposium of Circuits And Systems (ISCAS)*, 2018, to be published.

[4] M. Marzencki, 'Conception de microgénérateurs intégrés pour systèmes sur puce autonomes', PhD Thesis, Université Joseph-Fourier-Grenoble I, 2007.

[5] N. E. Dutoit, B. L. Wardle, and S.-G. Kim, 'DESIGN CONSIDERATIONS FOR MEMS-SCALE PIEZOELECTRIC MECHANICAL VIBRATION ENERGY HARVESTERS', *Integr. Ferroelectr.*, vol. 71, no. 1, pp. 121–160, Jul. 2005.

[6] 'IEEE Standard on Piezoelectricity', *ANSIIEEE Std 176-1987*, p. 0_1-, 1988.

[7] A. Erturk and D. J. Inman, 'An experimentally validated bimorph cantilever model for piezoelectric energy harvesting from base excitations', *Smart Mater. Struct.*, vol. 18, no. 2, p. 025009, 2009.

Design of broadband nonlinear vibration energy harvester with magnetic coupling

Zakaria Zergoune*, Najib Kacem, Jean-Louis Raynaud and Noureddine Bouhaddi

Univ. Bourgogne Franche-Comté, FEMTO-ST Institute, CNRS/UFC/ENSMM/UTBM, Department of Applied Mechanics, 25000 Besançon, France

*corresponding author e-mail: zakaria.zergoune@femto-st.fr

***Abstract*— The work reported here deals with the design and modeling of vibration energy harvesting from a nonlinear quasi-periodic structure. This proposed harvesting system consists of moving magnets held by elastic structures and coupled by a nonlinear magnetic force. The harvester has been modeled by forced Duffing equations for each moving magnet, including the geometric and magnetic nonlinearities and the mechanical damping. The forced Duffing equations have been solved using the harmonic balance method coupled with the asymptotic numerical method. The numerical and experimental results of the mistuning effect have been analyzed and discussed in depth.**

I. INTRODUCTION

The trend of using wearable and portable devices had significantly increased over the last years. Various energy harvesting techniques from different energy sources have been proposed and designed. Ambient vibration-based energy harvesters with the ability to convert mechanical vibrations to electrical energy are among these technologies with potential applications for low-powered electronic devices.

One of the important issues concerning the vibration harvesters is their frequency bandwidth in which they are effectively operating. Most of the proposed vibration energy harvesting devices are effectively operating within a limited bandwidth close to their resonance frequency. The nonlinear and multimodal methods have been studied for increasing the effective frequency bandwidth and gave more reliable results [1,2].

The purpose of this study is to investigate and to analyze the modeling of a broadband nonlinear vibration energy harvester with magnetic coupling. The effects of the mistuning and nonlinearities of the proposed system are discussed. The damping factor of the harvesting system was estimated experimentally by the half-power bandwidth method. The geometric and magnetic nonlinearities introduced in the model as well as the mistuning effect of the mechanical stiffness allow enlarging the frequency bandwidth and the energy localization.

II. SYSTEM MODELING

The proposed concept in this paper uses the energy localization for the sake of taking advantage of the multimodal approach. The mechanical and magnetic forces have been used for guiding and coupling the center moving magnets as well as reducing the mechanical damping factor (figure 1). The designed system is composed of $n+2$ magnets, two fixed magnets placed in the top and bottom harvester and n moving magnets. The magnets' poles have been oriented to repel each other. The proposed harvester allows tuning the separating distance between the n+2 magnets by a specific mechanism in order to adjust the magnetic coupling force as well as the linear resonance.

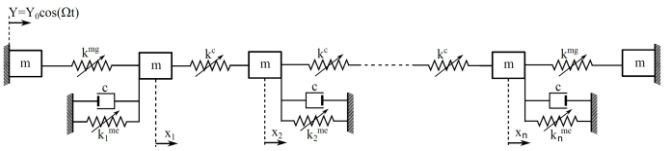

FIGURE 1. EQUIVALENT MECHANICAL MODEL FOR TWO MOVING MAGNETS

A. Magnetic force

The repulsive magnetic force between two magnets, as a function of the gap, was expressed by an analytical model (equation 2) proposed in reference [3] and called the equivalent surface current model (ESC model). The model assumes that the magnets are coaxially positioned which are the current case.

$$F(d_0) = \mu_0 \pi (r M_s)^2 \int_0^\infty J_1(\varepsilon r)^2 [2e^{-\varepsilon(d_0+h)} - e^{-\varepsilon.d_0} - e^{-\varepsilon(d_0+2h)}] \varepsilon^{-1} d\varepsilon, \quad (1)$$

where r, h, and M_s are the radius, height, and saturation magnetization, respectively. J_1 stands for the 1st order Bessel function.

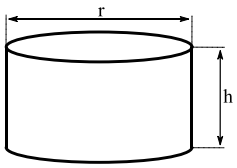

FIGURE 2. GEOMETRICAL PARAMETERS OF THE MAGNETS

As shown figure, the result of the magnetic force obtained by the ESC model has been checked by FEMM. Then, the ESC has been fitted for gap $d_0 = 60\,mm$ using a least-squares procedure. So, the total magnetic force can be identified as [4]:

$$F^{mg}(x) = k_1^{mg} x + k_3^{mg} x^3, \quad (2)$$

where $k_1^{mg} = 2\alpha_1 + 4d_0\alpha_2 + 6d_0^2\alpha_3$ is the linear stiffness coefficient and $k_3^{mg} = 2\alpha_3$ is the cubic nonlinear stiffness coefficient in which d_0 is the gap between the magnets.

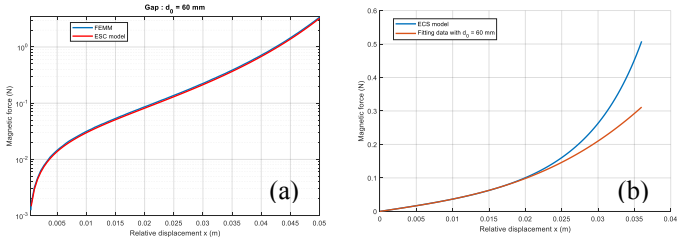

FIGURE 3. COMPARISON OF : (A) THE ESC MODEL WITH FEMM, (B) THE ESC MODEL AND THE FITTING DATA

The fitting data of equation 3 by the expression 2 is able to describe the total repulsive magnetic force up to 30% of the relative displacement compared to the ESC model as shown in figure 3.

The magnetic field B of the permanent magnets has been obtained analytically by the expression developed for cylindrical magnets in reference [5].

$$B(x) = \frac{\mu_0 M_s}{2}\left[\frac{h-x}{\sqrt{r^2+(h+x)^2}} - \frac{x}{\sqrt{r^2+x^2}}\right] \quad (3)$$

where μ_0 stands for the vacuum magnetic susceptibility.

B. Governing equation

The proposed model of the harvesting devise is modeled using forced duffing equations in the case of open circuit loop. The governing equation of the designed harvester can be written as:

$$m\ddot{x}_j + c\dot{x}_j + F_j^{mg}(x) + F_j^{me}(x) = -m\ddot{Y} \text{ with } j = 1,..,n \quad (3)$$

Two center moving magnets are only considered in the equivalent mechanical model. So, the proposed harvesting devise is modeled using two forced duffing equations. It is assumed that the two center moving magnets have the same mass, mechanical damping, and magnetic properties.

The nonlinear equations have been solved by combining the classical harmonic balance method with the asymptotic numerical method. This technique allows transforming the nonlinearities present in the governing equations into purely polynomial quadratic terms.

III. RESULTS AND DISCUSSION

In the present section, several numerical simulations have been performed in the case of two moving magnets. These simulations enable us to highlight the importance of the nonlinearity and mistuning of the designed harvesting device.

The mistuning coefficient α represents the ratio of the mechanical linear stiffness of the second moving magnet to the ones of the first moving magnet while the coupling coefficient represents the ratio of the linear magnetic stiffness and the linear mechanical stiffness.

Figure 4 represents the variation of the maximum amplitudes for the two dofs with the mistuning and coupling coefficients α and β. At $\alpha = 0.97$ and $\beta = 0.005$, there is a maximum amplitude of the mistuning dof x_2 compared to the 1st dof as depicted in the two spectrums. At this maximum, the amplitude of the 2nd dof is 20 % more than the 1st dof.

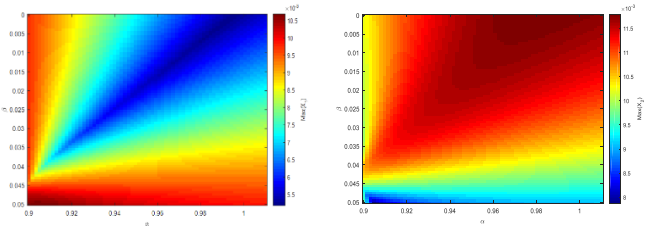

FIGURE 4. MAXIMUM AMPLITUDES IN TERMS OF THE MISTUNING AND COUPLING COEFFICIENTS

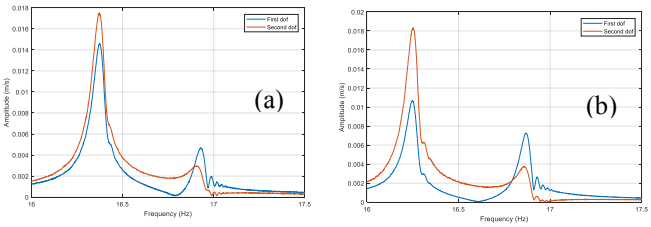

FIGURE 5. EXPERIMENTAL RESULTS FOR THE ENERGY LOCALISATION

Figure 5 shows experimental tests performed for two dofs. Figure 5a represents the reference case with a negligible mistuning coefficient while figure 5b represents the proposed harvesting systems with mistuning coefficient $\alpha = 1.07$ of the mass. The experimental results show that there is an increasing of the 2nd dof approximately 3%.

IV. CONCLUSION

In the present work, the effect of the nonlinearity as well as the mistuning and coupling coefficients on the frequency response of a periodic structure have been studied. The obtained results show that the perturbation of one of the moving magnet, the magnetic coupling coefficient and the nonlinearity increase the oscillation amplitude of the periodic system and enlarge the bandwidth as well. Thus, we can take advantage of these aspects to enhance the harvested power of a vibration energy harvesting mechanism. The proposed approach can be generalized to a large-scale quasi-periodic system.

REFERENCES

[1] I. Abed, N. Kacem, N. Bouhaddi, M.L. Bouazizi, "Multi-modal vibration energy har-vesting approach based on nonlinear oscillator arrays under magnetic levitation," Smart Materials and Structures, vol.25, pp.025018, 2016.

[2] S. Mahmoudi, N. Kacem, N. Bouhaddi, "Enhancement of the performance of a hybrid nonlinear vibration energy harvester based on piezoelectric and electromagnetic transductions," Smart Materials and Structures, vol.25, pp. 075024, 2014.

[3] P. Marco, A. F. Ferreira, A. O. Simões, R. Pascoal, J. Torrão, X. Xue, and P. Furlani, "Magnetic levitation-based electromagnetic energy harvesting: a semi-analytical non-linear model for energy transduction," Scientific Reports, 2016.

[4] B.P. Mann, N.D. Sims, "Energy harvesting from the nonlinear oscillations of magnet-ic levitation," Journal of Sound and Vibration, vol.319, pp.515-530, 2009.

[5] Camacho JM, Sosa V, "Alternative method to calculate the magnetic field of per-manent magnets with azimuthal symmetry". Revista Mexicana de Fisica, vol.59, pp.8-17, 2013.

Towards fault tolerant two-stage DC-DC converters under open-circuit switch fault: an original circuit design approach

Saima Siouane, Slaviša Jovanović, Etienne Tisserand and Philippe Poure
Institut Jean Lamour (UMR7198) , Université de Lorraine, Vandoeuvre lès Nancy, France
philippe.poure@univ-lorraine.fr

***Abstract*—This contribution proposes an original circuit design approach to perform fault tolerant operation of cascaded single switch non-isolated DC-DC converters under Open Circuit Switch Fault (OCF). We propose to implement in the electrical circuit an additional three-port equivalent synchronous switch as the redundant counterpart for the two main switches. Two examples of cascaded converters are provided: a Boost/Buck and a Buck/Buck-boost. Simulation results confirm that the continuity of service is guaranteed in OCF case, whatever the converter is concerned by the switch failure.**

I. Introduction

As shown in Fig. 1, a classical energy harvesting system for renewable DC sources, typically Photovoltaic (PV) or Thermoelectric (TE), includes two cascaded DC-DC conversion stages, separated by a DC bus, which can be associated to a battery for energy storage. The first DC-DC conversion stage performs Maximum Power Point Tracking whereas the second one supplies the load at the required voltage level. A failure may occur in any part of the system such as PV panel, TE module or DC-DC conversion. According to a survey [1], failures in switches take up 34% of electronic conversion failures. Thus, to ensure service continuity, an approach based on a fault tolerant DC-DC circuit is mandatory.

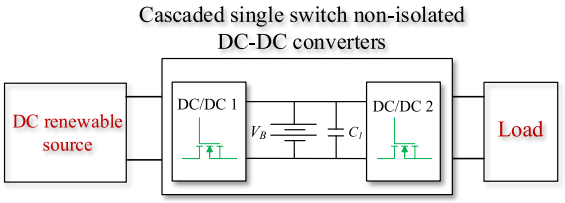

Fig. 1. Classical energy harvesting system for renewable DC sources.

II. Design approach

This contribution proposes an original circuit design approach to perform fault tolerant operation of cascaded DC-DC converters under Open Circuit Switch Fault (OCF). In this study, each converter is a single switch (Mosfet) non isolated DC-DC converter, such as a Buck, a Boost or a Buck-Boost. In the classical approaches, fault tolerant circuit design lays on switch redundancy; each of the two cascaded converters can be considered separately [2] or both converters could be considered together, if it is possible to share a common redundant switch associated to linking components [3]. The

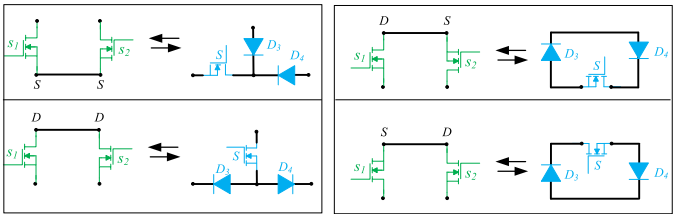

Fig. 2. The four possible common nodes two switch connections and their equivalent three ports synchronous switches

new circuit design approach we propose is based on the synchronous equivalent switches presented in Fig. 2. If the two switches S_1 and S_2 are synchronously controlled, these switches sharing a common node are equivalent to a three ports synchronous switch, based on a single switch and two diodes.

In the proposed approach, the design of the fault tolerant two-stage DC-DC circuit first consists on moving towards each other the two switches while maintaining the same electrical behavior of the converter. Thus, the two switches share a common node (Drain or Source) in the resulting equivalent electrical circuit and correspond to one of the four equivalent synchronous switches in Fig. 2. To obtain the final fault tolerant conversion circuit, the suited three-port equivalent synchronous switch is implemented in the electrical circuit previously obtained as the redundant counterpart for the two main switches, in offline scheme.

In Fig. 3, two examples are provided for classical two-stage DC-DC conversion topologies: a Boost/Buck and a Buck/Buck-Boost. In the same spirit, other combinations of cascaded single switch non-isolated converter can be studied.

TABLE I
Parameters of the fault tolerant converters.

Elements	Value			Elements	Value		
V_{in}	$10V$	L_2	$100\mu H$	V_{in}	$18V$	L_2	$100\mu H$
V_B	$12V$	C_1	$100\mu F$	V_B	$12V$	C_1	$100\mu F$
R_L	2.5Ω	C_2	$100\mu F$	R_L	25Ω	C_2	$22\mu F$
L_1	$50\mu H$	f	$20kHz$	L_1	$15\mu H$	f	$50kHz$
		D	0.2			D	0.56

III. Simulation results

For the two above-mentioned fault tolerant circuits (See Fig. 3), simulation results are provided under synchronous control, in Figs. 4, 5, 6 and 7. A single switching pattern δ (with duty cycle D and frequency f) is used to drive the two switches

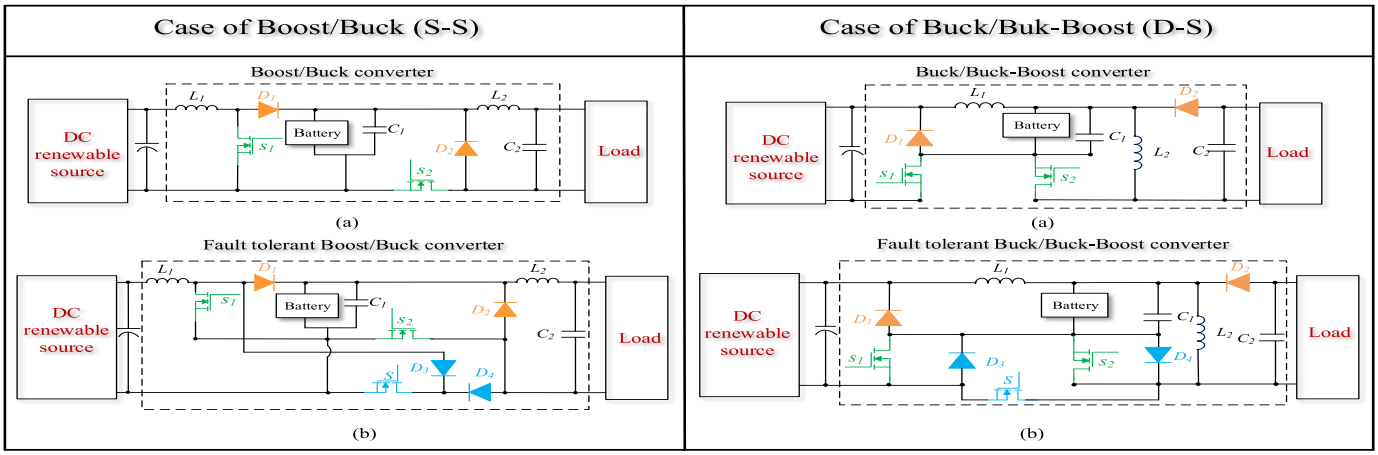

Fig. 3. Illustration of Boost/Buck and Buck/Buck-boost two-stage converters and the proposed fault tolerant circuits.

S_1 and S_2 in healthy conditions (S is OFF) or S in post OCF operation (S_1 and S_2 are OFF). In healthy conditions, D controls the first converter in discontinuous conduction mode whereas f control the second converter in continuous conduction mode. In post fault operation, the switching pattern δ controls the single switch S. The two fault tolerant circuits from Fig. 3b have been modeled and simulated with the parameters given in Table I (left ones for the Boost/Buck and right ones for the Buck/Buck-Boost converter). One can notice that the continuity of service is guaranteed in OCF case, whatever the converter is concerned by the switch failure.

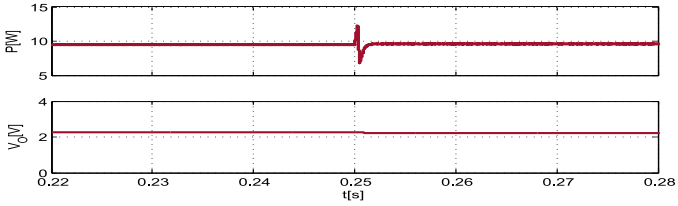

Fig. 4. P and V_O: OCF in S_1 at $t = 0.25s$ in the case of Boost/Buck.

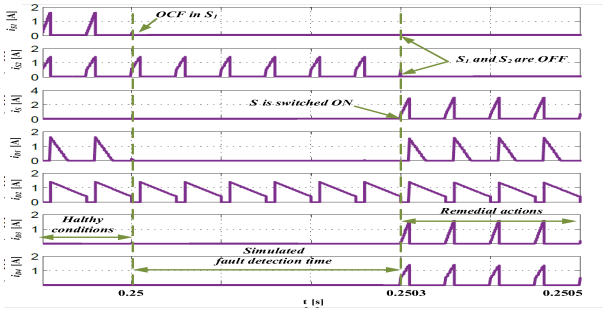

Fig. 5. Currents in the switches and the diodes in the case of Boost/Buck converter (OCF in S_1 at $t = 0.25s$).

IV. Conclusion

We have presented an efficient approach to design fault tolerant cascaded DC-DC converter. Under synchronous control, the circuit guarantees the service continuity of the full power conversion, whatever the converter is concerned by the open-circuit switch failure. The proposed design approach is general and can be applied to any two-stage single switch non-isolated DC-DC converters.

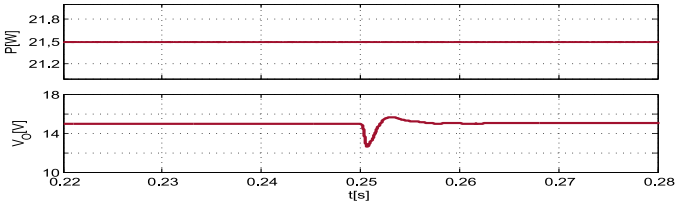

Fig. 6. P and V_O: OCF in S_2 at $t = 0.25s$ in the case of Buck/Buck-Boost.

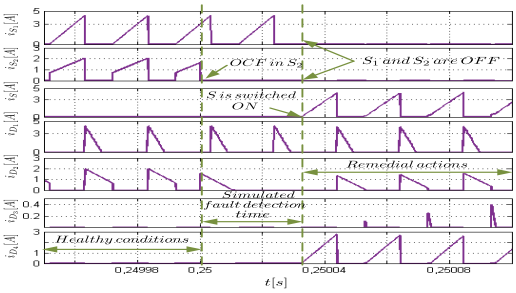

Fig. 7. Currents in the switches and the diodes in the case of Buck/Buck-Boost converter (OCF in S_2 at $t = 0.25s$).

References

[1] W. Zhang, D. Xu, P. N. Enjeti, H. Li, J. T. Hawke, and H. S. Krishnamoorthy, Survey on fault-tolerant techniques for power electronic converters, IEEE Transactions on Power Electronics, vol. 29, pp. 6319 6331, Dec 2014.

[2] E. Jamshidpour, P. Poure, and S. Saadate, Single switch dc-dc converter with fault-tolerant capability under open and short-circuit switch failures, IEEE Transactions on Power Electronics, vol. 30, pp. 27032712, May 2015.

[3] E. Jamshidpour, P. Poure, and S. Saadate, Photovoltaic systems reliability improvement by real-time fpga-based switch failure diagnosis and fault-tolerant dc-dc converter, IEEE Transactions on Industrial Electronics, vol. 62, pp. 72477255, Nov 2015.

Heartbeat Electrostatic Energy harvesting using Multimodal-shaped springs MEMS and Fractioning Interface Circuit

Bogdan Vysotskyi[1,2,*], Denis Aubry[2], Philippe Gaucher[2], Xavier Le Roux[1], Fabien Parrain[1] and Elie Lefeuvre[1],
[1] *Centre de Nanosciences et Nanotechnologies, CNRS, Univ. Paris-Sud, Université Paris-Saclay, C2N-Orsay, 91405 Orsay cedex, France*
[2] *MSSMat, CentraleSupélec, Université Paris-Saclay, CNRS UMR 8579, Gif sur Yvette, 91190, France*
* bogdan.vysotskyi@u-psud.fr

***Abstract*— This article presents the comparative study of the heartbeat energy harvesting with the variety of interface circuits of fractioning type. The MEMS electrostatic energy harvester with Multimodal-shaped springs had been chosen for the tests because of its high bandwidth (10-100 Hz) and high sensitivity to the small accelerations (down to 3 m/s²). The device had been tested under the heartbeat excitation signal with the different configurations of fractioning interface circuit. The recharging of the storage capacitor had been performed for each circuit, and the power output is found for every type of studied circuit, allowing to find the optimal circuit configuration for chosen MEMS device under the given vibrational excitation – the one produced by the heart.**

I. Introduction

Today energy harvesting aims towards offering solutions for supplying a variety of standalone devices with electrical energy [1]. The main engineering challenges for energy harvester for biomedical applications are miniaturization (typical volume <1cm^3), high sensitivity (<1g of acceleration) on a large bandwidth of low frequencies (1-50Hz), combined with a power output constantly delivering 1-10µW. It had been demonstrated that the configuration of the chosen interface circuit can have a significant impact on the overall performance of the energy harvesting system [2, 3]. The effect of the circuit configuration on the performance of nonlinear harvester under non-sine excitation is studied in this work. The fractioning interface circuit family based upon the voltage multiplier interface circuits [4] allows to choose the size of the biasing voltage of the transducer over the rectangular QV cycle by choosing the configuration of its structural elements. These circuits are fully passive and consist only of diodes and capacitors.

II. Overview of the Energy Harvester

The energy harvester design includes a Multimodal-shaped double curved beam mechanism, a central seismic mass and a biased transducer of variable capacitance (see Fig. 1). The suspension springs of the multimodal-shaped type [5] had been chosen in order to achieve a near-zero stiffness region in the force-displacement characteristics to increase the acceleration sensitivity and the overall bandwidth (originating in structural nonlinearity). The variable capacitance have been chosen to be implemented in overlap geometry in order to equilibrate between the maximum allowed displacement and electrostatic attraction force with the variation of the capacitance itself (Cmin and Cmax). The MEMS device had been fabricated using the developed silicon-on-glass (SOG) technology.

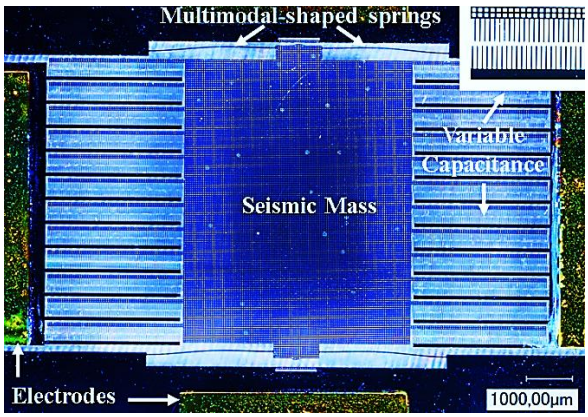

FIGURE 1. Photo of fabricated electrostatic energy harvester using Multimodal-shaped springs.

III. Fractioning Circuits

Fractioning circuits are the innovative interface circuits for electrostatic electret-free energy harvesting. The general configuration schematics of these circuits is shown on the Fig. 2.

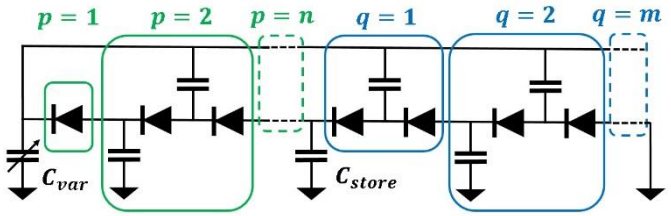

FIGURE 2. Scematics of fractioning interface circuit.

Their configuration permits to achieve a rectangular QV cycle while controlling precisely the maximum (V_{max}) and minimum (V_{min}) operating voltage of the transducer. These maximum and minimum voltages are shown to be the fraction of the voltage of the storage capacitor (or battery) V_{store}. The expression of V_{max} and V_{min} as a function of storage capacitor voltage reads:

$$\begin{cases} V_{max} = \dfrac{p+q-1}{q} V_{store}; \\ V_{min} = \dfrac{p+q}{q} V_{store}; \end{cases}$$

with p and q being the quantity of particular building block cells in the fractioning circuit.

Photo of the variety of fabricated PCBs of fractioning circuits with different parameters is shown on Fig. 3.

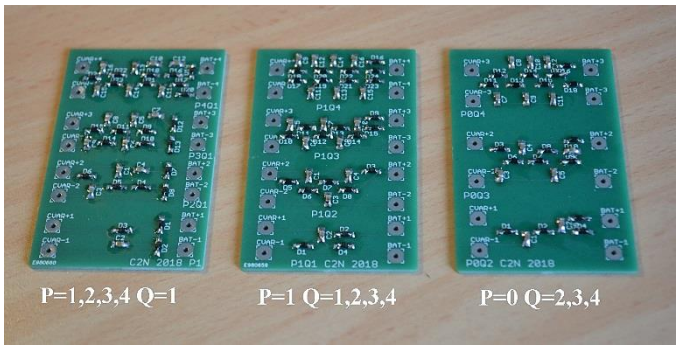

FIGURE 3. PHOTO OF FABRICATED PCBS WITH THE WARIETY OF FRACTIONING CIRCUITS.

IV. ENERGY HARVESTING EXPERIMENT

The experimental set-up consists of the shaker controlled by the arbitrary voltage source and voltage amplifier, accelerometer to adjust the studied acceleration glued to the shaker, MEMS device mounted on the shaker and positioned parallel to the gravity to achieve its full efficiency. Thus, an effective force-displacement characteristics of the system is shifted to the lower forces, similar to [6].

The cardiac excitation signal presented on the Fig. 4 had been sent to the energy harvesting system and the recharging of the storage capacitor had been measured with the various fractioning interface circuits. The result of characterizations shows that the highest power output from the heartbeat signal had been obtained with p = 1, q = 1 configuration (Bennet's doubler) and corresponds to the average of 351 nW. Obtained results normalized to the power harvested with Bennet's doubler are shown in the Table 1. It also been shown that with both increasing q and p the overall power output of the system decreases.

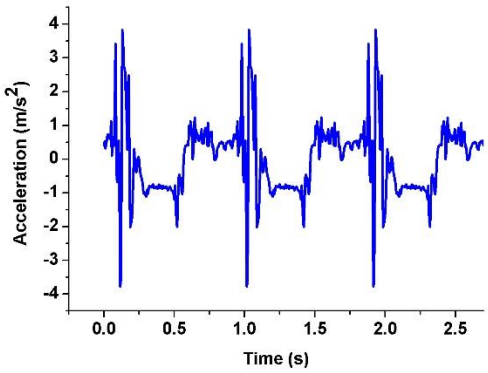

FIGURE 4. CARDIAC EXCITATION SIGNAL.

P | Q	1	2	3	4
0	-	100%	70%	56.7%
1	90.3%	70%	54.7%	36.5%
2	27.1%	-	-	-
3	21.1%	-	-	-
4	12.5%	-	-	-

TABLE 1. RELATIVE HARVESTED POWER UNDER CARDIAC EXCITATION AS A FUNCTION OF FRACTIONING CIRCUIT CONFIGURATION, COMPARED TO THE HARVESTED POWER WITH BENNET'S DOUBLER.

CONCLUSION

This article addresses a subject of the choice of the interface circuit for optimizing the power output under the particular excitation – of the cardiac type. A sensitive and wideband MEMS device of electrostatic type is selected to compare the variety of fractioning interface circuits. It can be shown that the Bennet's doubler (p = 1 and q = 1) is the most efficient configuration in terms of power output (351 nW), and the absolute value of harvested power decreases with the increasing of p and q. The future study can concentrate upon the defining the impact of the fractioning interface circuit configuration (the choice of p and q) upon the resulting bandwidth of the energy harvesting system.

ACKNOWLEDGMENT

This work is supported by the "IDI 2015" project funded by the IDEX Paris-Saclay, ANR-11-IDEX-0003-02 and has benefited from the financial support of the LabeX LaSIPS (ANR-10-LABX-0040-LaSIPS) managed by the French National Research Agency under the "Investissements d'avenir" program (n°ANR-11-IDEX-0003-02).

REFERENCES

[1] K.V. Selvan, M.S. Mohamed Ali, Renewable and Sustainable Energy Reviews 54, 1035–1047, 2016;

[2] A. Karami, D. Galayko, P. Basset, IEEE Transactions on Circuits and Systems I: Regular Papers, 64, 227-240, 2017;

[3] K. Peterson, G. A. Rincón-Mora, IEEE International Symposium on Circuits and Systems (ISCAS), Seoul, 20-23 May, 2012;

[4] J. Wei, S. Risquez, H. Mathias, E. Lefeuvre, F. Costa Proceedings of Sensors 2015, IEEE, 1-4 Nov., Busan, 2015;

[5] B. Vysotskyi, F. Parrain, D. Aubry, P. Gaucher, X. Le Roux and e .Lefeuvre, Journal of Microelectromechanical Systems 99, 1-7, 2017;

[6] K. Yamamoto, T. Fujita, A. Badel, F. Formosa, K. Kanda and K. Maenaka, Proc. PowerMEMS 2015, pp. 1-4

Energy Harvesting with lead free $LiNbO_3$

Giacomo CLEMENTI[1*], Ausrine BARTASYTE[1], Bernard DULMET[1] and Samuel MARGUERON[2]
[1] *FEMTO-ST Institute, Université de Bourgogne Franche-Comté, 25030 Besançon – France*
[2]*LMOPS, Université de Lorraine et CentraleSupélec, 57070 Metz – France*
*giacomo.clementi@femto-st.fr

***Abstract*—$LiNbO_3$ crystals and thin films are investigated for energy harvesting vibrational motion under low frequency (<100 Hz). The geometrical parameters and crystal orientations of the piezoelectric element are investigated by finite element software (FEM) in order to maximize the figure of merit. In addition, the structure of the device is simulated in a bending cantilever, including electrodes and resistance loading. The $LiNbO_3$ crystal orientation is investigated under transverse excitation mode.**

I. Introduction

Lead-free piezoelectric transducers and energy harvesters are intensively investigated to replace Lead Zirconate Titanate (PZT) due to EU Regulation. Zinc oxide (ZnO) piezoelectric has been studied in the form of films or nanowires. However, more complex oxides like Lithium Niobate ($LiNbO_3$) present several advantages such as high chemical stability, high temperature stability (Curie temperature is 1198°C [1]) and high electromechanical coupling. Even though $LiNbO_3$ has been widely studied in optics and surface acoustic waves field, little investigations have been done concerning its application for energy harvesting. High quality 6-inch wafers are sold for relative low price, allowing mass production of custom orientation cuts wafer. Moreover, $LiNbO_3$ can be found in ions slide film on silicon, grown epitaxially by MOCVD with different orientations [2]. Meanwhile, as compared to cubic PZT, the strong anisotropic piezoelectric, dielectric and mechanical properties have to be investigated. Moreover, one of the constraints in vibration energy harvesting, is its ability to harvest low frequency vibrations.

For instance, from the signal recorded with triaxial accelerometer in a car driving along an urban road, is possible to study acceleration levels (see Real Vibrations database [3]). If we take the signal when the sensor is positioned on the steering wheel of a diesel car, with gravity along x-axis, we can find that the root mean squared value of the signal is Xrms=0.52g, where g=9.81m/s^2. Once performed spectrogram analysis, it appears that the strongest frequency response intensity is below 40Hz. These vibrations are due to the running engine, and we can assume that this frequency is dominant and stationary. In this case it is possible to use a cantilever device to exploit vibrations as a source of kinetic energy.

One of the most common way to harvest energy is done by exploiting transverse piezoelectric mode in cantilevered beam configuration. The strain and electrical field are related by the constitutive relations:

$$\begin{cases} S_1 = s_{11}^E T_1 + d_{31} E_3 \\ D_3 = d_{31} T_1 + \epsilon_{33}^T E_3 \end{cases} \qquad (1)$$

where S is the strain tensor, s^E is compliance fourth order tensor at constant electric field, T is the stress tensor, d is the third order piezoelectric tensor, E is the electric field vector, D is the dielectric displacement vector and ϵ^T is the permittivity at constant stress. Here, charges are collected in transverse excitation mode with top-bottom electrodes, where '3' is polarization direction, while the piezoelectric element undergoes strain in '1' direction. The coupling factor k_{31} is the efficiency of transduction from mechanical to electrical energy, and for transverse mode it is described by (Eq. 2):

$$k_{31}^2 = \frac{d_{31}^2}{s_{11}^E \epsilon_{33}^T} \qquad (2)$$

II. Orientation Study of Lithium Niobate

$LiNbO_3$ has a trigonal structure R3c. It presents piezo-, pyro- and ferro-electrical properties and strongly anisotropic dielectric, mechanical properties represented in tensor form. The value of these tensors are well documented [4].

In transverse excitation mode, the rotation of the piezoelectric tensor shows that not only d_{31} will contribute to the piezoelectric response, but other coefficients as well. In order to have optimal values for the piezoelectric coefficients, we investigate the effect of rotation of the crystal. In Fig. 1, the rotation of piezoelectric tensor around x-axis by ψ angle shows strong variation of piezoelectric coefficients. The best configuration is achievable with Y-128° wafer cut, where we find higher d_{23}=27pC/N, and higher coupling factor k_{23}=0.45.

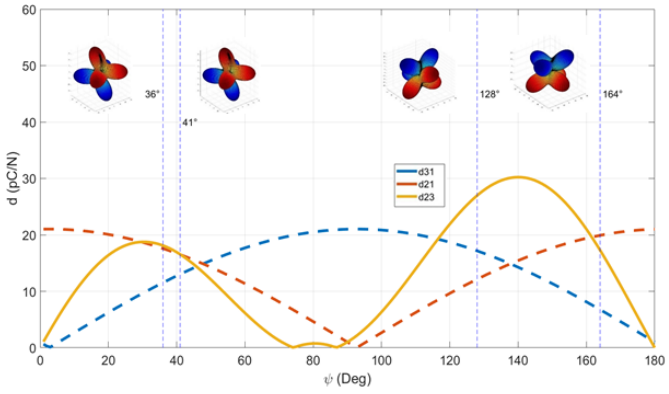

FIGURE 1. Orientation study of $LiNbO_3$ piezoelectric tensor

III. Finite Element Modeling

In order to test the validity of our energy harvester, we designed a 3D unimorph cantilevered beam for eigen-frequency analysis, and then a 2D model for frequency domain analysis. Our proposed device is smaller than 1 cm^3, whose dimensions and 3D representation are reported in Fig. 2. The acceleration level is introduced as a parameter to simulate the excitation inside the car (0.5g).

Cantilver dimensions (µm)		
Length	Width	Thickness
7E3	2E3	20
Tip mass dimensions (µm)		
2E3	2E3	400

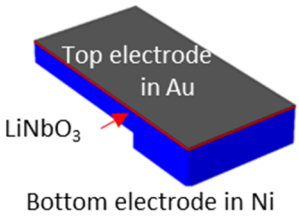

FIGURE 2. DIMENSIONS AND CONFIGURATION OF PIEZOEELCTRIC CANTILEVER

$LiNbO_3$ is the piezoelectric element for electromechanical conversion (1µm thickness). The hosting structure and mass load are made of nickel and the top contact is a gold electrode. Parametric sweep is performed to implement simulation on $LiNbO_3$ orientation and optimal load.

IV. Results

The eigen-frequency analysis allows to find the resonance frequency of our system, whereas the first mode is the bending mode (Fig. 3). The value computed is 35Hz, although other modes can be found at higher frequency (>100Hz). Bending mode value is in the same range as the one found in the experimental data.

FIGURE 3. BENDING MODE OF CANTILEVER

While voltage response is investigated in the frequency domain, parametric sweep is performed to implement the orientation study for $LiNbO_3$ piezoelectric element (Fig. 4).

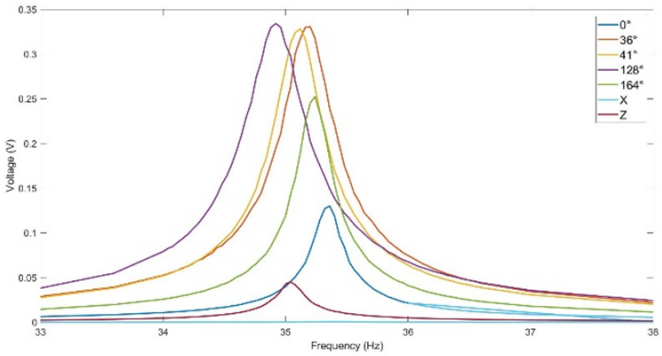

FIGURE 4. VOLTAGE RESPONSE FOR DIFFERENT ORIENTATIONS

The response of the device is centered around 35Hz as expected. The maximum amplitude is found at Y-128° orientation and leads to 0.34V with a load of 200kΩ. These values are in good agreement with the orientation study presented in Fig. 2. Moreover for Y-36°, orientation close to epitaxial thin-film [2], we have encouraging result in terms of voltage.

Finally it is possible to study voltage and power harvested varying the resistive load coupled with our cantilever. In this case the simulation allows to investigate the maximum power-point (Fig. 5). Maximum efficiency is reached when the cantilever resonates at 35Hz and its orientation is Y-128°. The power harvested is 340nW at 150kΩ with an output voltage of 0.3V, and the figure of merit is about 10µW/cm^2/g^2.

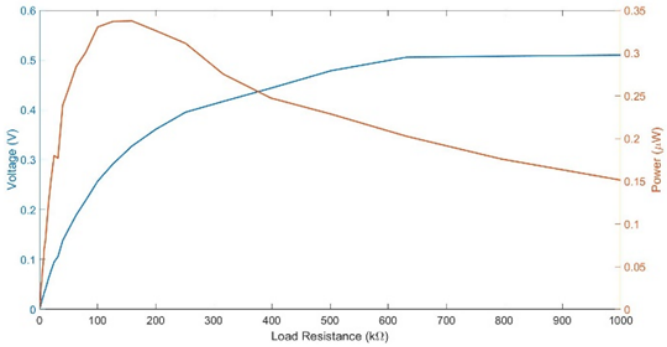

FIGURE 5. OPTIMAL LOAD FOR POWER AND VOLTAGE STUDY

V. Conclusion

A piezoelectric cantilever is a suitable choice for vibrational energy harvesters exploiting low frequency vibrations in cars. Y-128° $LiNbO_3$ cut presents high piezoelectric coefficient (d_{23}=27pC/N) and coupling (k_{23}=0.45). Modeling the cantilever with FEM allows to investigate power and voltage generated, but further optimization is needed in order to obtain higher figure of merit.

References

[1] J. R. Carruthers, G. E. Peterson, and M. Grasso, "Nonstoichiometry and Crystal Growth of Lithium Niobate" *J. Appl. Phys,* (1971) 42:5, 1846-1851

[2] A. Bartasyte, S. Margueron, T. Baron, S. Oliveri, P. Boulet, "Toward High-Quality Epitaxial $LiNbO_3$ and $LiTaO_3$ Thin Films for Acoustic and Optical Applications" *Adv. Mater. Interfaces*, 4(8), 1600998 (2017).

[3] I. Neri, F. Travasso, R. Mincigrucci, H. Vocca, F. Orfei, L. Gammaitoni, "A real vibration database for kinetic energy harvesting application." *J. Intell. Material Syst. Struct.* 23.18 (2012): 2095-2101

[4] R. S. Weis and T. K. Gaylord, "Lithium Niobate: Summary of Physical Properties and Crystal Structure" *Appl. Phys. A* ,37, 191-203 (1985)

Design and microfabrication of a Microscale-Stirling Engine (M-SE) for low temperature heat recovery

Alpha DIALLO*, Ravinder CHUTANI, Magali BARTHES, Sylvie BEGOT, Sylwester BARGIEL, Michel DE LABACHELERIE and François LANZETTA

FEMTO-ST institute, Univ. Bourgogne Franche-Comté, CNRS
15B avenue des Montboucons, BESANCON, France

* alpha.diallo@femto-st.fr

***Abstract*—This study concerns the design and microfabrication of a Microscale-Stirling Engine (M-SE) for the recovery of low temperature thermal energy ranging from 50 to 200°C. This M-SE consists of a stack of silicon, glass and hybrid membranes (HMs) based on a silicone elastomer embedded in a planar silicon spring. Design of hybrid membrane is briefly presented in this paper, followed by M-SE design and their microfabrication process. In addition, numerical simulations (finite element model) were performed in order to check mechanical and dynamic behavior of hybrid membrane salong with the expected power budget of the assembled M-SE using Schmidt analysis.**

I. INTRODUCTION

A reliable source of energy is essential for the industrial progress that underpins the economic development of any country. The world is going through an energy crisis that affects the stability of countries and consequently people's lives [1]. One of the important ways to reduce the energy crisis could be the recovery of heat at low and medium temperatures (from 50 to 200°C), such as from industrial waste heat, heating energy, solar heat, biomass, friction, Joule effect, exhaust pipes of vehicles and so on. In this paper, we mainly concern about MEMS based energy devices. Many MEMS devices need a high energy density to achieve a long operating time. Therefore, there is a need for high energy density micro power generation systems to replace the existing electrochemical batteries, which are not sufficient (~ 1 kJ / g) to sustain the power requirements of long periods [2]. Dynamic heat engines are more efficient than electrochemical conversion systems and achieve higher conversion efficiencies than static heat engines [2]. Therefore, several designs for micro-scale dynamic heat engines have been fabricated. For example, a microscale rotary engine (Otto cycle) [3], a microscale heat engine with reciprocating liquid piston (Otto/Diesel cycle) [4] and a microscale gas turbine engine (Brayton cycle) [5, 6] were fabricated. A micro heat engine (called P^3) for MEMS power system based on expansion and compression of a two-phase working fluid was developed [2]. Among the dynamic engines, the Stirling engine has many advantages, including no internal combustion and a very high efficiency in terms of energy conversion. This engine is based on a reversible cycle of compression and dilatation of a gas (e.g. air). In this paper, we propose a membranes-based microfabricated Stirling engine to harvest waste heat for temperature ranging from 50°C to 200°C.

II. DESIGN AND FABRICATION

A. Hybrid Membrane design

While miniaturizing classical engine, sliding piston must be replaced in order to avoid friction losses and fluid leakage through the cylinder–piston gap, designated as one of the main limitations [7,8]. For this reason, membrane are preferred in order to replace pistons in MEMS engine. The hybrid membranes (HMs) presented in this paper are based on the work of Chutani et al. [9] and were designed to be used for miniaturized Stirling engine. These HMs consisted of thin RTV silicone polymer based membrane embedded in silicon spiral spring with central disk (Figure 1). These membranes have been numerically simulated [10]. Moreover, they were dynamically characterized, and their aging and temperature stability were previously studied [10].

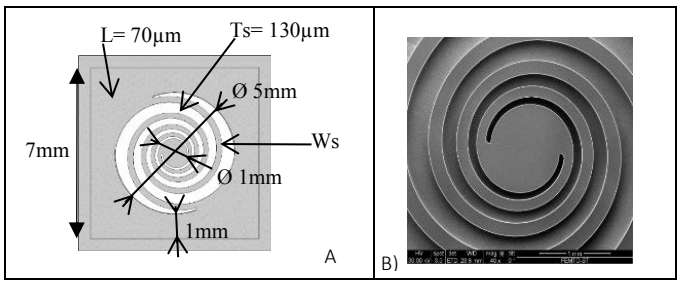

FIGURE 1. A) SILICON SPIRAL SPRING ARCHITECTURE AND GEOMETRICAL PARAMETERS; L IS THE LOCATION AND THICKNESS OF THE RTV-SILICONE LAYER THERE, WS IS THE WIDTH OF THE TURNS OF THE SPIRAL AND TS IS THE THICKNESS OF THE SPIRAL. B) A SEM IMAGE OF A SPIRAL

The role of each part of the HM is summarized in TABLE 1.

TABLE 1. THE ROLE OF EACH PART OF THE PLANAR SPRING AND THE POLYMER OF THE HM.

Components	Control/Role
Spiral spring	Stiffness, Flexural shape, Uniform stress distribution (width vs angle), Spring restoring force
Central disc	Inertia and Swept volume
RTV-silicone	Sealing, Spiral Robustness reduction, elasticity

B. M-SE design and microfabrication

M-SE (Figure 2A) consists of five different parts: four silicon plates (two, top and bottom on which compression and relaxation chambers are etched, the other two carrying the

HMs) and in between a thick glass plate with through holes to encapsulate incompressible liquid (Vaseline in this case).
The assembly of the M-SE consisted of four major microfabrication steps (cf. FIGURE 2.b)): two thermocompression bonding steps to assemble the silicon plates followed by two anodic bonding steps to assemble the latter with the thick glass plate.

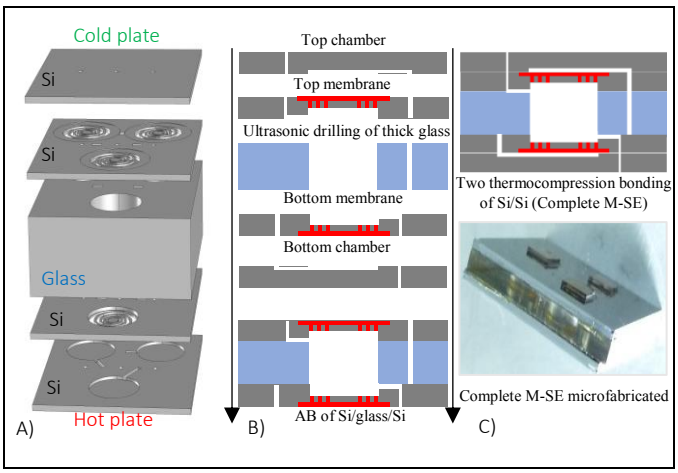

FIGURE 2. A) SCHEMATIC VIEW OF COMPONENTS OF THE M-SE, B) MICROFABRICATION PROCESS FLOWCHART AND C) PICTURE OF THE FULLY ASSEMBLED M-SE

All these microfabrication and assembling steps have been successfully completed, which led to the realization of the first M-SE entirely realized in a clean room at wafer level.

III. RESULTS

A FEM model, using COMSOL Multiphysics, was carried out to study the influence of the HM geometric parameters on the resonance frequency and the mechanical constraints resulting from a displacement. For the specific HMs used for the present M-SE, a resonance frequency of 2.9 kHz was found.

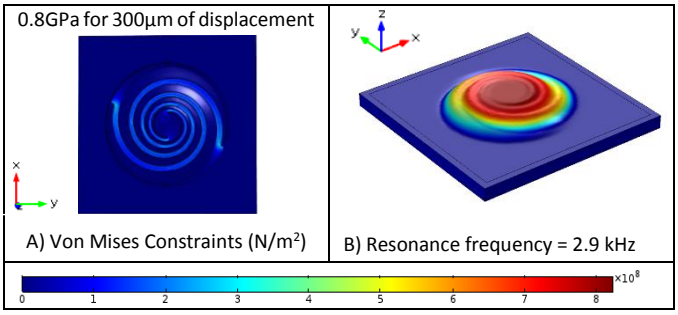

FIGURE 3. A) VON MISES CONSTRAINTS OF HMS FOR 300µM PRESCRIBED DISPLACEMENT, B) HMS RESONANCE FREQUENCY.

Static displacement of HMs versus air pressure was also experimentally determined: for a single membrane, a displacement of about 0.4 mm at 0.2 bar was found while for the same pressure, a displacement of about 0.15 mm was achieved for a hybrid fluidic membrane (ie. two HMs linked with the Vaseline in between [9]). Further, an isothermal simulation of the machine was done to determine the engine performance prediction, based on Schmidt analysis. Set parameters are given on TABLE 1. A mechanical Power output of 177 mW was found for the engine, and its yield was estimated to reach 37% of Carnot efficiency.

TABLE 2. PARAMETERS USED IN THE SCHMIDT MODEL. WITH V_{swc} THE SWEPT VOLUME; P THE PRESSURE, TH THE HOT PLATE TEMPERATURE, TC THE COLD PLATE TEMPERATURE, F THE OPERATING FREQUENCY AND α THE PHASE ANGLE

gas	v_{swc} (m^3)	P	Th(°k)	Tc(°k)	F(kHz)	α(rad)
Air	$0.3.10^{-6}$	Amb.	473	298	1	2.09

IV. CONCLUSION

We have designed and microfabricated a microStirling engine. The numerical simulation based on FEM model made it possible to determine the resonance frequency of the HM used in the micro-engine. Moreover, calculation based on the Schmidt analysis enable to predict the engine efficiency. The achieved machine will be characterized.

ACKNOWLEDGMENT

This work has been supported by the Labex ACTION project (contract "ANR-11-LABX-0001-01"), the Region Bourgogne Franche-Comté STIP'MEMS project and the French National Research Agency (ANR) under grant no. ANR-12-SEED-0005-01 (MISTIC Project). It has been partly supported by the French RENATECH network and its FEMTO-ST technological facility.

REFERENCES

[1] A-B. Awan, Z-A. Khan, "Recent progress in renewable energy – Remedy of energy crisis in Pakistan," *Renewable and Sustainable Energy Reviews*, vol. 33, pp. 236-253, 2014.

[2] S. Whalen, M. Thompson, D. Bahr, C. Richards, R. Richards, "Design, fabrication and testing of the P3 micro heat engine," *Sensors and Actuators A: Physical*, vol. 104, pp. 290-298, 2003.

[3] K. Fu, A-J. Knobloch, F-C. Marinez, D-C. Walther, C-F. Pello, A-P. Pisano and D. Liepmann, "Design and fabrication of a silicon based MEMS rotary engine," *Proceedings of the ASME IMECE*, Paper No. MEMS-23925, New York, 2001.

[4] W. Yang, "Liquid piston chip engine," *Proceedings of the DARPA/MTO MEMS/MPG/NMASP Principal Investigators*, Bloomington, CO, 2001.

[5] A-H. Epstein, S-D. Senturia, O. Al-Midani, G. Anathasuresh and al, "Micro-heat engines, gas turbines and rocket engines: the MIT micro engine project," *Proceedings of the 28th AIAA Fluid Dynamics Conference, Snowmass, Colorado*, Colorado, 1997.

[6] A. Mehra, X. Zhang, A-A. Ayon, I-A. Waitz, M-A. Schmidt and C-M. Spadaccini, "A six-wafer combustion system for a silicon micro gas turbine engine," *Journal MEMS*, vol. 9 , pp. 517-527, 2000.

[7] S-K. Chou, W. M. Yang, K. J. Chua, J. Li and K-L. Zhang, "Development of micro power generators – A review," *Appl. Energy*, vol. 88 , pp. 1-16, 2011.

[8] H-K. Bardaweel, M-J. Anderson, R-F. Richards and C-D. Richards, "Optimization of the dynamic and thermal performance of a resonant micro heat engine," *J. Micromechanics Microengineering*, vol. 18 , pp. 104014, 2008.

[9] R. Chutani, F. Formosa and M. de Labachelerie, A. Badel and F. Lanzetta, "Microfabrication of hybrid fluid membrane for microengines," *J. Micromechanics Microengineering*, vol. 26 , pp. 124009, 2016.

[10] A. Diallo, R. Chutani, M. Barthès, S. Bégot, M. De Labachelerie and F. Lanzetta "Study of dynamic response of silicone elastomer microfabricated hybrid membranes versus temperatures and aging time," *Proceedings of the PowerMEMS 2017* , pp. 154, 2017.

Thermoelectric nanogenerator networks: a viable source of power for autonomous wireless sensors

Dimitri TAINOFF[1], Anais PROUDHOM[1], Sébastien DUFRESNES[1], Sylvain DUMONT[1], Daniel BOURGAULT[1], Olivier BOURGEOIS[1]

[1] *Institut Néel, CNRS, Université Grenoble Alpes, 25 Avenue de Martyrs, BP 166, 38042, Grenoble, France*

*dimitri.tainoff@neel.cnrs.fr

***Abstract*— Here we report the design, the elaboration and the measurement of an innovative planar thermoelectric (TE) devices made of large array of suspended nanogenerators [1]. The miniaturized TE generators are arranged in serial and/or in parallel depending on the expected final resistance adapted to the charge. Devices are elaborated using MEMS clean room processes. They can produce enough power to send a signal with common communication protocol and feed basic functions, for example a temperature measurement.**

I. INTRODUCTION

With the emergence of low power communication protocols dedicated to the Internet of things (IoT), there is a real demand for autonomous micro-sources of energy that can supply batteries and deliver power of about 100 µW. That range of power can be supplied by standard TE module with a temperature gradient of few degrees under stationary operating conditions. However these conditions of use are not necessarily adapted for small wireless sensors specially when the energy source is intermittent or the volume available too limited.

II. ARRAY OF TE NANOGENERATORS BASED ON MEMBRANE

A. Concept

The expertise developed at the Institut Néel CNRS on the elaboration of suspended sensors dedicated to thermal measurements has been used to design suspended thermoelectric nano-generators [1,2]. The planar generators are made of suspended silicon nitride membranes functionalized with TE materials as described in the figure 1. Since membranes have a negligible mass, their temperature is free to fluctuate contrary to the bulk silicon frame that conducts well the heat. Thus a temperature gradient appears between the membranes and the bulk silicon frame when the whole setup is submitted to a heat source (air flow, radiation etc…). The small mass of the membrane allows avoiding the effect of thermal inertia. That makes the device working even in the case of intermittent thermal energy source. The proof of concept has been validated using Bi_2Te_3 TE thin films. Indeed this material has the best TE properties around room temperature with a conversion efficiency up to 10%.

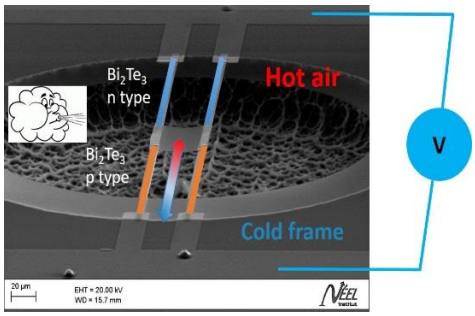

FIGURE 1. Scheme of a unique suspended membrane having two thermoelectric n and p junctions (Bi_2Te_3 materials), a nano-generator sensitive to heat flow.

B. Results

For temperature gradient of 8°C the power generated by an individual membrane is around 0.3 nW. The duplication of this thermoelectric nano-generator thanks to standard MEMS clean room techniques enabled us to obtain few hundreds of membranes. In that case, a power of approximately 60µW is harvested for a temperature gradient of 10°C and a surface of 10 cm². A concentration of several thousands of nano-generators per cm² may be reached by using state of the art clean room technology. This will lead to power production of up to 750 µW for 10 cm², a power value sufficiently high to make sober sensors infinitely autonomous in energy.

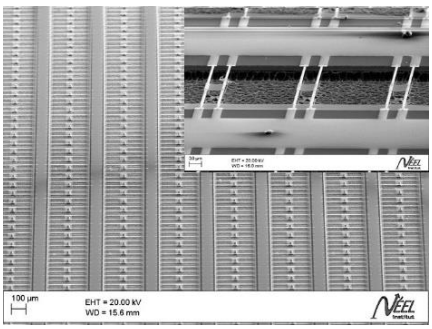

FIGURE 2. Array of thousands of membranes. The TE nano-generator are installed in series and parallel to adapt the internal resistance to the impedance of the charge.

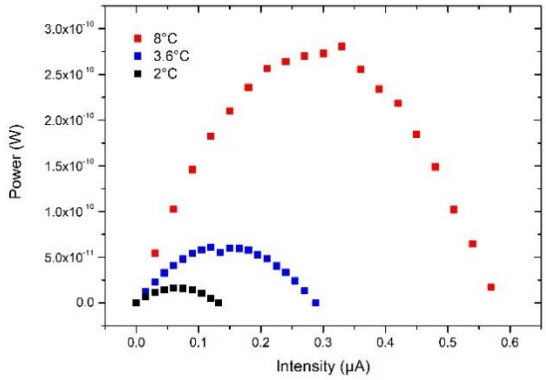

FIGURE 3. Power generated by a single membrane as the function of the bias current (in Peltier mode). The different temperature gradients used in the experiment are mentioned.

Prototypes including energy harvesting have been made and coupled to an ASIC in order to feed a wireless temperature sensor.

The patented design of the TE nano-generators array permits to arrange easily the micromodule in serial and/or in parallel depending of the expected final resistance [3]. The whole device is mechanically robust, versatile regarding the energy sources and not sensitive to aging having no moving part (see figures). Prototypes have been built with two industrial groups and coupled to an ASIC in order to get an operational autonomous sensor. A start-up commercializing that solution is going to be created.

III. Conclusion

As a conclusion, planar suspended thermoelectric devices have been developed and patented by CNRS. This device permits to convert small intermittent gradient of heat into electrical power. The design of the device permits to adapt the resistance of the thermogenerator depending on the exact use case. The efficiency of the device is sufficient to expect its use in real IoT use cases.

References

[1] O. Bourgeois, D. Tainoff and D. Bourgault *Thermoelectric device*, patent 16/51336 owned by CNRS (2016).

[2] D. Tainoff, and O. Bourgeois *Gas sensor device*, patent owned by CNRS (2017).

[3] D. Tainoff, A. Proudhom, C. Tur, T. Crozes, S. Dufresnes, D. Bourgault, and O. Bourgeois. *Thermoelectric nanogenerator networks: a viable source of power for the autonomous wireless sensors,* in prep. to be submitted to NanoEnergy (2018).

Posters

Development of nanostructured carbon/MnO_2 hybrid electrodes for energy storage applications

Clémence ROGIER[1,*], Grégory POGNON[1], Paolo BONDAVALLI[1], Gaëtan BRACCIALE[1], Christophe GALINDO[1], Giao T.M. NGUYEN[2], Frédércic VIDAL[2], Pierre-Henri AUBERT[2]

[1]*Thales Research & Technology, 1 avenue Augustin Fresnel, 91767, Palaiseau, France*

[2]*Laboratoire de Physicochimie des Polymères et des Interfaces (EA 2528), Université de Cergy-Pontoise, 5 mail Gay-Lussac, 95031 Cergy-Pontoise Cedex, France*

*clemence.rogier@thalesgroup.com

***Abstract* — Combining transition metal oxides and nanostructured carbon materials in one electrode is considered as one of the best ways of reaching high energy densities in supercapacitors. In this study, carbon nanotube/birnessite type manganese dioxide nanohybrids were synthesized for use in supercapacitors with high electrochemical performances. This material is then combined with graphene in a nano-architecture to create a synergetic effect and increase electrochemical performances. Graphene oxide and CNTs were physically mixed with the synthesized material to form a binder-free nanostructured electrode with a capacitance of 156 F/g.**

I. INTRODUCTION

Supercapacitors are energy storage devices mainly used as complementary systems to batteries [1]. Their main characteristics are high power densities, very long cycle life and fast charge/discharge rates. Two types of supercapacitors can be identified in regard to their electrochemical mechanisms: electrochemical double-layer capacitors (EDLCs) and pseudocapacitors. EDLCs present carbon based materials as electrodes and their charges are electrostatically stored on the electrode surface [2]. Pseudocapacitors have redox active materials as electrodes such as transition metal oxides. They store energy through reversible faradaic reactions [3]. Pseudo-type supercapacitors have been greatly studied recently because they allow much higher capacitance and energy densities than EDLCs. MnO_2 is a promising material for the positive electrode of supercapacitors with pseudocapacitive behavior because of its high theoretical maximum capacitance (~1370 F/g), low cost and environment friendly nature [4]. However its low conductivity prevents fast charge/discharge mechanism and leads to low power densities.

Our target is to develop a hybrid supercapacitor with high energy densities but also good cycle life and fast charge/discharge performances. Our strategy is to combine within a specific architecture carbon nanomaterials (graphene and carbon nanotubes) and manganese dioxide to form a hybrid positive electrode. The high capacitance of MnO_2 will be exploited and the carbon materials will give a good conductivity to the material creating a synergetic effect and much higher electrochemical performances compared to pristine materials thanks to their optimized association [5].

In this work we present a one-step low temperature synthesis of a MnO_2-carbon nanotubes hybrid with much higher capacities than pure MnO_2 nanomaterial. MnO_2 nanoflakes have been grown chemically on the surface of multiwall carbon nanotubes (CNTs) with covalent bounds [6].

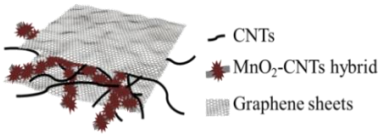

FIGURE 1: SCHEME OF THE GRAPHENE/CNTS/MNO_2-CNTS HYBRID

This material is then combined physically through non-covalent interaction to graphene oxide to create a porous hierarchical nano-architecture. The objective is to combine the faradaic behavior of the MnO_2 material with the electrostatic behavior of graphene and CNTs. Graphene is well known for its high surface area (~2630 m^2/g) [7]. Here we aim to use the hybrid MnO_2-CNTs material as spacers to render the surface of graphene sheets accessible to electrolyte ions. The obtained electrode material combining MnO_2 with a high surface area conductive scaffold should be the most promising architecture to enhance performances.

II. MATERIAL PREPARATION

A. *Hybrid MnO_2-CNT electrode material*

MnO_2-CNTs hybrid material was synthesized by a redox reaction in water between multiwall CNTs and $KMnO_4$ based on a procedure reported elsewhere [6]. Pure MnO_2 nanoparticles were synthetized through a similar method but without CNTs and with adding ethanol instead as a reducing agent. Free-standing electrodes of these materials were obtained in each case by mixing the synthesized powder with pristine CNTs and PTFE binder with a mass ratio of 68:17:15 (or a CNTs/PTFE 85:15 ratio for comparison with pure CNTs). By adding ethanol, a paste can be laminated in order to obtain a free-standing electrode with a thickness of ~60 µm.

B. *Graphene/CNTs/MnO_2-CNTs hierarchical structure*

The second type of electrode prepared is a binder free nano-structured Graphene/CNTs/MnO_2-CNTs electrode obtained by physical mixing of graphene oxide (GO), pristine CNTs and hybrid MnO_2-CNTs powder in alcohol under ultrasound with a mass ratio of 25:70:5. By evaporation of the solvent an ink is obtained and can be coated onto a graphite substrate by Doctor Bladder with a thickness of ~20 µm of material. This film is then treated under air at 200°C for 2h to remove oxidized functions in (GO).

III. Results and Discussion

A. MnO_2-CNT hybrid electrode properties

The MnO_2-CNTs hybrid is synthesized by a redox reaction between the C atoms of the nanotubes and MnO_4^- ions. SEM and TEM images show that the multiwall carbon nanotubes of ~10 nm diameter were functionalized by nanoflakes recovering the entire surface of the tube creating hybrid tubes of ~50 nm diameter (Figure 2A).

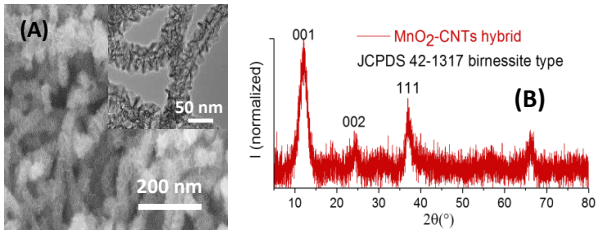

FIGURE 2: (A) SEM AND TEM (INSERT) IMAGE OF MnO_2-CNTS (B) XRD PATTERN OF MnO_2-CNTS HYBRID

XRD patterns (Figure 2B) show that a birnessite type MnO_2 phase is obtained for the hybrid materials (Ref. JCPDS 42-1317). The broad and ill-defined diffractions peaks are mainly due to the small particle size of MnO_2 in the nanocomposite but also to a low crystallinity.

Cyclic voltammetry measurements of MnO_2-CNTs were compared with pure CNTs and MnO_2 electrode materials and performed on the free-standing films (II.A) in Na_2SO_4 1M aqueous electrolyte from 0 to 0.9V vs Ag/AgCl in a three electrodes cell. The hybrid material shows a capacitance of 106 F/g at 5 mV/s which is much higher than for the pure MnO_2 (49 F/g) or for the pure CNTs (13 F/g) in the same conditions (Figure 3). As expected, electrochemical performances decrease when the scan rate increases, due to the high resistivity of the electrode material (38 F/g at 50 mV/s).

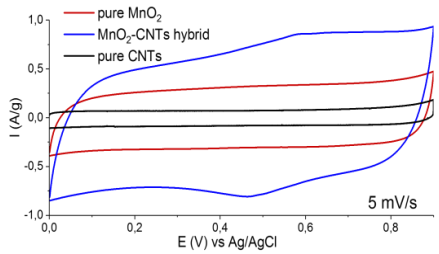

FIGURE 3: CV OF PURE CNTS (BLACK) PURE MnO_2 (RED) AND MnO_2-CNTS HYBRID (BLUE)

B. Graphene/CNTs/MnO_2-CNTs hierarchical structure

The electrode material obtained in II.B by mixing MnO_2-CNTs hybrid, pure CNTs and graphene oxide can be described as a hierarchical nanostructure or a nano-architecture. Graphene oxide is not a good conductive material, so the electrical conductivity of the electrode is enhanced by a thermal treatment after deposition. Indeed graphene oxide can be thermally reduced in more conductive Reduced Graphene Oxide (rGO) [8]. The thermal treatment enhances the electrochemical performances (Figure 4A). SEM images (Figure 4B) show that CNTs, MnO_2-CNT hybrid and rGO are evenly mixed in a hierarchical architecture.

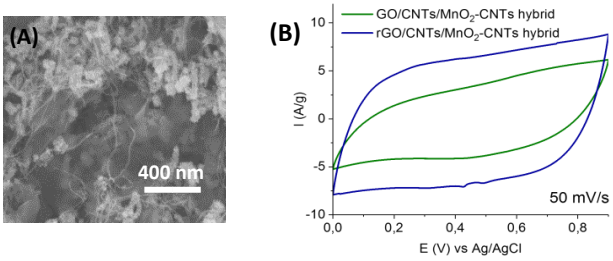

FIGURE 4: (A) CV OF GO-MnO_2-CNTS (GREEN) AND RGO-MnO_2-CNTS (BLUE) (B) SEM IMAGE OF RGO-MnO_2-CNTS

The specific capacitance measurements of the rGO/CNTs/MnO_2-CNTs coated material show higher performances than for the MnO_2-CNTs free standing film. On one hand, adding rGO and optimizing electrode formulation creates a synergetic effect and increases strongly the specific capacitance up to 156 F/g at 5 mV/s and to 109 F/g at 50 mV/s which indicates one the other hand that the material has also a good rate capability.

IV. Conclusion

In summary, a hybrid MnO_2-CNTs hybrid material was synthesized through a simple redox reaction and used as a component in a hierarchical architecture with rGO and CNTs. The hybrid MnO_2-CNTs nano-objects give the faradaic behavior necessary to enhance electrochemical performances, the rGO and CNTs provide for a high specific surface area and electrical conductive network.

The obtained electrode material exhibits a capacitance three times higher than that of pure MnO_2 material indicating a synergetic effect between carbon nanomaterials and MnO_2 nanoflakes.

References

[1] R. Kötz et M. Carlen, «Principles and applications of electrochemical capacitors,» *Electrochimica Acta,* vol. 45, n°115, pp. 2483-2498, 2000.

[2] A. Gonzalez, E. Goikolea, J. A. Barrena et R. Mysyk, «Review on supercapacitors: Technologies and materials,» *Renewable and Sustainable Energy Reviews,* vol. 58, pp. 1189-1206, 2016.

[3] J. Wang, S. Dong, B. Ding, Y. Wang, X. Hao, H. Dou, Y. Xia et X. Zhang, «Pseudocapacitive materials for electrochemical capacitors: from rational synthesis to capacitance optimization,» *National Science Review,* vol. 4, n°11, pp. 71-90, 2017.

[4] M. Huang, F. Li, F. Dong, Y. X. Zhang et L. L. Zhang, «MnO2-based nanostructures for high-performance supercapacitors,» *J. Mater. Chem. A,* vol. 3, pp. 21380-21423, 2015.

[5] R. B. Rakhi, W. Chen, D. Cha et H. N. Alshareef, «Nanostructured Ternary Electrodes for Energy-Storage Applications,» *Advanced Energy Materials,* vol. 2, n°13, pp. 381-389, 2012.

[6] L. Li, Z. A. Hu, N. An, Y. Y. Yang, Z. M. Li et H. Y. Wu, «Facile Synthesis of MnO2/CNTs Composite for Supercapacitor Electrodes with Long Cycle Stability,» *The Journal of Physical Chemistry C,* vol. 118, n°140, pp. 22865-22872, 2014.

[7] L. L. Zhang, R. Zhou et X. S. Zhao, «Graphene-based materials as supercapacitor electrodes,» *J. Mater. Chem.,* vol. 20, pp. 5983-5992, 2010.

[8] G. Lu, L. E. Ocola et J. Chen, «Reduced graphene oxide for room-temperature gas sensors,» *Nanotechnology,* vol. 20, n°144, p. 445502, 2009.

Optimization of a Bimorph Piezoelectric Energy Harvester Using Neural Network-Based Genetic Algorithm

Abbas Homayouni Amlashi[1,*], Abdenbi Mohand-Ousaid[1] and Micky Rakotondrabe[1]
[1] *Automatic Control and Micro-Mechatronic Systems (AS2M) Department, FEMTO-ST Institute*
Université Bourgogne Franche-Comté, CNRS, 24 rue Alain Savary, Besançon 25000, France.
*abbas.homayouni@femto-st.fr

***Abstract*—piezoelectric bimorph cantilever beam is used to harvest the energy from an external harmonic excitation source with constant amplitude and constant excitation frequency. To maximize the electric charge, an attachment has been added to the cantilever beam to perfectly match one of the natural frequencies of the beam equal to the excitation frequency. To choose the best attachment mass, mass moment of inertia, attachment location and force location on the beam, Genetic Algorithm (GA) is proposed while a multi-layer perceptron (MLP) neural network in the core of GA evaluation process has been utilized to obtain approximate functions for the natural frequencies based on the optimization variables. Simulation results demonstrate the successful performance of the neural network-based genetic algorithm in choosing the best combination of the variables to maximize the charge.**

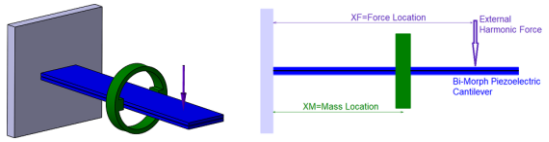

FIGURE 1. BIMORPH PIEZOELECTRIC CANTILEVER WITH ATTACHMENT

I. INTRODUCTION

Bimorph piezoelectric cantilevers are the most effective energy harvesters among other types of piezoelectric cantilever beams[1]. To modify natural frequencies of the beam and matching one of them to the excitation frequency, an attachment has been added to the beam. as can be seen in FIGURE 1, in contrast to previous researches in the literature in which the attachment is considered to be a lumped mass at the tip of the beam[2], in this paper the attachment can be placed anywhere in-span of the beam while the effect of mass moment of inertia is also considered. In term of optimization, contrary to geometrical parameters (in particular thicknesses) optimization [3], the paper suggests to more possibilities. Indeed, for any excitation frequency, different combination of attachment mass, mass moment of inertia and attachment location can be chosen to obtain equal natural frequency. In addition, the force application point on the beam is another factor which can affect the amplitude of charge. Therefore, in order to deal with this multi parameter optimization, GA has been utilized here. The variables related to physical specification of the attachment will change the structural properties of the beam including natural frequencies and mode shapes. Therefore, multi-layer perceptron neural network has been trained to obtain approximate functions for the natural frequencies based on the optimization variables. This trained network will be used in the evaluation process of the genetic algorithm to form a neural network-based genetic algorithm which can find the best combination of the optimization variables to match the natural frequency of the beam to the excitation frequency and maximize the output electric charge of the piezoelectric cantilever.

II. PIEZOELECTRIC CHARGE OPTIMIZATION

A. *Piezoelectric charge equation*

Piezoelectric cantilever output electric charge equation is a function of natural frequencies, mode shapes, excitation amplitude, excitation frequency and parametric constants. Except force location, the other three optimization variables do not appear directly in the charge equation. On the other hand, the natural frequencies of the beam are functions of those optimization variables. However, there are no analytical expression for the natural frequencies as a function of the optimization variables.

B. *Multilayer perceptron neural network*

The proposed approach here is to train a multi-layer perceptron neural network to obtain natural frequencies as a continuous function of the optimization variables. Training data consist of input data and target data. Input data is a matrix with 3 rows and 8000 columns for the combination of 20 different attachment location, 20 different attachment mass and 20 different mass moment of inertia. The target data is a matrix of natural frequencies with 4 rows and 8000 columns. Each rows is related to one natural frequencies.

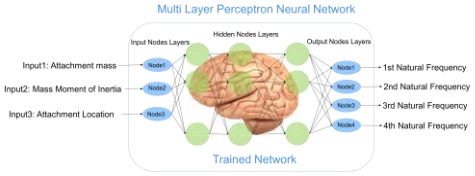

FIGURE 2. MULTI-LAYER PERCEPTRON NEURAL NETWORK

The trained network has been shown in FIGURE 2 which gets the optimization variables and gives the natural frequencies. After finding the approximate functions for the natural frequencies based on the optimization variables, the mode shapes can be found with the help of boundary and continuity equations as a function of the optimizations variables.

C. *Genetic algorithm optimization*

Genetic algorithm has been chosen to find the best attachment location, attachment mass, attachment mass moment of inertia and force location. The fitness function for GA is the piezoelectric charge equation. To avoid being trapped in local optimums, it is necessary to define big population for the GA. For example, here population is defined with 500 individuals while the crossover rate is 0.8 and mutation rate is 0.1. On the other hand, big population means higher amount of CPU time for optimization.

D. *Neural network-based genetic algorithm*

The evaluation process of neural network-based genetic algorithm has been shown in FIGURE 3. The trained network gives the natural frequencies of the selected individuals immediately. This is extremely less time consuming in comparison to numerical procedure for solving the frequency equation. Mode shapes, natural frequencies and force location will be used to find the fitness value of that individual. Therefore, GA can find the best optimization variables in reasonable CPU time.

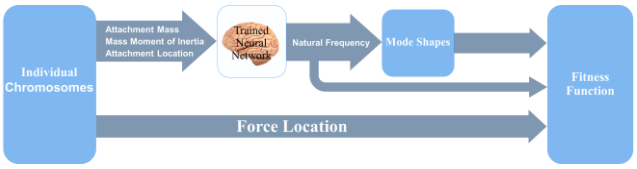

FIGURE 3. GENETIC ALGORITHM EVALUATION PROCESS

III. RESULTS

A. *effect of attachment location on piezoelectric charge*

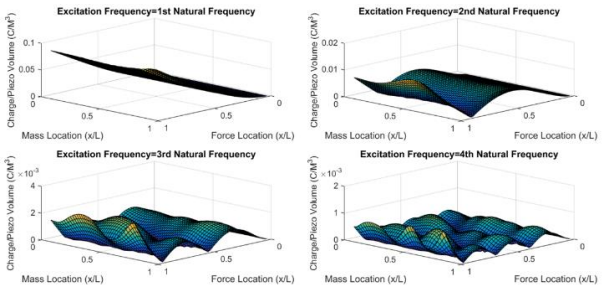

FIGURE 4. CHARGES FOR ATTACHMENT LOCATION VS. FORCE LOCATION

The effects of attachment vs. force location on the piezoelectric charge are demonstrated in FIGURE 4. Lots of local optimums can be seen due to changing the attachment location and force location. The similar results can be achieved for changing the attachment mass and mass moment of inertia. Therefore, decision making for choosing the best optimization variables to maximize the charge amplitude is not possible analytically.

B. *MLP neural network fitting function*

In FIGURE 5, the attachment mass moment of inertia considered to be constant. It can be seen that how the approximate function of the trained MLP network is fitted to the discrete training data.

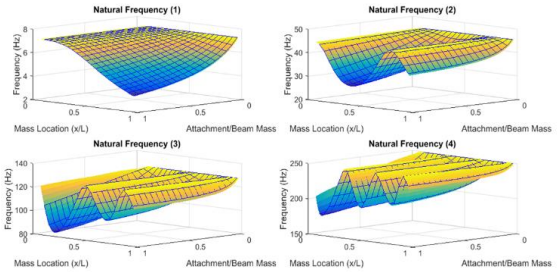

FIGURE 5. TRAINED NETWORK AND DISCRETE TRAINING DATA

C. *Neural network-based genetic algorithm Optimization*

Now, by having the approximate functions of natural frequencies based on the optimization variables, the neural network-based genetic algorithm can be used to find the best possible combination of optimization variables to maximize the charge amplitude. For this case Excitation frequency is the average of bare beam first and second natural frequency. Optimization start with 500 individuals. The optimization reaches the best value in the reasonable CPU time. As has been shown in FIGURE 6, Slight changes in GA suggested variables decrease the amplitude of charge. Second natural frequency of the bimorph and selected attachment is equal to the excitation frequency.

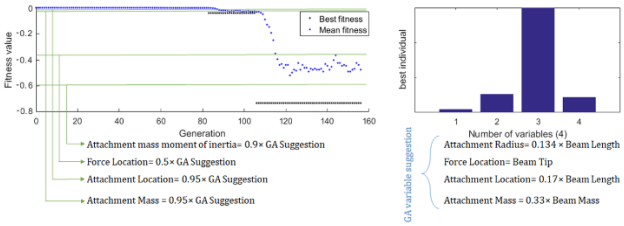

FIGURE 6. GENETIC ALGORITHM OPTIMIZATION PROCEDURE

IV. CONCLUSION

The proposed neural network-based genetic algorithm of this paper, has the ability to maximize the piezoelectric charge for any given external harmonic excitation by choosing the best parameters for the attachment on the beam to match one of the natural frequencies of the beam with the excitation frequency.

ACKNOWLEDGMENT

This work has been supported by the national CODE-Track project (ANR-17-CE05-0014-01, Control theory tools for Optimal Design of piezoelectric Energy harvesters devoted to birds tracking devices). This work has also been supported by the Labex ACTION project (contract "ANR-11-LABX-01-01").

REFERENCES

[1] K. Rabenorosoa and M. Rakotondrabe, "Performances analysis of piezoelectric cantilever based energy harvester devoted to mesoscale intra-body robot," in *Next-Generation Robotics II; and Machine Intelligence and Bio-inspired Computation: Theory and Applications IX*, 2015, p. 94940E.

[2] A. Erturk and D. J. Inman, *Piezoelectric energy harvesting*: John Wiley & Sons, 2011.

[3] T. Schlinquer, A. Mohand-Ousaid and M. Rakotondrabe,*'Optimal design of a unimorph piezoelectric cantilever devoted to energy harvesting to supply animal tracking devices'*, IFAC -WC , (World Congress), pp.15165-15170, Toulouse France, July 2017.

Hybrid synchronized switch harvesting using piezoelectric and electromagnetic conversion

Giulia Lombardi[1,*], Mickaël Lallart[1,†]
[1] *Univ. Lyon, INSA-Lyon, LGEF, EA682, F-69621, VILLEURBANNE, FRANCE*

[*] giulia.lombardi@insa-lyon.fr [†] mickael.lallart@insa-lyon.fr

***Abstract*—In the present work, a preliminary investigation of a hybrid nonlinear energy harvesting scheme based on the coupling of two energy conversion mechanisms is exposed. The proposed approach is derived from the Synchronized Switch technique and consists in combining piezoelectric and electromagnetic transduction. The working principle and preliminary simulations results obtained with the proposed scheme are presented, showing the enhancement of the voltage inversion compared to the sole use of piezoelectric effect.**

I. Introduction

A strong research effort in recent years has been done to harvest the energy available in the environment and to use it as a power source for wireless sensor nodes. Among ambient energy sources, mechanical vibrations are one of the most prevalent ones. Energy harvesting from vibrations has therefore become a focus of interest, motivated by the increasing use of autonomous sensors and sensor networks. Three main technologies are employed to convert mechanical energy into electrical energy: electromagnetic, piezoelectric and electrostatic energy scavengers thus leading to the concept of vibrational energy harvester. Due to their integration potential and power density, piezoelectric energy harvesters, based on the direct piezoelectric effect, have been widely studied and nonlinear treatments applied to the piezovoltage have been developed in order to enhance the energy conversion [1]. Energy extraction strategies have also been extended to electromagnetic vibration energy harvesters (based on the Faradays's law of induction), such as the nonlinear SMFE (Synchronous Magnetic Flux Extraction) technique, which provides a considerable optimization of the energy transfer irrespective of the load impedeance [2]. This paper proposes a new hybrid energy harvesting principle based on the coupling of these two energy conversion mechanisms, with a particular attention to the resulting enhancement of the piezoelectric element output voltage due to the synchronized switching interface.

II. Principles and theoretical analysis

A. Principles

The objective of this section is to expose a theoretical model of the proposed energy harvesting system. The proposed model is derived from the Synchronized Switch nonlinear interface [3] which consists of adding a switching device in series with an inductor to the piezoelectric element. The idea is therefore to convert the inductor from a passive electrical component to an active electrical system. The general resulting circuit is illustrated in Figure 1 and can be divided into two sub-sections, one corresponding to the piezoelectric (PZT) generator and the second one corresponding to the electromagnetic (EM) generator. The state of the switches S1 and S2 (respectively normally off and on) leads to open and short circuit configurations for the piezoelectric and electromagnetic generators respectively, as it will be explained in section B.

B. Theoretical Model

Assuming linear elasticity and near resonance conditions, the typical configuration of a vibration energy harvester can be modeled as a second-order system consisting of a modal mass *M*, a spring *K* and a damper *D*.

From an electrical point of view, a piezoelectric generator is equivalent to a current source proportional to the relative vibration velocity $\dot{u}$ connected in parallel with a capacitor while an ideal electromagnetic generator can be modeled as a velocity depended voltage source in series with an inductor. The constitutive equations of this model are therefore given by:

$$\begin{cases} M\ddot{u} + D\dot{u} + K_e u = F - \alpha V_p - \beta I_m \\ I_p = \alpha\dot{u} - C_0\dot{V_p} \\ V_m = \beta\dot{u} - L_0\dot{I_m} \end{cases} \quad (1)$$

where *u* is the displacement of the structure (assumed to be sinusoidal), V_p and V_m the piezoelectric and electromagnetic voltages respectively and I_p and I_m the piezoelectric and electromagnetic currents respectively; α and β are the force factors of the piezoelectric and electromagnetic elements respectively; C_0 represents the piezoelectric clamped capacitance and L_0 the inductance of the electromagnetic transducer at rest. The operations of the proposed configuration are described as follows. First, the switch S1 is open and S2 is closed, leading to open circuit condition for the piezoelectric element and

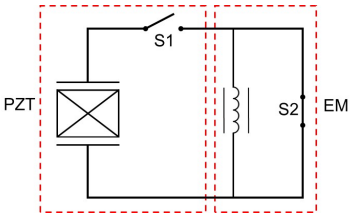

Fig. 1: Circuit schematic

short circuit condition for the electromagnetic element. Under these conditions, the mechanical speed is related to the voltage derivative for the piezoelectric element, following equation (2), and to the current derivative for the electromagnetic element, following equation (3):

$$I_p = 0 \Rightarrow \dot{V_p} = \frac{\alpha}{C_0}\dot{u} \tag{2}$$

$$V_m = 0 \Rightarrow \dot{I_m} = \frac{\beta}{L_0}\dot{u} \tag{3}$$

When the mechanical displacement reaches a maximum or a minimum value, the electronic switches S1 and S2 are briefly turned on and off respectively, so that the piezoelectric element is connected with the electromagnetic element establishing an oscillating electrical L-C circuit. Consequently, a current flow from the piezoelectric element appears as:

$$L\ddot{q} + R\dot{q} + \frac{q}{C_0} = 0 \tag{4}$$

where q is the charge of the piezoelectric element. Unlike the standard synchronized switch interface (null initial current flow), equation (4) is solved considering $I_p = I_m$ and $V_m = V_p$, leading to the voltage and current oscillation as defined in equations (5) and (6) respectively:

$$V(t) = e^{-\frac{R}{2L_0}t}[V_0\cos(\omega_0 t) + \frac{I_0}{C_0\omega_0}\sin(\omega_0 t)] \tag{5}$$

$$I(t) = e^{-\frac{R}{2L_0}t}[-C_0V_0\omega_0\sin(\omega_0 t) + I_0\cos(\omega_0 t)] \tag{6}$$

where I_0 is equal to $2\frac{\beta}{L_0}u_m$ and corresponds to the current provided by the electromagnetic element and V_0 corresponds to the maximum output voltage provided by the piezoelectric component (V_M). Focusing on the voltage inversion only, in order to achieve a quasi-instantaneous inversion, the switch S1 must be again turned off when the current is null. In the steady-state case, the relation between the output voltage magnitudes before and after the inversion process are given by:

$$\begin{cases} V_M - V_m = 2\dfrac{\alpha}{C_0}u_M \\ V_m = \gamma V_M \end{cases} \tag{7}$$

where γ is the equivalent inversion coefficient, defined as:

$$\gamma = e^{-\frac{R\pi}{2L_0}}e^{-\frac{R}{2L_0\omega_0}\arctan(\frac{I_0}{C_0V_M\omega_0})}\sqrt{1+\left(\frac{I_0}{C_0V_M\omega_0}\right)^2} \tag{8}$$

therefore possibly higher than the inversion coefficient in the non-hybrid case (that is equal to $e^{-\frac{R\pi}{2L_0}}$) thanks to the contribution of the electromagnetic generator (yielding non-zero initial current condition).

III. Numerical validation

As a preliminary validation process, the proposed scheme was analyzed with *Matlab* using Euler's integration method, where the parameter values used for the simulation are 50 *nF* for C_0, 30 *mH* for L_0 and 1 $mN{\cdot}V^{-1}$ for α. The results obtained are illustrated in Figure 2 depicting the enhancement of the voltage inversion when comparing the piezoelectric element alone and the hybrid configuration (considering β equals to 1 NA^{-1}). The corresponding converted energy in these conditions are 11.8 μJ and 17.5 μJ for the piezoelectric element alone and the hybrid configuration respectively, allowing a global energy gain of 40%. Increasing the value of the electromagnetic force factor, leads to an increase of the energy gain that can obtained with the hybrid model, as depicted in Figure 3.

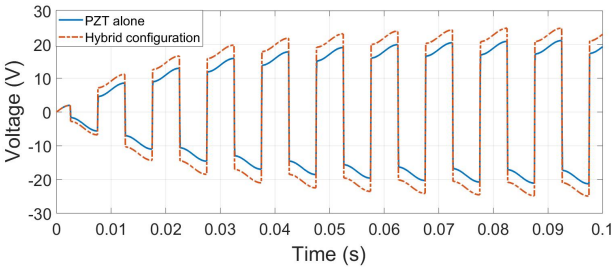

Fig. 2: Voltage waveforms

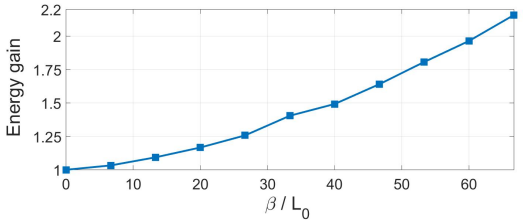

Fig. 3: Converted energy gain

IV. Conclusion

The proposed work, derived from the synchronized switch nonlinear interface, focused on the coupling of two energy conversion mechanisms, combining piezoelectric and electromagnetic transductions. The study has shown an enhancement of the voltage inversion due to the contribution of the electromagnetic generator, thus leading to a gain of 40% in terms of converted energy in the considered example. Further works aim at investigating the enhancement of the current inversion, taking into account the losses of the electromagnetic element, the actual evaluation of the harvested energy and an experimental validations of the proposed model.

V. Acknowledgments

The authors gratefully acknowledge the financial support from European Union's Horizon 2020 research and innovation programme under the Marie Skłodowska-Curie Grant Agreement No. 722496.

References

[1] E. Lefeuvre, A. Badel, C. Richard, L. Petit, D. Guyomar *A comparison between several vibration-powered piezoelectric generators for standalone systems*, Sensors and Actuators A: Physical, Volume 126, Issue 2, 2006, Pages 405-416, ISSN 0924-4247.

[2] E. Arroyo, A. Badel, *Electromagnetic vibration energy harvesting device optimization by synchronous energy extraction*, Sensors and Actuators A: Physical, Volume 171, Issue 2, 2011, Pages 266-273, ISSN 0924-4247.

[3] C. Richard, D. Guyomar, D. Audigier, H. Bassaler, *Enhanced semi passive damping using continuous switching of a piezoelectric device on an inductor*, Proceedings of SPIE Smart Structures & Materials Conference, Passive Damping and Isolation, Volume 3989, 2000, Pages 288.

Growth of KNN:LN Nanowires and thin films for vibrational energy harvesters

Anjneya Verma, Thomas Fischer and Sanjay Mathur
Department of Inorganic Chemistry, University of Cologne
anjneya.verma@uni-koeln.de

Abstract—Energy harvesting comprises all methods to produce energy locally from the sources for instance, solar-, thermal-, wind-, hydrothermal-, vibrational- energy, etc. In the present topic, the focus is on the power generation from vibrations which are counted as energy losses and decrease the efficiency of any particular device. To harvest this ambient energy, we are going to fabricate Piezoelectric Nanostructures. A Piezoelectric material is based on principles of piezoelectricity. On the application of mechanical stress, pressure, vibrations results in accumulation of electric charge. This process is reversible in nature. These Piezoelectric materials have application in vibrational energy harvesters.

The Piezoelectric materials such as Lead Zirconate Titanate (PZT) are widely used due to relatively high piezoelectric coefficients, coupling factors and dielectric permittivity. However, they have a disadvantage of being toxic in nature due to presence of lead, and hence create environmental problems. To overcome this, research is going on to find appropriate environment friendly lead-free materials. These materials have been extensively researched in the past, and progress has been made on a Niobate perovskite compound $KNaNbO_3$ (KNN) and Lithium Niobate (LN) [1]. This system has a morphotropic phase boundary (MBP) due to which it can transit between orthogonal and tetragonal crystal structure. This transition property gives it large piezoelectric constant (d_{33}= 689 pC/N at T_{O-T} = 83 °C) [2]. Until now only selected researchers have successfully fabricated this material using Vapor Phase Epitaxy Method.

In accordance with the ENHANCE, EU-Horizon 2020 program, we will try to fabricate KNN and LN piezoelectric materials in the form of Nanostructures using Vapor Phase Epitaxy. Our aim is to deposit of Thin films and Vertically Aligned Nanowires using environment friendly lead-free materials. With suitable precursors, precise fabrication of nano-structures by optimizing growth conditions, we are going to fabricate piezoelectric to make them usable for energy harvesting applications.

REFERENCES

[1] Jing Feng Li, Ke Wang, Fang-Yuan Zhu, Li-Quan Cheng, Fang-Zhou Yao "(K,Na)NbO_3 Based Lead-Free Piezoceramics: Fundamental Aspects, Processing Technologies, and Remaining Challenges" *Journal of the American Ceramic Society*, vol. 96, Issue 12, 26 November 2013.

[2] Jie Yang, Faqiang Zhang, Qunbao Yang, Zhifu Liu, Yongxiang Li, Yun Liu and Qiming Zhang"Large piezoelectric properties in KNN-based lead-free single crystal grown by a seed-free solid-state crystal growth mathod" *Applied Physics Letters,*108, 182904, 2016

Plate electrical analogue for multimodal energy transfer

Robin DARLEUX[1,*], Boris LOSSOUARN[1] and Jean-François DEÜ[1]

[1] *Laboratoire de Mécanique des Structures et des Systèmes Couplés (LMSSC)*
Conservatoire national des arts et métiers (Cnam), 292 rue Saint-Martin, 75003 Paris, France

*robin.darleux@lecnam.net

***Abstract* — This work presents the implementation of a plate electrical analogue and its validation by comparison between measurements and simulations. We also highlight the possible use of this network as an energy harvester.**

I. INTRODUCTION

Bonding piezoelectric patches on a vibrating structure creates an electromechanical coupling that enables the transfer of the vibration energy to an electrical circuit. The extracted energy can then be either dissipated in a resistive component, or recovered through suitable power electronics. In any case, the design of the electrical circuit has a significant influence on the energy conversion performance. More specifically, piezoelectric shunt damping has been studied to damp one [1] or several [2] modes. These solutions might be effective to extract energy from a few resonances, however the complexity of the electrical circuit increases when considering a large number of modes. Other solutions including interconnected piezoelectric patches coupling the vibrating structure to its electrical analogue have been developed [3,4]. These solutions can help scavenging energy over a wider frequency range but require bonding several piezoelectric transducers on the mechanical structure.

In this paper, we consider a plate as the mechanical structure from which vibration energy should be extracted. Based on a direct electromechanical analogy [5], the unit cell of the electrical network, analog to the unit cell of the mechanical structure, is derived from a discretization of the Kirchhoff-Love theory for plates. A model of the network is developed, in which the electronical damping induced by resistive components is taken into account. The computed currents distribution is then compared to measurements. The comparison validates the fully-passive electrical network that has been realized. Perspectives on further extension to energy harvesting are highlighted as well.

II. MODELING OF A PLATE ELECTRICAL ANALOGUE

A. Unit cell of the electrical network

To define the analogous electrical network of a plate, a discrete model of the mechanical structure is derived from a finite difference model of the Kirchhoff-Love equation in harmonic motion. We then use a direct electromechanical analogy [5], which is summed up in TABLE 1. The discrete mechanical equations are then transformed in electrical equations, from which the equivalent unit cell of the analogous electrical network is identified. Complete details are given in [4].

Mechanical quantity	Electrical quantity
Force	Voltage
Velocity	Electrical current
Compliance	Capacitance
Mass	Inductance
Viscous damping	Resistance

TABLE 1. DIRECT ELECTROMECHANICAL ANALOGY

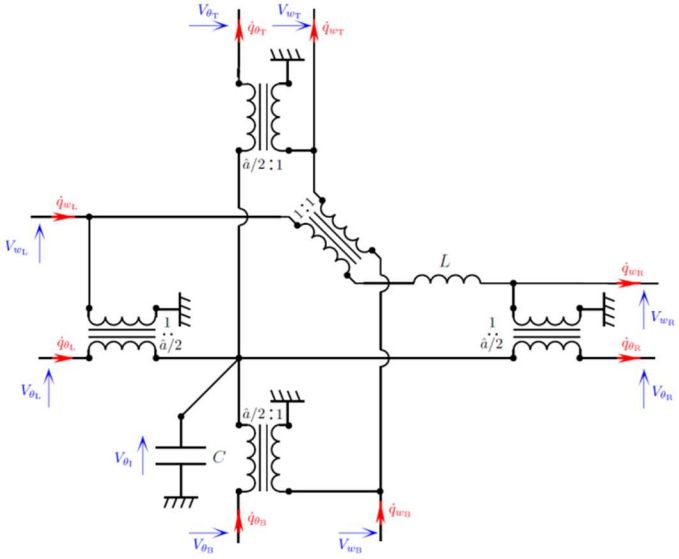

FIGURE 1 : UNIT CELL OF THE ELECTRICAL ANALOGUE OF A PLATE (B. LOSSOUARN ET AL. [4])

The unit cell of the electrical network we obtain is represented in FIGURE 1. The inductance L, the capacitance C and the transformer of ratio 1:1 represent the mass of the mechanical cell, the bending stiffness, and the coupling between the two directions of the mechanical structure, respectively. Transformers of ratio $\hat{a}$/2:1 represent mechanical levers that appear in the finite difference model, where $\hat{a}$ is equivalent to the length of the square cell. Additional components, such as the internal resistances of the inductance L and of the transformer windings, are taken into account as well.

B. Numerical implantation of the finite difference model

The unit cell previously defined is reproduced in two orthogonal directions to form the electrical network. Following an assembly process like in the finite element method, the electrical currents and voltages that appear in FIGURE 1 are then calculated in the case of external voltages applied at nodes of the network. The frequency response function (FRF) of the

voltage drop across the inductors L is computed, and will be compared to experimental results in the next section.

III. Measurements on a Fully-Passive Plate Electrical Analogue

A. Experimental setup

A fully passive network has been realized and is shown in FIGURE 3. Inductive components have been made following the method proposed in [6] and piezoelectric capacitances have been replaced by ceramic capacitors. A voltage excitation induces an electrical current distribution through the network. Those currents are measured by a differential voltage measurement across the inductors.

B. FRFs and currents distribution in the network

The FRF of the current flowing through the inductors divided by the excitation voltage amplitude has been measured at all 42 centers of the unit cells of the network. A comparison of the results obtained by simulation and measurements at one specific unit cell is shown in FIGURE 3. The measured operational current modes shapes, which mimic the vibration modes of the mechanical structure such as in FIGURE 4, can be compared to numerical results as well. These comparisons validate the electrical network, which has been developed as an electrical analogue of a mechanical plate.

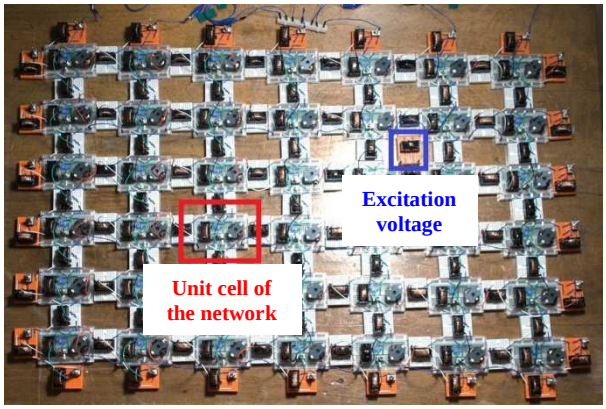

FIGURE 2. Electrical network analogous to a simply supported plate. The network is made of 6x7 identical unit cells.

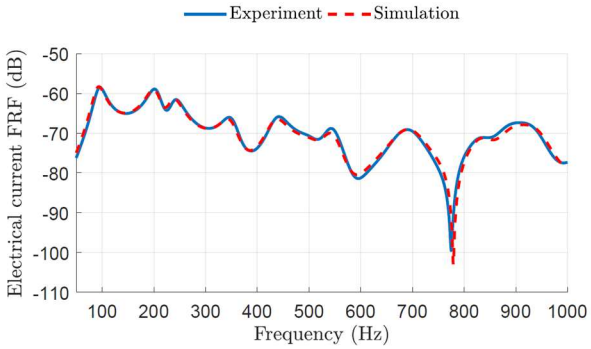

FIGURE 3. Comparison between experiments and simulations of the current FRF in the electrical network

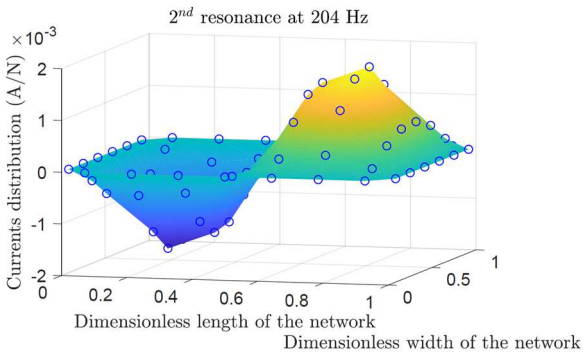

FIGURE 4. Electrical current distribution in the electrical network near the second resonance

IV. Conclusion

In this work, a plate electrical analogue dedicated to multimodal energy transfer is proposed. The analogue network is designed by discretizing the Kirchhoff-Love theory equations and using a direct electromechanical analogy. The unit cell we obtain is periodically repeated to create the network. Simulations and measurements of the currents distribution across the inductors of the network validate the concept of a plate electrical analogue.

Now validated, the network would be able to extract vibration energy from the considered plate over a frequency range of nearly 1 kHz that includes 10 modes. The connection to the vibrating structure will be done thanks to piezoelectric patches, first for a broadband vibration damping purpose, and then for an energy harvesting purpose. As it stands, the main limitation to develop a piezoelectric energy harvester with such an electrical analogous network is that the inductors and transformers of the network are too resistive. The ensuing energy dissipation leads to damped resonances (see FIGURE 3), which limits the energy that could be recovered. The electrical components should thus be optimized as to reduce the internal resistances of the network, and so enable scavenging of the energy transferred from the mechanical structure.

References

[1] O. Thomas, J. Ducarne and J.-F. Deü, "Performance of piezoelectric shunts for vibration reduction", *Smart Materials and Structures*, vol. 21, pp. 015008, 2012.

[2] S. Wu, "Method for multiple mode piezoelectric shunting with single PZT transducer", *Journal of Intelligent Material Systems and Structures*, vol. 9, pp. 991-998, 1998.

[3] S. Alessandroni, F. Dell'Isola and M. Porfiri, "A revival of electrical analogs for vibrating mechanical systems aimed to their efficient control by PZT actuators", *International Journal of Solids and Structures*, vol. 39(20), pp. 5295-5324, 2002.

[4] B. Lossouarn, M. Aucejo and J.-F. Deü, "Design of a passive electrical analogue for piezoelectric damping of a plate", *Journal of Intelligent Material Systems and Structures*, pp. 1045389X17731232, 2017.

[5] R.H. MacNeal, "The solution of partial differential equations by means of electrical networks", *PhD Thesis*, California Institute of Technology, 1949.

[6] B. Lossouarn, M. Aucejo, J.-F. Deü and B. Multon, "Design of inductors with high inductance values for resonant piezoelectric damping", *Sensors and Actuators A: Physical*, vol. 259, pp. 68-76, 2017.

Enhancement of the performances of a quasi-periodic electromagnetic vibration energy harvester by energy localization

Kaouthar Aouali[1,2,*], Najib Kacem[1], Elyes Mrabet[2], Noureddine Bouhaddi[1] and Mohamed Haddar[2]

[1]Univ. Bourgogne Franche-Comté, FEMTO-ST Institute, CNRS/UFC/ENSMM/UTBM, Department of Applied Mechanics, 25000 Besançon, France
[2]National Engineering School of Sfax, Research Laboratory of Mechanics Modeling and Production, Sfax, Tunisia
*Corresponding author: aouali.kaouthar@gmail.com

Abstract

Vibration energy harvesting by exploiting the multimodal approach in a quasi-periodic system is investigated. The quasi-periodic system, based on magnetic transduction, consists of two weakly coupled magnets guided by elastic beams. Mistuning is achieved by varying the mechanical stiffness of one of the beams. These imperfections will lead to the vibration energy localization in regions close to the imperfections which will be exploited to maximize the harvested energy.

Keywords: Vibration energy harvesting, energy localization, quasi-periodic structure, mistuning.

I. Introduction

The diversity of ambient sources of energy arouses researchers to made its scavenging a focus of interest. Many efforts have, recently, been made to develop techniques for vibration energy harvesting based on various energy conversion mechanisms. In the following, we are interested in a vibration energy harvester (VEH) by exploiting the multimodal approach [1], which involves operating multiple modes in a periodic system.

Depending on the magnitude of the disorder and the strength of the internal coupling of the system, it is possible to localize the vibration energy in regions close to the imperfections [4]. Thus, we introduce an irregularity in the mechanical stiffness of one of the two beams. This phenomenon will be exploited to maximize the harvested energy.

Numerical simulations have been performed to highlight the benefits of the localization on the VEH in terms of harvested power. Thus, the optimal mistuning can be determined in order to enhance the performances of the proposed device.

II. System Modeling

A. Design

The harvester proposed, inspired from the work of Mahmoudi and al [3] and depicted in figure 1, is based on magnetic transduction. It is composed of two weakly coupled magnets guided by elastic beams. The magnetic poles are oriented in such a way that repulsive forces are created between each two adjacent magnets. These forces lead to "nonlinear magnetic stiffness". Wire-wound copper coils are wrapped around the moving magnets. When the device is subjected to a harmonic base excitation, each moving magnet oscillates around its equilibrium position and a current is induced in each coil.

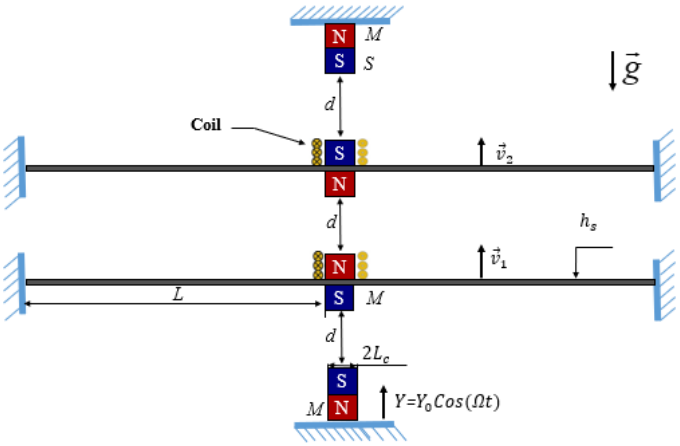

FIGURE 1. DESIGN OF THE PROPOSED VIBRATION ENERGY HARVESTER

The design and physical parameters are reported in Table 1.

TABLE 1. DESIGN PARAMETERS

Parameter	***Designation***	***Value***
L(m)	Beam Length	$60\ 10^{-3}$
b(m)	Beam width	$4\ 10^{-3}$
Lc(m)	Magnet Length	$5\ 10^{-3}$
hs(m)	Beam thickness	$0.6\ 10^{-3}$
d(m)	Gap between magnets	$26\ 10^{-3}$
M(Kg)	Beam mass	$60\ 10^{-3}$
δ	Parameter of magnet and coil	5 Vs/m
S(m)	Magnet surface	$26\ 10^{-4}$
ρ(Kg/m^3)	Steel's Density	7800
Rint (Ω)	Internal resistance	180
E(Pa)	Steel's Young modulus	$210\ 10^9$

B. Problem formulation

In this study, the fourth order partial differential equations of the continuum system are derived using the Hamilton principle. Then, a reduced-order model is generated by Galerkin method, transforming the system into a finite-degree-of-freedom system in terms of generalized coordinates.

III. Solution Procedure

A. Equation of motion

After normalization and generation of a reduced order model, the coupled multi-physics problem, for two degrees of freedom (dof), can be written as:

$$\begin{pmatrix} -\Omega^2+i\Gamma\Omega+(1+2\beta) & -\beta \\ -\beta & -\Omega^2+i\Gamma\Omega+(\alpha+2\beta) \end{pmatrix}\begin{pmatrix} A1 \\ A2 \end{pmatrix}=\begin{pmatrix} F\Omega^2 \\ F\Omega^2 \end{pmatrix} \quad (1)$$

Where

α : mistuning, β : coupling factor, Ω : frequency ratio,

Γ : damping factor and F : ratio of base excitation

The damping factor is proportional to $c=c_m+c_e$ which is the sum of mechanical and electrical damping. The mechanical damping is taken equal to $c_m = 0.19$ Ns/m and according to Mann and Sims [3], the electrical damping is defined as follows:

$$c_e = \frac{\delta^2}{R_{load}+R_{\text{int}}} \quad (2)$$

Where

R_{load}:load resistance and R_{int}:internal resistance

B. Harvested power

The induced current flowing in the load resistance provides an electric power expressed as follows:

$$P(t) = R_{load}.i(t)^2 \quad (3)$$

IV. Results and Discussion

The amplitude of the excitation is $Y_0 = 1.510^{-5} m$ and simulations are performed using the parameters of Table 1.

The load resistance is equal to a value wish is around the internal resistance. We have chosen, thereafter, that its domain of variation is limited to 800Ω.

Figure 2 shows the maximum amplitudes of the two magnets with respect to the load resistance and the mistuning. The displacement of the first magnet is important compared to the second one where we have introduced an irregularity. The vibration energy will be, therefore, localized on this magnet. Thus, an electric circuit is implemented to harvest the vibration energy. The harvested power is expressed as follows [3]:

$$\bar{P}=R_{load}\left[\frac{\delta d}{(R_{load}+R_{\text{int}})T}\right]^2\left[\omega_1^2(\alpha,\beta)A_{1\max}^2(\alpha,\beta,R_{load})\right] \quad (4)$$

Where $T = L^2\sqrt{\frac{12\rho S}{Ebh^3}}$

The effects of mistuning and coupling on the harvested power are investigated by mean of both maximization of the harvested power and the difference between maximum peak amplitudes. The harvested power, depicted in figure 3 is maximum when $\alpha\in[1.033,1.056]$ and $R_{load}\in[270,370]$ and is equal to 0.517 mW.

Notably, in this domain, the level of modal localization is about 25% as shown in figure 4.

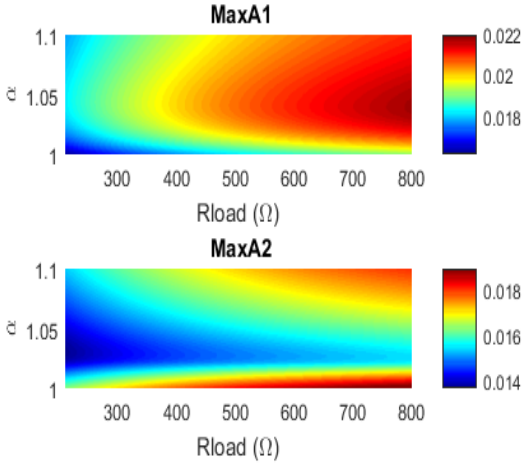

FIGURE 2. MAXIMUM DIMENSIONLESS AMPLITUDES OF TWO BEAMS

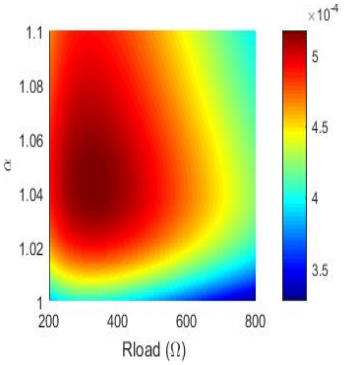

FIGURE 3. POWER (W) VARIATION WITH MISTUNING AND LOAD RESISTANCE

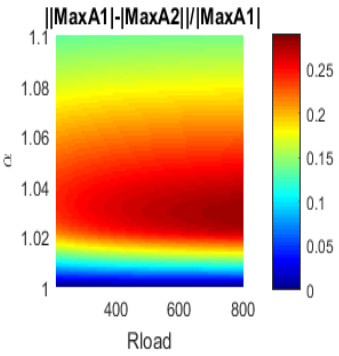

FIGURE 4. PERCENTAGE OF LOCALIZATION

V. Conclusion

In this paper, we propose a multimodal electromagnetic energy harvester. We have introduced an imperfection in the structure in order to enhance the harvested power by energy localization. The harvested power is enhanced by up 28% compared to that from a periodic structure. Its maximum value is equal to 0.517 mW with a localization about 25%.

References

[1] Y. TADESSE, S. ZHANG and S. PRIYA: Multimodal energy harvesting system: Piezoelectric and electromagnetic. *Journal of Intelligent Material Systems and Structures*, 20(5): 625-632, 2009.

[2] S. MAHMOUDI, N. KACEM and N. BOUHADDI: Enhancement of the performance of a hybrid non-linear vibration energy harvester based on piezoelectric and electromagnetic transductions. *Smart Materials and Structures*, 23(7):075024, 2014.

[3] B.P. MANN and N.D. SIMS: Energy harvesting from the nonlinear oscillations of magnetic levitation. *Journal of Sound and Vibration*, 319 (1-2):515-530,2009.

[4] P.V. MALAJI and S.F. ALI: Energy harvesting from near periodic structures, *Vibration Engineering and Technology of Machinery*, Mechanisms and Machine Science 23, 411–420,2015.

Dy-doped BiFeO3 films grown by MOCVD on single crystal substrate

Quentin MICARD[1,*], Anna L. PELLEGRINO[1], Gugliemo G. CONDORELLI[1] and Graziella MALANDRINO[1]
[1] *Dipartimento di Scienze Chimiche, Universitá Catania, and INSTM UdR Catania, Viale A. Doria 6, I-95125 Catania, Italy*
* qmicard@gmail.com

Abstract

The deposition of BiFeO3 on various substrates has attracted great attention in the recent years for multifunctional applications since its ferroelectric and magnetic transition temperatures are well above the room temperature. Recent work has focused on A-site doping with rare-earth ions, and in particular on partial substitution of Bi3+ ion with Dy3+ has been considered.

Bi(1-x)DyxFeO3 films have been grown on conductive Nb-doped SrTiO3 (100) substrates by MOCVD. Films have been deposited using a multi-metal source, consisting of the Bi(phenyl)3, Dy(hfa)3diglyme and Fe(tmhd)3 (phenyl = –C6H5, H-hfa = 1,1,1,5,5,5-hexafluoro-2,4-pentanedione, diglyme = H-tmhd = 2,2,6,6-tetramethyl-3,5-heptandione) precursor mixture.

The piezoelectric and ferroelectric properties are correlated to the structural and compositional properties of the deposited layers with attention to the Dy doping. This correlation has been done using X-ray diffraction (XRD) for the structural characterization, field-emission scanning electron microscopy (FE-SEM), atomic force microscopy (AFM) and energy dispersive X-ray (EDX) analysis for the morphologic and chemical characterizations, respectively. Piezo- and ferroelectric response of deposited films has been investigated by Piezoelectric Force Microscopy (PFM) and Piezoelectric Force Spectroscopy as a function of the Dy doping properties of deposited films.

ACKNOWLEDGMENT

This work is supported by the European Community under the Horizon 2020 Programme in the form of the MSCA-ITN-2016 ENHANCE project, Grant Agreement N.722496.

A PSpice model of a thermo-magnetically triggered piezoelectric generator

Adrian A. RENDON-HERNANDEZ[1,*] and Skandar BASROUR[1]
[1] Univ. Grenoble Alpes, CNRS, Grenoble INP†, TIMA, 38000 Grenoble, France
†Institute of Engineering Univ. Grenoble Alpes
*adrian.rendon@univ-grenoble-alpes.fr

***Abstract*—This paper deals with an equivalent electric circuit model of a Thermo-magnetically activated piezoelectric generator (TMAPEG) along with its PSpice implementation. The model, which is developed of lumped circuit elements, is valid under both parallel and series wired TMAPEG operation modes. It also takes into account the effect of mechanical losses due to damping as well as dielectric and mechanical losses linked to the materials. A curve fitting and parameter estimation process are presented in order to determine the losses elements values from experimental measurements of the electrical admittance of the TMAPEG.**

I. INTRODUCTION

Energy harvesters able to recover energy from thermal sources by two-step process such as for instance i) conversion of temperature fluctuations into mechanical movement of a structure, and then ii) mechanical energy conversion into electricity, have gained much attention in recent years [1–3]. The conversion of thermal energy into mechanical movement can be obtained using temperature-dependent and reversible magnetization, which is typical of soft magnetic alloys such as for example iron-nickel alloys, while the conversion of mechanical movement into electricity may be achieved by means of piezoelectric transduction. When designing this kind of energy harvesters, an equivalent model of the system is very helpful in estimating its main features, including the achievable energy output before manufacturing prototypes, assessing the performance of the generator, and the effects of design changes. And efficient design of energy harvesters is particularly advantageous if the theoretical model of the whole energy harvester system (i.e., energy harvester and power management electronics) is implemented using a common software tool, such as PSpice. Therefore, we are developing an equivalent electric model of the whole energy harvesting system we are proposing using PSpice that is extremely convenient to analyze the complete system (i.e., thermo-magnetic, mechanical, and electrical parts).

This work presents the PSpice implementation of a thermo-magnetically triggered piezoelectric energy harvester system previously presented [1] (see Fig. 1). The PSpice model takes into account the effect of dielectric, and mechanical losses due to transducer's material. Mechanical damping of the system is also considered. This work is organized as follows. Section II gives a brief overview of the theoretical model of our TMAPEG, while Section III presents its electrical equivalent model implementation in PSpice. A curve-fitting and parameters estimation process of the electrical admittance of the system are presented in section IV. Validation of simulation results and experimental measurements are outlined in section V.

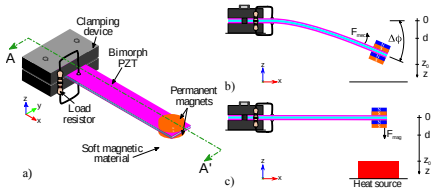

Fig. 1. (a) schematic view of our proposed thermo-magnetically triggered piezoelectric based generator showing its two stable positions; (b) closed position and (c) open position.

II. THEORETICAL MODEL

We observe from Fig. 1 that the transducer part of the TMAPEG consists of piezoelectric cantilever bimorph with a permanent magnet on the free end, which has a double role (i.e., providing a constant external magnetic field and acting as a proof mass). And the conversion principle of mechanical strain to an electrical charge is practically the same of that of vibration-based generators. Therefore, we adapted the theoretical model of a vibration based generator detailed in [4], to model our generator system. The electrical equivalent model is detailed in next section.

III. ELECTRICAL EQUIVALENT MODEL

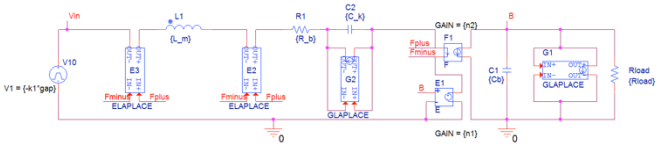

Fig. 2. TMAPEG electromechanical circuit model.

The simplified model takes into account the vibration-based generator geometrical, mechanical, electromechanical coupling parameters, and losses elements linked to materials as shown in Fig. 2. The mechanical elements such as mass, spring and damper are represented by their electrical analogous items, i.e., equivalent inductance L_m, resistance R_b, and capacitance C_k, respectively. The electromechanical conversion block, relating input stress on mechanical side to the voltage on electric domain, is represented by means of controlled sources (i.e., piezoelectric mechanical-electrical conversion is modeled using the Voltage Controlled Voltage Source and the electrical-mechanical conversion is modeled using the Current Controlled Current Source). Stress and force are related to through the geometrical constant K_1 [4]. The equivalent inductance, $L_m = K_1 K_2 m$ which relates the second derivative of strain to stress, represents the inertia of the permanent magnet (proof mass). The geometrical constant K_2 can be derived from the relation between the

displacement, z, and strain [4]. The equivalent resistance, $R_b = K_1K_2b$ which relates stress to strain rate, considers the mechanical losses due to damping; b is the damping coefficient. The equivalent capacitance, C_k, which represents the compliance, relates stress and strain, and it is simply equal to the inverse of the Young's modulus of the piezoelectric material. The capacitance between the electrodes of the bimorph can be written as $C_b = (wl\varepsilon)/(2h_P)$. Where, w, l, ε, and h_P are, respectively, the width, length, absolute piezoelectric dielectric constant, and thickness of piezoelectric layer. The dielectric losses in piezoelectric materials can be described using a complex dielectric constant. This behavior can be modeled with a frequency-dependent resistance in parallel with the piezoelectric capacitance C_b. The losses elements, implemented in PSpice using GLAPLACE and ELAPLACE items (i.e., G_1, G_2, E_2, and E_3), can be described as follows:

$$\begin{aligned} G_1 &= sqrt(-sxs)C_b tan(\delta_d) \\ G_2 &= sqrt(-sxs)C_b tan(\delta_m) \\ E_2 &= s/abs(s)\,K_1K_2b \\ E_3 &= sqrt(-sxs)K_1K_2m \end{aligned} \quad (1)$$

Where δ_d and δ_m are the dielectric and mechanical losses tangents, respectively. The input excitation of the model is considered as a pulse voltage source in order to describe the counter balancing between the mechanical restoring force of the transducer beam and the attraction magnetic force with the magnets and the iron-nickel alloy. Thus, the input force, $F_{in} = -Kz$, where, K is the equivalent stiffness of the transducer, and z, the separation distance between magnet and soft magnetic alloy. The material parameters are listed in Table 1.

IV. Curve Fitting and Parameters Estimation

Initial measurements of the electrical admittance of the generator were carried out using the conditions described as follows: an increase in temperature of the soft magnetic alloy was produced up to reach the opening state of the generator, then, measurements were executed using HIOKI im3570 impedance analyzer. Following this, data was introduced on the optimizer tool of PSpice to estimate the loss parameter values. Our proposed model considers complex material parameters. The model is presented in actuator mode, in such a manner that the admittance can be computed at the input of the electrical block.

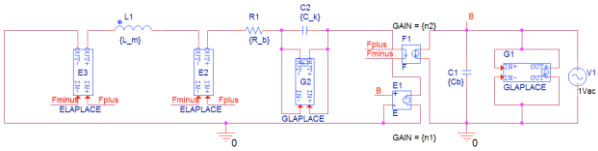

Fig. 3. PSpice schematic of the thermo-magnetically triggered piezoelectric generator in actuator mode to conduct the curve-fitting study and to finding the losses elements values

After 12 iterations of the curve fitting process, using the LSQ solver available in PSpice, the losses elements were estimated as listed in Table 1.

TABLE 1. Material Parameters.

Symbol	*Description*	*units*	*Real part*	*Imag. part*
b	Damping ratio	-	24.8×10^{-3}	0
$\tan(\delta_d)$	Dielectric loss tangent	-	29×10^{-3}	0
$\tan(\delta_m)$	Mechanical loss tangent	-	37×10^{-3}	0
d_{31}	Piezoelectric constant	CN^{-1}	-98.8×10^{-12}	3.02×10^{-12}
ε_{33}^T	Permittivity constant	Fm^{-1}	1.35×10^{3}	-316.98
S_{11}^E	Elastic compliance	Pa^{-1}	25.7×10^{-12}	-1.3×10^{-12}

V. Results and Discussion

This methodology represents a viable alternative to investigate our generator behavior from an electrical point of view. Including the losses elements, which are predominant during the dynamic response of the generator. Fig. 4 illustrates the results of the curve fitting and parameter estimation process of the electrical admittance of the generator. It can be seen that the resonant frequency of the transducer is not constant during its open state. Fig. 5 shows a transient response comparison using our proposed model and observed data. A good agreement is found.

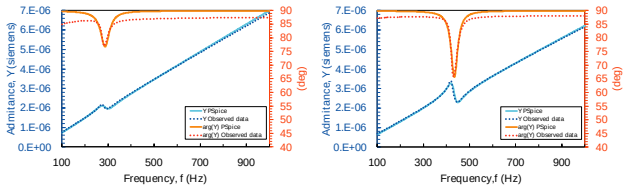

Fig. 4. The curve fitting on the admittance is showing a good agreement with the equivalent model, (left) measurements at the moment when the generator reaches its opening commutation and is heated up until 70°C; (right) measurements at at the instant before the closing commutation of the generator, near to the closing temperature.

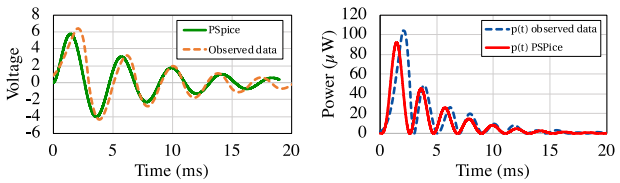

Fig. 5. Results comparisson in transient domain between measurements and simulation after solvinf by curve-fitting for the losses elements. When a load resisitor of 390kΩ is connected (as the optimal resistance for opening commutation).

Future works include implementation of a charging circuit in PSpice to efficiently optimize the whole generator system.

References

[1] Rendon-Hernandez A and Basrour S 2016 Coupled multiphysics finite element model and experimental testing of a thermo-magnetically triggered piezoelectric generator *Journal of Physics: Conference Series* **773** 012024

[2] Gueltig M, Wendler F, Ossmer H, Ohtsuka M, Miki H, Takagi T and Kohl M 2017 High-Performance Thermomagnetic Generators Based on Heusler Alloy Films *Advanced Energy Materials* **7** 1601879

[3] Chun J, Song H-C, Kang M-G, Kang H B, Kishore R A and Priya S 2017 Thermo-Magneto-Electric Generator Arrays for Active Heat Recovery System *Scientific Reports* **7** 41383

[4] Roundy S and Wright P K 2004 A piezoelectric vibration based generator for wireless electronics *Smart Materials and Structures* **13** 1131–42

MEMS Harverster based on PMN-PT/SOI beam

Mihaela IVAN[1,*], Ioan Alexandru IVAN[2,3], Joel AGNUS[1], Thomas BARON[1] and Philippe LUTZ[1]
[1] *FEMTO-ST Institute, Univ. Bourgogne Franche-Comté, CNRS, 25000 Besançon, France*
[2] *Université de Lyon, ENISE/ LTDS, 42023 Saint-Etienne, France*
[3] *Université Valahia de Targoviste, 130104 Targoviste, Romania*
*mihaeeugenia.ivan@femto-st.fr

Abstract— **In this paper we present the design, manufacturing and characterisation of an innovative piezoelectric micro-electro-mechanical (PiezoMEMS) device made from advanced materials of the PMN-PT (Lead Magnesium Niobate-Lead Titanate) family on a SOI (silicon-on-insulator) substrate, able to more efficiently convert electrical energy from low levels of ambient vibrations and impulses.**

I. INTRODUCTION

Energy harvesting systems, also called microgenerators, convert energy from irregular motion, mechanical deformation, ambient vibrations, wind, heat or light into electrical energy using a variety of principles (inductive, piezoelectric, capacitive, thermoelectric, piezoelectric, electromagnetic, biomechanical etc.). They are good candidates for small electronic devices, low energy applications, were using finite lifetime battery is not suitable.

PMN-PT is a single crystal piezoelectric material presenting a significantly higher electromechanical coupling (over 3 times) than conventional PZT piezoceramics [1] so is a very promising material for energy harvesting domaine. A harvester prototype made of a composite PMN-PT cantilever based on a PDMS layer and having a proof mass manufactured from PDMS (poly-dimethilsiloxane) was demonstrated by Mathers et al [2] wih a size of 7.4 mm x 2 mm x 110µm. Its interdigited electrodes configuration (IDE) improves the efficiency of the energy conversion. G-T Hwang and & [3] designed, fabricated and tested a flexible piezoelectric energy harvester, based on PMN-PT thin film of 8.4 µm, wich was employed to enable a cardiac pacemaker.

The harvester structure presented here is based on PMN-PT/SOI bimorph beam manufactured by means of clean room micro technologies. To obtain the cantilever structure, thinned and diced PMN-PT pieces are bonded to SOI etched cavities using gold-gold bonding techniques. The first results are presented.

II. DEVICE DESIGN & MANUFACTURING

A. *Materials Choice & Design*

PMN-PT was considered in two crystalline poling orientations, [001] and [011]. Although the [011] orientation provided improved piezoelectric coefficient by 30% with respect to [001] orientation, we discovered that ageing (depolarization) is increased for the [011] orientation due to low coercive field at room temperature. Therefore, after extensive tests, we established that the PMN-PT [001] is a more appropriate candidate.

The device structure consists of a bimorph cantilever (PMN-PT/SOI) of 2mm x 1mm x 40µm active size (figure 1), and a seismic mass of 10mm in length. The width of each cantilever is 1mm and the thickness ranges from 420µm at the base down to 40µm at the active area level.

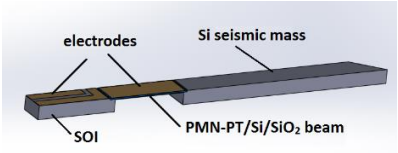

FIGURE 1. 3D sketch of PMN-PT/SOI cantilever

B. *Microfabrication*

The fabrication process is detailed in figure 2. The substrate consists on SOI oxidized wafer 60µm/2µm/450µm thick ; its top side is patterned by BHF etching process performed in SiO2 layer (1.2µm), followed by top side structure releasing in wet etching process with KOH solution. The resulting cavities have about 50µm deep (figure 3a).

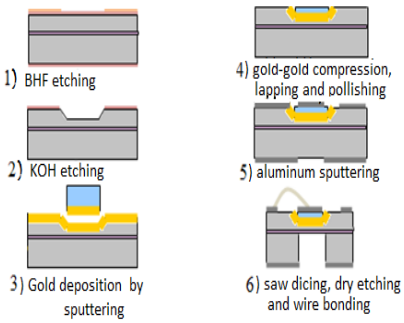

FIGURE 2. Flow chart used for harvester micro-fabrication

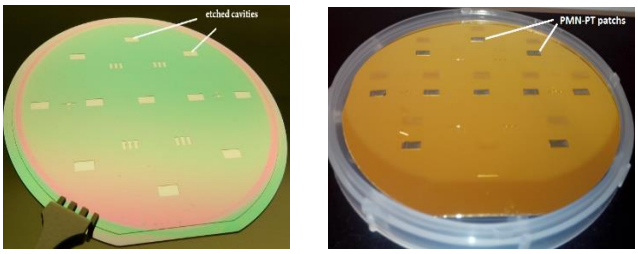

a) b)

FIGURE 3. SOI wafer : a) after KOH etching b) Au-Au bonding

In the next step, chromium/gold layer (30nm/170nm) is deposited on SOI top side by sputtering. The previously diced PMN-PT patches are also gold-sputtered on a side and bonded instantly into the etched cavities by compression of the gold layers at environmental temperature (figure 3b). The bonded PMN-PT layer is then thinned from 150µm to 50µm thickness by lapping and polishing using adapted diamond suspensions with size particles. Top side electrodes and bottom side patterning are performed by aluminum sputtering. After that, the wafer is cut by saw dicing, devices are separated (Figure 4) and bottom side structure is released by dry etching performed on individual device. For this goal, 450µm thickness from handle layer was etched up to silicon dioxide barrier. The result is shown on Figure 4b.

a) b)

FIGURE 4 a) Device after saw dicing and separation

b) Device after DRIE process

On figure 5 we can see that the cavities sidewall are not perfectly vertical but the beam is completely released.

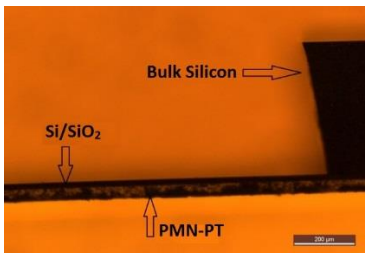

FIGURE 5. Microscopy image showing the bimorph beam

III. Measurements and Results

A. Characterization set-up

The device was characterized on the custom-built testing platform (figure 6) which includes a real-time processor.

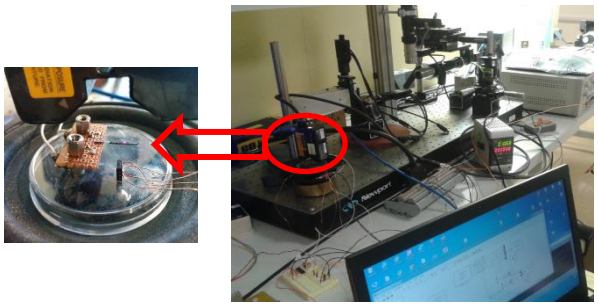

FIGURE 6. Experimental set-up for device characterization

To accurately characterize the voltage and charge harnessing under different mechanical vibration conditions (amplitude, frequency spectrum), the test bench was equipped with an accelerometer, a precision triangulation laser sensor, the required operational amplifier and electronics for precise voltage and charge conversion. The embedded system data acquisition, conversion and control have been finally developed on a Speedgoat™ rapid control prototyping real-time control board running Matlab™/Simulink scripts.

B. Preliminary Results

The charge and voltage response for unpackaged harvester are measured under 0.2*g* vibration input level. First results show the generation of 0.46µC in short-circuit at 113Hz resonant frequency and 1.2V on open circuit conditions at 121Hz (Figure 7).

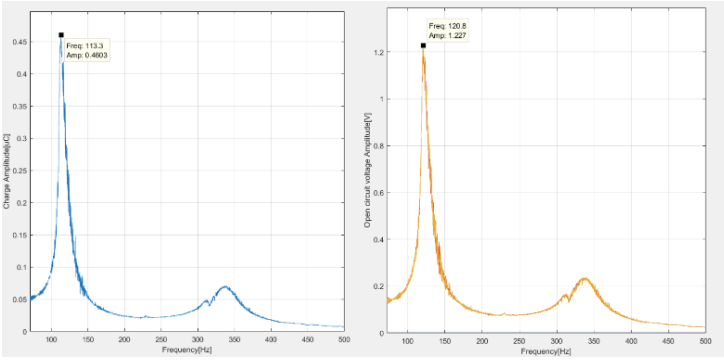

FIGURE 7. Frequency response of charge and open circuit voltage. Experimental Results

IV. Conclusion

The MEMS harvester structure presented in this paper is based on PMN-PT/SOI bimorph beam manufactured by means of clean room micro technologies. A prototype with a size of 2mmx1mmx40µm outputs 0,46µC together with a voltage of 1,2V at a frequency around 120Hz under a peak-to-peak excitation of 0,2*g*.

Acknowledgment

This work has been supported by the Marie Curie European Re-Integration Grant (ERG), called MICROGENS "MicroElectroMechanical Generators Based on High Performance Piezoelectric Materials" and by a BQR project SiMaPe of AS2M Department in collaboration with Time-Frequency Team of FEMTO-ST Institute. The devices were manufactured at MIMENTO clean-room, member of French Renatech Networkte.

References

[1] http://www.trstechnologies.com/Materials/High-Performance-PMN-PT-Piezoelectric-Single-Crystal

[2] A.Mathers, K.S.Moon and J.Yi *"A Vibration-Based PMN-PT Energy Harvester"*, IEEE Sensors Journal, Vol.9, No.7, July 2009

[3] G-T Hwang, H. Park, J-H. Lee, S. Oh, K. Park, M. Byun, H. Park, G. Ahn, Chang K. Jeong, K. No,HS Kwon, S-G Lee,B. Joung and K J Lee, *"Self-Powered Cardiac Pacemaker Enabled by Flexible Single Crystalline PMN-PT Piezoelectric Energy Harvester"*, in Advanced Materials, Volume 26, Issue 28, pages 4880–4887, July 23, 2014

Autonomous Wireless Network Sensor (WSN) general approach for Energy Harvesting (EH) power supply solutions

Gabriel BARRIENTOS[1,2,*], Prof. Graziella MALANDRINO[1] and Dr. Salvatore RINAUDO[2]
[1] *Dipartimento Scienze Chimiche, Università di Catania (UniCT), Viale Andrea Doria, n.6, I-95125 Catania (CT), Italy*
2 STMicroelectronics SRL (ST), Via Primosole, n.50, 95121 Catania (CT), Italy
* g.a.barrientos.r@gmail.com

***Abstract*—The automotive industry has been developed in recent years taking into account the advantages of obtaining data from the different sub-systems that exist in a vehicle. The industry offers more and more sensors for various functionalities in a vehicle and the added value continues growing. But by increasing the amount of sensors the power consumption is higher, the current methods of connectivity of devices become more complicated, the weight of the vehicle increases making the production of CO2 higher, etc. The solution proposed in the project "Piezoelectric Energy Harvesters for Self-Powered Automotive Sensors: from Advanced Lead-Free Materials to Smart Systems (ENHANCE)" presents two main innovations. The first one is the implementation of a Wireless Sensor Network (WSN) to avoid extra weight and simplify devices' installations. And the second one is the implementation of technologies based on Energy Harvesting (EH) which would make the devices autonomous and would decrease not only the energy consumption of the vehicle, but also the maintenance. The WSN is composed of Master, Slave or Master/Slave devices that are responsible for acquiring the information at the ends of the network and transmit them to the center to be processed. Once the network topology to be used is established, the data generated from the sensor element until the user application mode is established by a Protocol Stack. Using the OSI model defined with 5 layers we can establish an accurate method for the collection, identification and packing of the data and transmit it in an organized and standardized way. A sensing module is needed and it can be designed in a generic way for the different sensors in a vehicle. It is only necessary to take into account that the sensor changes according to its application and the EH method as it can be exploited in its location. The most important aspect of all the designing is saving power consumption.**

REFERENCES

[1] A. A. Alhameed Alkhatib, G. Singh Baicher "Wireless Sensor Network Architecture", International Conference on Computer Networks and Communication Systems (CNCS), IPCSIT vol.35, 2012.

[2] W. Charfi, M. Masmoudi and F. Derbel "A LAYERED MODEL FOR WIRELESS SENSOR NETWORKS", 6th International Multi-Conference on Systems, Signals and Devices, 2009.

[3] K. Ma, Y. Zheng, S. Li, K. Swaminathan, X. Li, Y. Liu, J. Sampson, Y. Xie and V. Narayanan "Architecture Exploration for Ambient Energy Harvesting Nonvolatile Processors", IEEE, 978-1-4799-8930-0/15, pages 526-537, 2015.

Harvesting indoor light to supply power to nomad embedded systems

Bastien POLITI[1,3] , Alain FOUCARAN[1], Marie PIQUEMIL[3], Nicolas CAMARA[1,2]
[1]Univ. Montpellier, IES, UMR5214, 860 rue Saint Priest, Montpellier, France
[2]EPF Engineering School, 21 boulevard Berthelot, Montpellier, France
[3]Bureaux A Partager, 21 place de la République, Paris, France
bastien.politi@ies.univ-montp2.fr

It is possible to design a system to supply power to low consumption systems (hundreds of µW to tens of mW) from industrial devices. To develop an autonomous system based on harvesting energy from mixed artificial and natural light, it is mandatory to know which solutions are available and suitable to the conditions of use of the system to be designed. In this paper a comparison of solar cells exposed to different indoor light sources is made. This allows to establish which technology is the most relevant to use in different light environments, in terms of power generation. In addition, the difference in behavior between the two most widely produced solar cells, crystallin and amorphous Si, is depicted. We conclude that for new efficient light sources as fluorescent tubes, CFLs and LEDs, amorphous silicon is the best solution to generate power. On the other hand, crystallin silicon is the most efficient under incandescent, halogen or sunlight exposition.

I. INTRODUCTION

Harvesting enough energy to compensate the mW power consumption of our modern wireless electronic devices is still challenging. Industrials have started to be more and more present on the market, proposing solutions to develop autonomous systems based on energy harvesting solutions. The aim of this paper is to introduce and describe some of these new industrial low-cost possibilities applied to a concrete example: a commercial e-ink wireless touch screen display in an indoor environment.

II. POWER CONSUMPTION CHARACTERIZATION

The first step of this study is to characterize the mean power consumption of our sample nomad device. Using an ultra-low cost bidirectional current/power monitor IC (less than USD $2) from Texas Instrument (INA219), we have measured for several hours, every 6ms, the instantaneous power consumption of the device. The results are displayed in FIGURE 1. In average the measured device uses 35mWh every hour and becomes energetically autonomous by harvesting a mean power of 35mW in its environment.

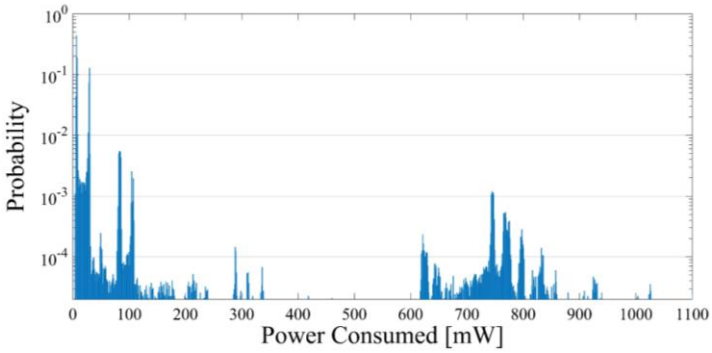

FIGURE 1: POWER CONSUMPTION OF A NOMADIC EMBEDDED DEVICE

III. INPUT POWER TO HARVEST

In an indoor environment like offices, several kinds of energy to harvest can be found: RF energy from WIFI or GSM; mechanical energy from sounds, building vibrations or even user touch, and finally light, from fully artificial to a mix of artificial and natural light during the day. Considering the very low amount of input power of RF and mechanical vibrations compared to the 35mW necessary to harvest, we will focus on light, the major source of power.

Traditionally, the indoor lighting industry gives the light specifications in lux and temperature units that relate more to the perceptions of the human eye than the actual standard units. In order to characterize the input power, we used a "BLACK-Comet-SR" spectrometer covering a range of 200-1100nm that gives the electromagnetic spectrum associated to each artificial and natural light in $W.m^{-2}.nm^{-1}$. We used different light with various spectrums, which can be found in indoor environment: A common halogen light bulb, a "warm" LED (2700K) and two compact fluorescent lights (CFL) of different "color" (2700K and 6500K) and daylight sources through anti-IR double glazing windows. In our example, a 500 lux of fluorescent light correspond to an incident power of $212\mu W/cm^2$ when integrating the whole spectrum. The measures were set at 500 lux, value in which meets most recommendations for indoor space lighting in Europe (EN 12464-1 standard).

IV. PV TRANSDUCERS

The transducers associated to light harvesting are the photovoltaic cells that include a lot of different technologies; monocrystalline Silicon, polycrystalline Silicon, amorphous Silicon, GaAs, thin films inorganic semiconductor cells with CIS, CIGS and CdTe, also organic cells (OPV), Dye cells and finally Perovskite cells. Each one of these technologies exhibits different External Quantum Efficiency (EQE). Based on these EQE differences, the power generated by a cell under a particular light source can be higher than with other cells [1]. The key to indoor energy harvesting is to optimize the match between the indoor input light spectrum

and the EQE of the chosen PV technology used to harvest this input power.

For clarity, the cells studied for this abstract are only based on pc-Si and a-Si cells shown in TABLE 1. They will be considered as references for the other technologies that will be presented at the conference.

TABLE 1. CELLS STUDIED

Cell Array	Cell Array Characteristics			
	Technology	***Num. of cells***	***Dimensions***	***Cost***
Mars Rock Science SC-6733-9	a-Si	9	67 x 33mm	USD $2.1
Chinese Manufacturer SP-107*61	pc-Si	2 x 10	107 x 61mm	USD $1.75

V. EXPERIMENTAL SETUP

The setup, used to characterized photovoltaic devices for indoor light, already used for this purpose in the literature [2,3], consists in a standard current-voltage (I-V) measurement under different light sources. These measurements were performed in an enclosure surrounding the cell in order to limit exposure to the interfering lights as much as possible. The light source distance from the cell can be adjusted allowing to set the desired illuminance level. The used source meter is a commercial SMU Keithley 2450.

VI. RESULTS AND DISCUSSION

A significant difference of behavior between the pc-Si cell and a-Si emerges in the results shown in FIGURE 2. Under halogen exposure, the poly-crystallin silicon cell performs more than 7 times better than the amorphous one (123µW/cm² vs 16µW/cm² under 500 lux). However, under artificial lights the pc-Si cell performances fall dramatically down to half of what other cells can output. In contrast, amorphous cells show consistent power generation irrespective of the type of light source they are exposed to. As a matter of fact, it is noticeable that this type of cell can provide from 8µW/cm² under 200 lux of illumination to 19.8µW/cm² under 500 lux.

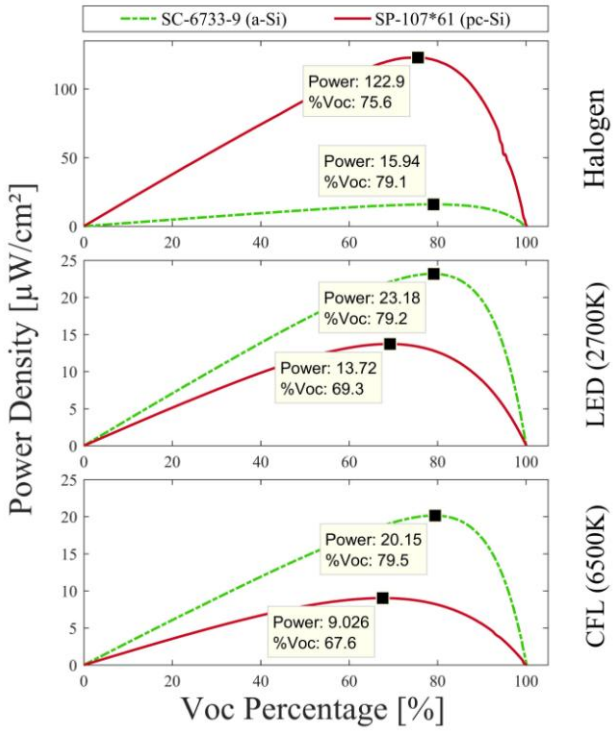

FIGURE 2: POWER PRODUCTION UNDER 500 LUX

Furthermore, amorphous silicon cells generate more power under most efficient light sources such as CFL, and even more power, with LED due to their band gap around 1.7eV. In contrast, poly-crystallin silicon's band gap of 1.1eV makes it the most efficient for harvesting energy from light of a wavelength above 1100nm.

VII. HARVESTED POWER

To complete this paper, testing and measuring the energy which can be harvested from a cell, managed by a Power Management IC (PMIC), has to be accomplished. This will conclude whether the setup used to characterize and estimate the recoverable power is capable of providing correct estimations or not. This part of the study will be presented at the conference.

VIII. CONCLUSION

We reported that the power density of solar cells in indoor environments can vary dramatically depending on its technology. Depending on the luminous indoor environment a device has to be powered from, the choice of the photovoltaic cell is decisive. Under light merely composed of efficient artificial illumination (i.e. LEDs, fluorescent lamp or tube), crystallin silicon is prescribed. However, with light coming from halogen or incandescent lights, it becomes interesting to use crystallin silicon.

In conclusion, a steady power generation level of 20µW/cm² is achievable with amorphous silicon. In our case a device consuming 35µW with a surface of 1750cm² of a-Si cells will be autonomous under 500 lux illuminance exposure. To go further a study of the behavior of the different cells under various mixt indoor light environment has to be done.

ACKNOWLEDGMENTS

Project funded by the National Research and Technology Association (ANRT: CIFRE N° 2017/0331)

REFERENCES

[1] B. Minnaert and P. Veelaert, "WHICH TYPE of solar cell is best for low power indoor devices ?," *Innov. Sustain. Prod.*, pp. 8–12, 2010.

[2] C. Carvalho and N. Paulino, "On the Feasibility of Indoor Light Energy Harvesting for Wireless Sensor Networks," *Procedia Technol.*, vol. 17,

[3] Y. Li, N. J. Grabham, S. P. Beeby, and M. J. Tudor, "The effect of the type of illumination on the energy harvesting performance of solar cells," *Sol. Energy*, vol. 111, pp. 21–29, 2015.

[4] F. De Rossi, T. Pontecorvo, and T. M. Brown, "Characterization of photovoltaic devices for indoor light harvesting and customization of flexible dye solar cells to deliver superior efficiency under artificial lighting," *Appl. Energy*, vol. 156, pp. 413–422, 2015.

An electromagnetic vibration energy harvester using a two degree of freedom oscillator for railway applications

M. Perez[1*], S. Chesné[1], C. Jean-Mistral[1], S. Bouvet[2], and C. Clerc[2]

[1] *Université de Lyon, CNRS INSA-Lyon, LaMCoS UMR5259, F-69261 Villeurbanne, France*
[2] *VibraTec, 28 chemin du petit bois, F-69130 Ecully, France*
* *matthias.perez@insa-lyon.fr*

This paper presents an inertial energy harvester exploiting the vibrations on a tramway to turn the relative motion between a permanent magnet stack and several coils into electricity. This paper includes a short review of the vibratory environment encountered on the tramway, the design and optimization of the harvester and some results of simulation. Among all the geometries tested, a 0.2dm³ device has been highlighted, with an output power of 6.7mW (33.5mW/dm³) on all the travels simulated.

Keywords— Vibration energy harvesting, Electromagnetic conversion, Permanent magnets, Inertial linear generator

I. INTRODUCTION

Railway networks sustain high mechanical solicitation, whether on the rail or on the embedded structures (suspensions, wheels, frames…). Tramways operate every day of the year, with very limited disruption. Consequently, many parts are expected to wear out or even break out. The idea is therefore to conduct health monitoring of the structures (SHM) with energetically autonomous devicein order to anticipate potential failures and change the relevant parts in time. Many publications were published on this topic since 2007, with piezoelectric solutions [1][2], or electromagnetic transducers [3][4] embedded on the rail [5][6][7], or on the bogie… In this study, we focused only on the production of electricity from vibration to supply the different sensors used for the SHM (accelerometers, strain gauges, GPS…).

II. VIBRATORY ENVIRONMENT OF THE TRAMWAY

As a first step, it is necessary to know the reel vibratory environment of a tramway in operation. A complete campaign has allowed to characterize the actual vibratory environment of an operating tramway on the entire rail network of the city of Lyon in France and to collect a considerable amount of data (Fig. 1). The bogie turned out to be an ideal location for both detecting the potential failures and harvesting vibration energy.

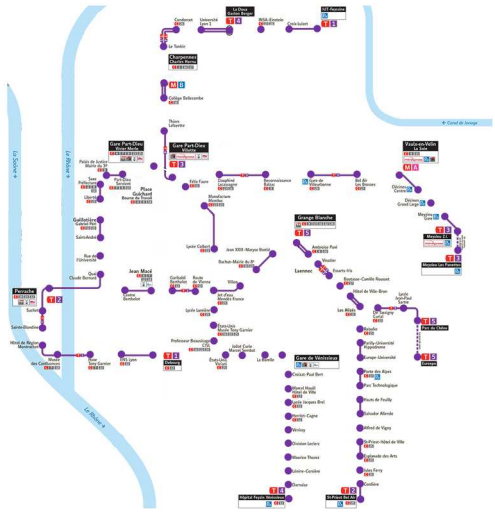

Fig. 1. Map of Lyon's tramway network and travels performed.

By post-treating all the data, an RMS acceleration of 4.7m.s^{-2} and associated displacements lower than ±500µm on the bogie location are noted. These experiments also allowed us to identify the characteristic spectrum and underline two predominant frequencies between 0 and 100Hz (Fig. 2).

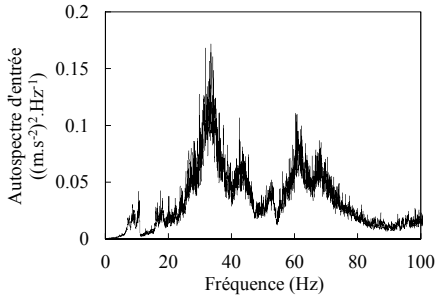

Fig. 2. Auto-power spectrum calculated on all the tests.

III. DESIGN AND OPTIMIZATION OF THE HARVESTER

An inertial two degree of freedom vibration energy harvester combined with a permanent magnet linear generator has been designed. The mechanical and electrical differential equations discussing our transducer are:

$$\begin{cases} \ddot{x}_1 + \dfrac{c_{mec\_1}}{m_1}\dot{x}_1 + \dfrac{\alpha^2}{m_1(r_b+R)}(\dot{x}_1-\dot{x}_2) + \dfrac{k_1}{m_1}x_1 = -\ddot{x}_0 \\ \ddot{x}_2 + \dfrac{c_{mec\_1}}{m_1}\dot{x}_2 + \dfrac{\alpha^2}{m_2(r_b+R)}(\dot{x}_2-\dot{x}_1) + \dfrac{k_2}{m_2}x_2 = -\ddot{x}_0 \end{cases}$$

with x_i the position of each degree of freedom, c_{mec_i} the coefficient of friction, k_i the stiffness, m_i the mass, $\alpha = \frac{\partial \phi}{\partial x}$ the electric coupling coefficient, r_b the resistance of the coils, R the load resistance and $\ddot{x}_0$ the acceleration of the bogie.

Experimental vibratory data have been used as input parameters. The device has been design to be as compact as possible, while providing a sufficient amount of electric power for the supply of the sensors. The solution we propose is made up of two moving parts comprising basically the NdFeB permanent magnets arrangement on one side and the coils on the other (Fig. 3). The two degree-of-freedom of the harvester have been tuned to resonate in perfect adequacy with the spectrum of the input signal (Fig. 2). Both parts are linked to a common frame thanks to two double spring membranes.

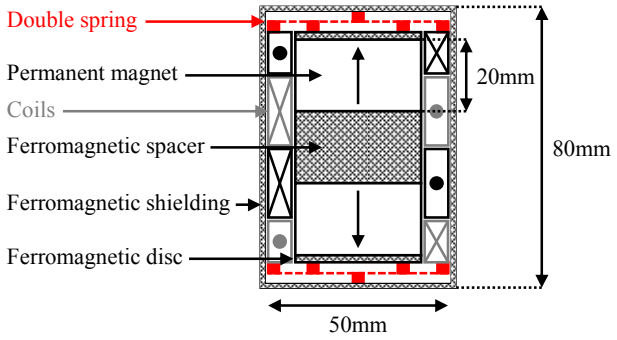

Fig. 3. Schematic representation of the energy harvester at rest.

IV. Simulation Results

In order to maximize the output electric power, a high electric coupling coefficient is mandatory. In the case of an electromagnetic converter, this coefficient α depend on the geometry and the strength of the permanent magnets, and on the number of turns of the coils N. An optimization helped us to identify the following configuration:

- 2 NdFeB permanent magnets (radius : R_a=17.5mm, height : H_a=20mm, remanence Br=1.35T)
- Separated by a ferromagnetic spacer (radius: 17.5mm, height: 20mm)
- 4 cylindrical copper coils are located around the permanent magnet stack (inner radius: 18.5mm, outer radius: variable)

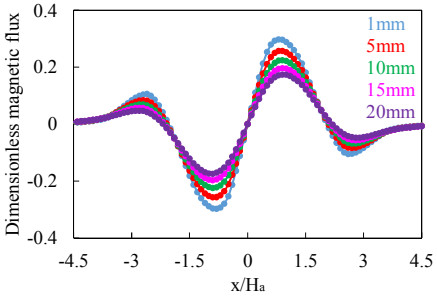

Fig. 4. Variation of the dimensionless magnetic flux $\left(\frac{\phi(x)}{N\pi {R_a}^2 B_r}\right)$ for different coil thicknesses.

Fig. 4 shows the evolution of the dimensionless magnetic flux according to the thickness of the coils. It may be noted that the spatial variation of the magnetic flux is maximum around the point of equilibrium (x=0). Considering the relatively small displacement of the two degree of freedom during the operation (x/H_a<<1), we can consider that the electric coupling coefficient α is constant.

Fig. 5 presents the simulated average electrical power depending on the thickness of the coils. The best results has been obtained with the magnet stack tuned to resonate at 32Hz while the coils was tuned to resonate at 64Hz. By comparison, the blue curve has been achieved by fixing the second degree of freedom (i.e. the winding). Therefore, we can clearly notify the profit of the second degree of freedom, especially for high coil thicknesses.

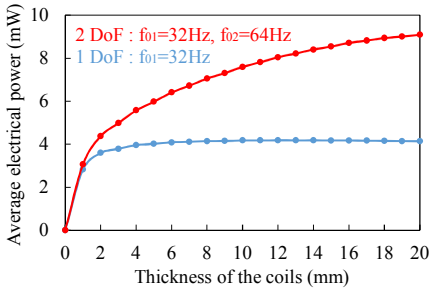

Fig. 5. Evolution of the electric power for different parameters and the optimal load resistance $\left(\frac{\sqrt{k_1 m_1}}{c_{mec\_1}} = \frac{\sqrt{k_2 m_2}}{c_{mec\_2}} = 10\right)$.

V. Conclusion

We have presented some results of the optimization of an electromagnetic vibration energy harvester. In our case, we found that the best option was to use a two degree of freedom oscillator, due to the input spectrum and the very low levels of relative displacement. Experimental results are currently under development and will be published soon.

References

[1] G. De Pasquale, A. Soma, and F. Fraccarollo, Piezoelectric energy harvesting for autonomous sensors network on safety-improved railway vehicles, Institution of mechanical engineers, part C : Journal of mechanical engineering science (2011).

[2] J. Li, S. Jang, and J. Tang, Design of a bimorph piezoelectric energy harvester for railway monitoring, Journal of the Korean society for nondestructive testing (2012).

[3] H. Park and J. Kim, Electromagnetic induction energy harvester for high-speed railroad applications, Precision engineering and manufacturing-green technology (2016).

[4] M. Gao, P Wang, Y. Cao, R. Chen, and D. Cai, Design and veri_cation of a rail-borne energy harvester for powering wireless sensor networks in the railway industry, Transactions on intelligent transportation systems (2016).

[5] C.A. Nelson, S. R. Platt, S. E. Hansen, and M. Fateh, Power harvesting for railroad track safety enhancement using vertical track displacement, Active and passive smart structures and integrated systems (2009).

[6] A. Pourghodrat, C. A. Nelson, K. J. Phillips, and M. Fateh, Improving an energy harvesting device for railroad safety applications, Active and passive smart structures and integrated systems (2011).

[7] J. Wang, T. Lin, and L. Zuo, High e_ciency electromagnetic energy harvester for railroad application, International design engineering technical conferences and computers and information in engineering conference (2013).